Universiteit Leiden
The Netherlands

From stress to success: how actinobacteria exploit life witout a cell wall

Ongenae, V.M.A.

Citation
Ongenae, V. M. A. (2025, March 11). *From stress to success: how actinobacteria exploit life witout a cell wall*. Retrieved from https://hdl.handle.net/1887/4197402

Version:	Publisher's Version
License:	Licence agreement concerning inclusion of doctoral thesis in the Institutional Repository of the University of Leiden
Downloaded from:	https://hdl.handle.net/1887/4197402

Note: To cite this publication please use the final published version (if applicable).

From stress to success: how actinobacteria exploit life without a cell wall

Véronique Margriet Antoinette Ongenae

From stress to success: how actinobacteria exploit life without a cell wall

ISBN: 978-94-6506-967-8

Printing of this thesis was financially supported by the Netherlands Society of Medica Microbiology (NVMM) and the Royal Netherlands Society for Microbiology (KNVM).

The studies in this thesis were financially supported by VICI grant no. VI.C.192.002.

Cover design: Niki Savelkoel and Véronique Ongenae
Layout: Véronique Ongenae
Printing: Ridderprint, ridderprint.nl

Copyright © 2025, Véronique Ongenae

From stress to success: how actinobacteria exploit life without a cell wall

Proefschrift

ter verkrijging van
de graad van doctor aan de Universiteit Leiden,
op gezag van rector magnificus prof.dr.ir. H. Bijl,
volgens besluit van het college voor promoties
te verdedigen op dinsdag 11 maart 2025
klokke 14:30 uur

door

Véronique Margriet Antoinette Ongenae

Geboren te Enschede, Nederland
In 1996

Promotores:
Prof. dr. D. Claessen
Prof. dr. A. Briegel

Promotiecommissie:
Prof. dr. A. H. Meijer
Prof. dr. H. P. Spaink
Prof. dr. F. Barona Gomez
Prof. dr. J. Frunzke (Forschungszentrum, Jülick, Gemany)
Prof. dr. S.J.J. Brouns (University of Delft)

Contents

Chapter 1.	General introduction	7
Chapter 2.	Cell wall-deficiency as an escape mechanism from phage infection	13
Chapter 3.	Genome sequencing and characterization of *Streptomyces* phage Pablito, representing a new species within the genus *Janusvirus*	27
Chapter 4.	Genome sequencing and characterization of *Streptomyces* phage Vanseggelen and Verabelle, representing two new species within the genus *Camvirus*	41
Chapter 5.	Reversible bacteriophage resistance by shedding the bacterial cell wall	61
Chapter 6.	YidC2 is required for insertion of the holin-endolysin system during phage infection in *Streptomyces coelicolor*	89
Chapter 7.	Summary and general discussion	119
Nederlandse samenvatting		127
References		135
Curriculum vitae		157
Publications		158

Chapter 1

General introduction

Streptomyces are soil-borne multicellular bacteria, well-known for their ability to produce many clinically important antibiotics, like neomycin, streptomycin and many more [1-3]. Compared to most bacterial model species, Streptomycetes have a rather unique lifecycle, which starts from spores. If spores encounter a favorable and nutrient-rich environment, typically one or two germ tubes are formed at the distal end of each spore. These tubes form filaments, or hyphae, that grow by tip extension. Subsequently, the growing hyphae branch, leading to the formation of a vegetative mycelium that degrades organic material in the soil [4]. The vegetative hyphae contain semi-permeable cross-walls and are multinucleated [5]. When nutrients are exhausted, differentiation is initiated, leading to the formation of hydrophobic aerial hyphae that grow out of the substrate and which subsequently develop into long spore chains. These spores possess a thick cell wall, which makes them resilient to harsh conditions. Following dispersal to more favorable environments, the spores can reinitiate this lifecycle.

In their natural environment, *Streptomyces* are exposed to numerous stressors in their environment, such as heat stress, changes in acidity of the soil, competetive bacteria and bacteriophages [6-9]. The bacterial cell wall is a shape-defining and stress-bearing structure that can protect bacteria against exposure to most of these stresses. This wall is either a single layer of peptidoglycan between an inner and an outer membrane in diderm bacteria, or a thick peptidoglycan layer outside the cytoplasmic membrane in monoderm bacteria, such as *Streptomyces* [10].

Counterintuitively, *Streptomyces* can transiently lose their cell wall under hyperosmotic growth conditions or during antibiotic treatment, resulting in the formation of so-called cell wall-deficient (CWD) cells [11, 12]. These spherical cells are able to survive in an osmoprotective environment and can revert to the mycelial mode-of-growth when the stressors are no longer present. However, little was known about the relevance of these cells in nature [10].

Bacteriophages, or in short phages, recognize their hosts by binding to receptor proteins located on, or attached to, the cell wall of bacteria. Therefore, we hypothesized that the shedding of the cell wall may also protect the cells from phage infection. In this case, the phages might be unable to recognize their host when the cell wall and its associated receptor

proteins are absent. Since most research has been done on phage-host pairs in non-osmoprotective media and with unicellular model bacteria, like *Escherichia coli* and *Bacillus subtilis* [13, 14], the unique lifecycle of *Streptomyces,* requires another perspective on phage infection dynamics (Fig. 1).

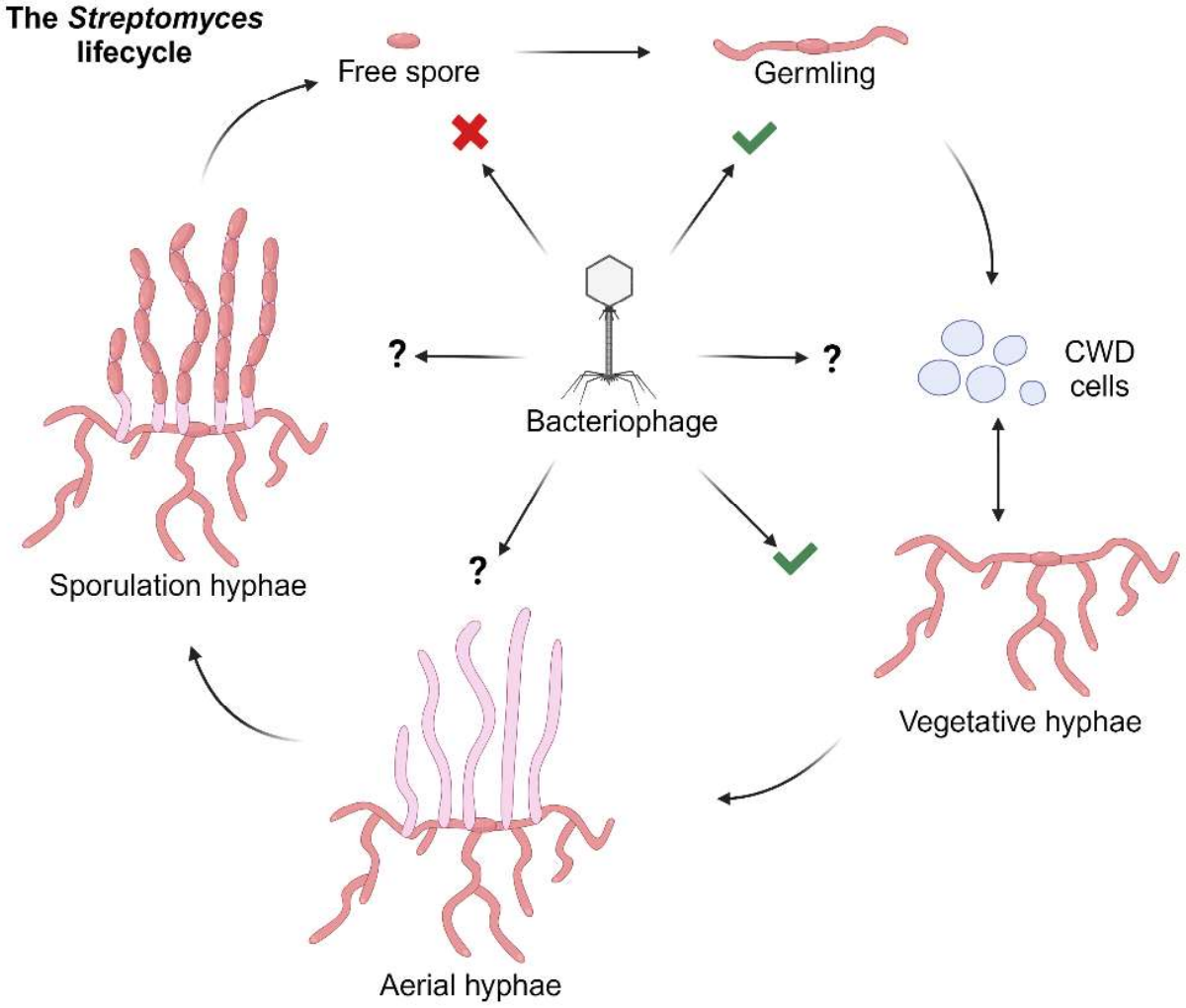

Figure 1. Schematic representation of phage infection in the *Streptomyces* lifecycle. The *Streptomyces* lifecycle starts as a free spore, which in turn grows into a germling. These germlings form a network of mycelium with vegetative hyphae, which under osmoprotective stress can form cell wall-deficient cells. Phages cannot infect the dormant spores and prefer young germlings and vegetative hyphae. After nutrient depletion, aerial hyphae are formed, which produce spores. It is unknown whether phages can attach and infect aerial hyphae, sporulation hyphae and CWD cells.

In general, little is known about the interaction of phages with *Streptomyces* bacteria during their different morphological states, from multicellular hyphae to cells after shedding their cell wall. So far, it has been shown that phage infection is optimal in young germlings and vegetative mycelium [15, 16]. Additionally, we know that phages cannot infect spores, probably due to their metabolic inactivity or different cell surface, and that the production of aerial hyphae can prevent spreading of phage infection [17]. However, the infection dynamics during the cell wall-deficiency stage remain largely unexplored.

The aim of this thesis is to study phage infection in *Streptomyces*, focused on cell wall-deficient cells. The results of this thesis contribute to a better understanding of phage infection dynamics in multicellular bacteria.

In **Chapter 2**, I review and discuss the hypothesis that bacteria can evade phage infection by shedding the cell wall. Phages recognize and attach to receptor proteins on, or attached to, the bacterial cell wall, like peptidoglycan and (lipo)teichoic acids in Gram-positive bacteria. Gram-negative bacteria on the other hand, have a wide range of structures on the outer membrane that phages can recognize, like lipopolysaccharides, transporter proteins and pores. However, some bacteria are known to shed their cell wall in response to environmental stressors. Without the protection of the cell wall, bacteria become spherical, only enclosed by a membrane and very fragile, but also lack most of the receptor proteins necessary for successful phage recognition.

Since little is known about the infection dynamics in multicellular bacteria, I sequenced and characterized three new bacteriophage species in **Chapter 3 and 4**. When compared to unicellular bacteria like *E. coli* or *Pseudomonas aeruginosa*, relatively few *Streptomyces* phages have been properly sequenced and characterized. Therefore, these phages increase our knowledge on the viral dark matter and are now called *Streptomyces* phage Pablito, belonging to the genus *Janusvirus,* and *Streptomyces* phage Vanseggelen and *Streptomyces* phage Verabelle that belong to the genus *Camvirus*. All three new phage species are used in future studies and their availability will contribute to expand the knowledge on phage-host dynamics in multicellular bacteria.

In **Chapter 5**, I show that phage infection converts the mycelium of most *Streptomyces* species into cell wall-deficient cells in osmoprotective medium, which we hypothesized in **Chapter 2**. *Streptomyces* spp. MBT86 was infected with *Streptomyces* phage Pablito and the presence of cell wall-deficient cells was quantified. The response to shed the cell wall was independent of the tested bacteriophage; several other phages could also induce this reaction. The wall-less cells were protected from phage infection and could revert to their canonical mycelial mode-of-growth, demonstrating that a significant fraction of the population survived the phage infection. To our surprise, not only strains MBT86, but all other tested *Streptomyces* strains could form cell wall-deficient cells after infection with a susceptible phage. Interestingly, we also found this behavior in the unicellular bacteria *E. coli* and *B. subtilis,* which was shown with fluorescent microscopy, phage growth curves and cryo-electron microscopy.

Since the mechanism behind shedding the cell wall in *Streptomyces* and the overall phage infection dynamics in multicellular bacteria remains largely unknown, we tested a knock-out library of 28 *Streptomyces coelicolor* cell wall mutants for their ability to be infected by our in-house phage collection. In **Chapter 6**, I describe the discovery of the role of the membrane insertase YidC2 in *S. coelicolor* during phage infection. With adsorption assays and cryo-electron microscopy, we discovered that phage CF3 could not lyse *S. coelicolor* Δ*yidC2* and the phages remained inside the infected bacterium, while the wildtype was killed. We showed that YidC2 plays an important role during the insertion of the holin-endolysin system from the phage inside the bacterial membrane, which subsequently leads to lysis of the infected bacteria.

The main findings of this thesis are summarized and discussed in **Chapter 7**. Here, I give my perspective for future directions in the research field of cell wall-deficiency associated with bacteriophages.

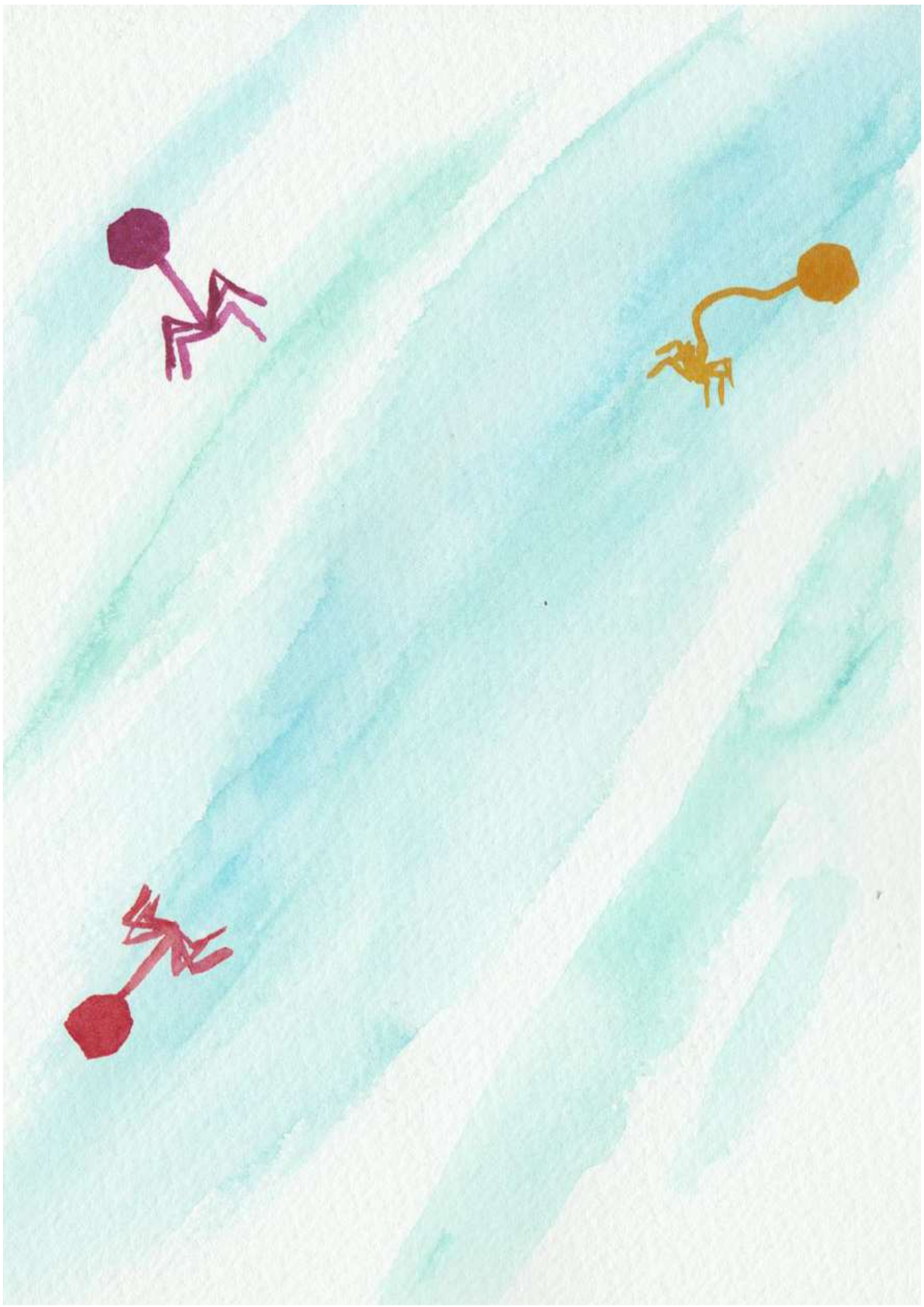

Chapter 2

Cell wall-deficiency as an escape mechanism from phage infection

Véronique Ongenae, Ariane Briegel and Dennis Claessen

This chapter was published as:

Ongenae, V., Briegel, A., & Claessen, D. (2021). Cell wall-deficiency as an escape mechanism from phage infection. *Open biology*, *11*(9), 210199.

Abstract

The cell wall plays a central role in protecting bacteria from some environmental stresses, but not against all. In fact, in some cases, an elaborate cell envelope may even render the cell more vulnerable. For example, it contains molecules or complexes that bacteriophages recognize as the first step of host invasion, such as proteins and sugars, or cell appendages such as pili or flagella. In order to counteract phages, bacteria have evolved multiple escape mechanisms, such as restriction-modification, abortive infection, CRISPR/Cas systems or phage inhibitors. In this perspective review, we present the hypothesis that bacteria may have additional means to escape phage attack. Some bacteria are known to be able to shed their cell wall in response to environmental stresses, yielding cells that transiently lack a cell wall. In this wall-less state, the bacteria may be temporarily protected against phages, since they lack the essential entities that are necessary for phage binding and infection. Given that cell wall-deficiency can be triggered by clinically administered antibiotics, phage escape could be an unwanted consequence that limits the use of phage therapy for treating stubborn infections.

Introduction

Bacteriophages, or (in short) phages, are viruses that infect bacteria. It has been estimated that they outnumber bacteria in the biosphere by a factor of 10 and are present in almost all natural environments [18, 19]. As phages are non-motile microorganisms, it is presumed that the initial contact between a phage and a suitable host occurs via random collisions as a result of free diffusion [20]. Phages recognize their host species by interacting with specific receptors, especially sugars and proteins, exposed on the bacterial cell surface. Here, we propose that the ability of bacteria to shed their wall may be an underappreciated mechanism to evade phage infection, as phages may no longer be able to recognize their host.

In this perspective review, we will start with discussing the detailed structure of the bacterial cell envelope and its specific components that enable phage attachment to their hosts. Currently, all known mechanisms for this first step of host infection involve bacterial surface-associated macromolecules. We then discuss the ability of several bacteria to shed their cell wall under influence of stressors and the consequences of a cell wall-deficient (CWD) lifestyle. Finally, we will discuss how phage infection may be evaded by shedding of the cell wall. We hypothesize that phages will no longer be able to recognize their bacterial host and render such wall-less cells immune to phage infection. Since cell wall-less states have been reported to occur in pathogenic species [21, 22], this evasion mechanism may be highly relevant for the development of phage therapy treatments.

Phage–host attachment

Bacteriophages used to be classified according to morphological types, while more recently, sequence similarity and phylogenetic relationships have become the primary method to distinguish taxa [23, 24]. The majority of phages contain double-stranded DNA in their capsid heads, although single-stranded DNA, single-stranded RNA and even double-stranded RNA are also common in nature [25-27]. Approximately 96% of all known phages are tailed phages (Fig. 1) belonging to the order *Caudovirales*, which can vary

tremendously in size, structure and DNA content. This order can be sub-divided into three families, based on the contractility of the tail, whereby phages with non-contractile tails can be divided into those with short and long tails [23, 28]. The best-studied organism in this order is the bacteriophage T4. This *Myoviridae* is well studied by cryo-electron microscopy, and detailed information on the structure and infection process of its host *Escherichia coli* are available [29-31].

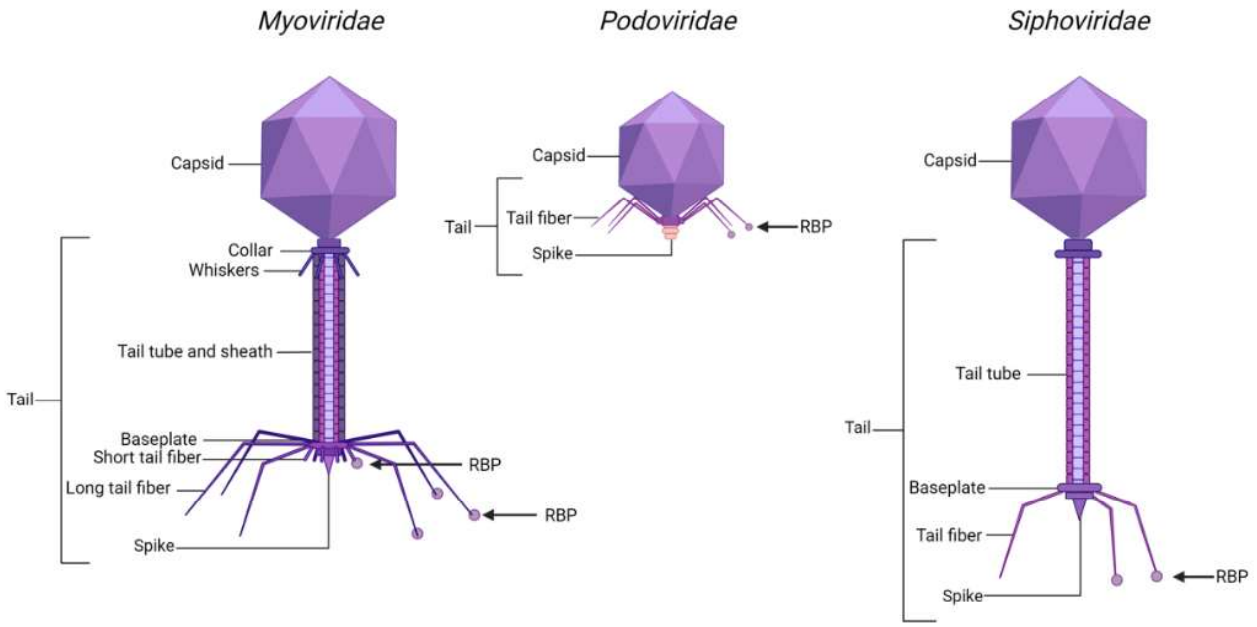

Figure 1. Tailed bacteriophages. The *Caudovirales* order consist of three families: (a) *Myoviridae*, with a contractile tail, (b) *Podoviridae*, which have no baseplate and are short-tailed and (c) *Siphoviridae* with a long non-contractile tail. Receptor binding proteins (RBPs) can be found on long- or short-tail fibres and sometimes even on the spike. Created with BioRender.com.

Although phages come in various shapes and sizes, one common feature is the need to identify and attach to a suitable host. The receptor-binding proteins (RBPs), often located at the tip of the phage's tail, recognize surface-associated molecules on a host bacterium. The nature of the bacterial molecules recognized by phages differs between various taxonomic groups and is commonly highly specific for the host cell wall or cell envelope composition. A major component of the bacterial cell wall is peptidoglycan, which is often associated with phage adsorption in monoderms (formerly

called Gram-positive bacteria) [32]. Peptidoglycan strands are composed of chains of monomers consisting of N-acetylglucosamine and N-acetylmuramic acid, which are covalently cross-linked via peptide stems to create a gigantic molecule, called the sacculus [33]. Besides peptidoglycan, other macromolecules can be found in the cell wall of monoderm bacteria (Fig. 2a), such as teichoic acids, which are also known to be involved in phage adsorption [34]. In fact, over 96% of the molecules identified on monoderm bacteria so far are associated with either residues or structures of teichoic acid and peptidoglycan [35]. Diderm (Gram-negative) bacteria on the other hand display a large variety of molecules, as seen in Figure 2b [29]. Molecules that can be recognized by phages are for instance, enzymes, transporter proteins, substrate receptors and many more structures located on the outer membrane [36]. Multiple studies have used the model organism *E. coli* and more recently also *Salmonella* to identify new molecules that are necessary for phage infection in diderm bacteria, such as the important proteins OmpA, OmpC, OmpF and LamB, but also many lipopolysaccharides [37-41].

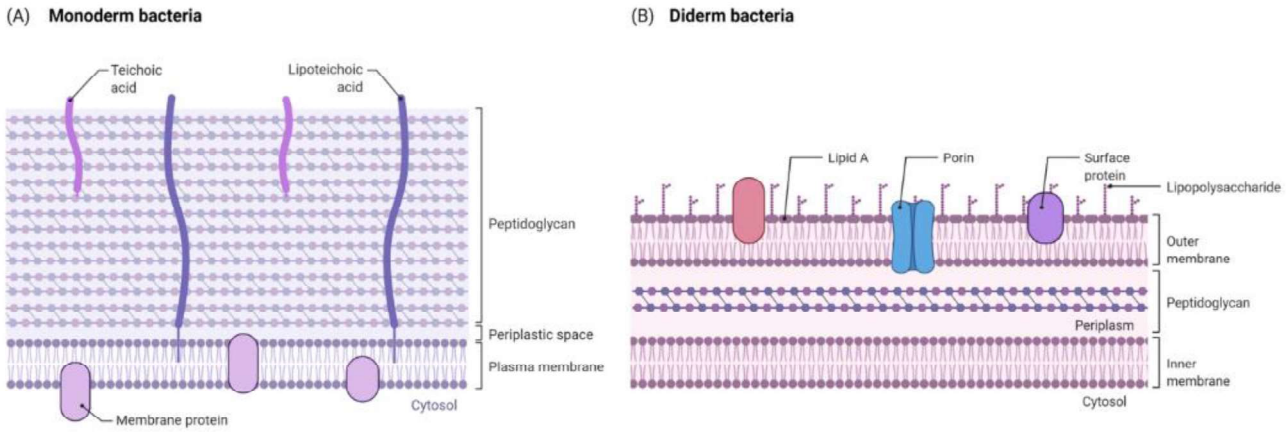

Figure 2. Bacterial cell wall. (a) The cell wall of monoderm bacteria consists of a thick peptidoglycan layer intertwined with teichoic acid, which can both be recognized by RBPs of phages. (b) Diderm bacteria have a thinner peptidoglycan layer and an additional outer membrane with several components that phages can recognize for attachment. Created with BioRender.com.

In addition to receptors molecules, proteins and lipopolysaccharides, some phages can also attach to structures that are not located directly on the cell

wall or outer membrane of bacteria, such as flagella, pili and capsules. The adhesion of phages to a flagellum often starts as a process that initially is reversible. However, the rotating movement of the flagellum guides the phages towards the cell body, where it then tightly attaches to surface molecules located near the base of the flagellum [35, 42]. In addition, some phages can 'hitchhike' on non-host bacterial flagella to increase their chances of meeting a host species. This has been shown for the bacteriophage PHH01 that can attach to the flagella of the carrier bacteria *Bacillus cereus* to help encounter its host *E. coli* [43]. Another recent example is the transport of *E. coli* lambda phage by *Capnocytophaga gingivalis* swarm [44]. Phages can also attach to extracellular structures such as pili or fimbriae, which are proteins that help bacteria to attach to each other or surfaces. For phages ϕCb13 and ϕCbK, it has been shown that the initial attachment to pili is necessary for successful attachment to *Caulobacter crescentus*, as mutant bacteria without pili could not be infected [42]. These studies demonstrate that loosing structures like pili or flagella is an effective defense mechanism from bacteria to evade phage attachment. It further suggests that the loss of the entire cell wall may be an additional effective mechanism for phage evasion.

Bacterial defense mechanisms against phages

To prevent phage infection, bacteria have developed multiple and impressive anti-phage strategies. Restriction-modification systems act as the prokaryotic innate immune system, consisting of a restriction nuclease and methyltransferase. Bacteria prevent self-cleavage by methylation of their own DNA, while incoming phage DNA is generally not methylated [45]. A more costly defense system is called the abortive infection process, where the infected cell initiates programmed cell death before the phage can replicate, thereby protecting other cells in the bacterial colony [46]. The toxin-antitoxin system can be seen as one of the components of abortive infection and consists of a toxin that inhibits bacterial cell growth upon phage infection and an antitoxin, which protects the cell during normal conditions [47]. The phage growth limitation (Pgl) system is often described as an inverted restriction-modification system or abortive infection-like mechanism, where the primary

infected bacteria do not survive the infection, but mark the progeny phage DNA by methylation [48, 49]. If such modified phages subsequently infect neighbouring Pgl+ bacteria, the phage is restricted. Although Pgl systems are only found in Actinomycetes, a comparable mechanism, called the BacteRiophage EXclusion (BREX) system was discovered in *Bacillus cereus* [50]. This system possesses two genes that are homologous to the Pgl system. However, unlike Pgl, the BREX system prevents initial phage replication by methylation [48]. In addition to protein-mediated anti-phage defenses, some *Streptomyces* species can use a chemical defense mechanism. Here, small molecules are produced that serve as phage inhibitors [51]. The only known adaptive immune system in prokaryotes is the CRISPR/Cas defense mechanism, which protects against phages and other foreign genetic elements, like plasmids and transposons [52]. Recently, a new counter-defense mechanism against CRISPR/Cas has been uncovered, where phage T4 restores the broken genomic material, thereby making progeny phages resistant against future CRISPR attacks [53]. For those interested in more detailed information on anti-phage systems and the phage-bacteria arms race, we refer to some excellent recent reviews [49, 52, 54, 55].

Bearing anti-phage systems is associated with a trade-off between fitness costs and the benefit of resisting phages [56]. As bacteria typically only carry a small subset of the available defense mechanisms, the 'pan-immune system' was recently proposed [54]. Here, the authors suggest that although a single bacterial strain cannot carry all existing defense mechanisms, it can use horizontal gene transfer to access defense mechanisms encoded by closely related species.

However, the bacterial cell wall remains the first barrier a phage needs to overcome during host infection. The prime defense of bacteria is therefore directed at the initial prevention of phage attachment to the bacterial surface-associated macromolecules. When bacteria are living in a biofilm, this mode of growth already acts as the first layer of protection. Amyloid fibre networks inhibit phage transport into the biofilm and also coat the surface of individual cells to prevent phage attachment [57]. Another defense strategy used by the diderm bacterium *Vibrio cholerae* is the production of outer membrane

vesicles with an almost identical cell surface as the bacteria itself, to serve as natural decoys against phages [58].

Other common mechanisms to prevent phage attachment are shielding surface-associated molecules by glycosylation, masking them with polysaccharide capsules or mutating the molecules on the bacterial cell surface [59-61]. If phages cannot recognize and attach to the molecules on the cell surface of bacteria, the host will remain uninfected. However, the production of a capsule or adaptation of receptor molecules can be metabolically expensive [62]. Therefore, a possible energetically more favourable way to escape phage binding would be by shedding the cell wall altogether. In this case, not only the molecules located on the bacterial cell surface will vanish, but also structures like the capsule, flagella and pili are no longer present.

Cell wall-deficiency as a possible mechanism to escape phage attack

Some filamentous actinobacteria have the ability to shed their cell wall under influences of hyperosmotic stress or limited oxygen availability, which may be common in soil ecosystems [63]. Under these conditions, CWD cells are extruded from the vegetative mycelia. These cells are unable to proliferate without their wall and will ultimately revert to the mycelial mode of growth [10]. However, if these CWD cells acquire mutations due to prolonged exposure to hyperosmotic stress conditions, L-forms are formed that can proliferate without a cell wall [11, 64]. To start a CWD lifestyle, cells first have to escape the sacculus, followed by coping with the increased oxidative stresses in the environment [10]. Thereafter, an upregulation of membrane synthesis is required, resulting in an enlarged surface area to volume ratio [65]. Not only filamentous actinobacteria, but many other bacteria, including both monoderm and diderm species, are able to switch to a CWD state. CWD cells of different species have been found in the urine of patients suffering from recurrent urinary tract infection [66]. Additionally, such CWD cells have been detected in the biofilms of individuals with chronic and aggressive periodontitis [22]. These studies support the assumption that CWD bacteria could hide inside

their host for an extended amount of time, as they are insensitive to wall-targeting antibiotics and can possibly also evade elements of the host's immune system. In fact, exposure to cell wall-targeting antibiotics could even promote the formation of CWD cells. This response is best studied for β-lactam antibiotics like penicillin, which targets the catalytic enzymes involved in cell wall synthesis, resulting in lysis of the bacterial cell wall of for instance *E. coli* [67]. Prolonged exposure to these antibiotics can be used to induce cell wall-deficiency in an osmotically stable environment [67]. While cells without their wall are inherently fragile, wall-deficiency probably provides bacteria with some crucial advantages over walled bacteria. In their natural environment, bacteria are challenged by various stresses, such as changing environmental conditions, competing organisms and the possibility of phage attack. The formation of CWD cells has been observed as a response to escape various environmental stresses [10]. For example in *Mycobacterium bovis*, where L-forms were isolated after nutrient starvation and cryogenic stress treatments [68] or in *E. coli*, which could survive lethal treatments like autoclaving and boiling by shedding their cell wall [69]. This indicates that cell wall-deficiency could be a temporary coping strategy to protect the bacteria during unfavourable environmental conditions, like the possibility of phage infection.

As the vast majority of molecules phages can attach to, are located in or associated with the cell wall, transient loss of the wall could render bacteria immune for phage binding and infection (Fig. 3). In monoderm CWD cells, the shedding of the wall would result in the loss of almost all known molecules a phage can recognize, as these are almost invariably associated with peptidoglycan and teichoic acids in the cell wall. The formation of diderm CWD cells is less well understood. For example, it remains debatable whether diderm bacteria that can form CWD cells retain their outer membrane, which contains the majority of the known molecules that phages recognize. Literature of CWD diderms with and without their outer membrane have been reported, and even thin-section electron microscopy cannot clearly distinguish between a single membrane and two membranes if the periplasm is pressed closely together [70, 71]. On the other hand, more recent papers have shown that a rigid outer membrane is essential for the formation and survival of wall-

deficient cells in *E. coli* [72, 73]. Here, the outer membrane proteins Lpp, OmpA and Pal are necessary for this rigidity. These and many more outer membrane proteins could also serve as molecules for phage attachment and, perhaps in this manner, serve as a sink for phages. In this way, such CWD cells could help to protect the other cells in the colony similar to the previously described decoy outer membrane vesicles of *V. cholera* [58]. Additionally, when bacteria shift to a CWD lifestyle, small fragments of the original cell wall probably remain in close proximity of the newly formed CWD cells for some time. It may be that these small cell wall particles can also serve as a decoy for phages, just like outer membrane vesicles [58]. Building upon the theory that cell wall-deficiency could be an escape mechanism for phage attack, the holin-endolysin system might also play an important role. Lytic phages use endolysins to degrade the peptidoglycan layer from inside a bacterium, which have a similar outcome as penicillin treatment. We know that penicillin is often used to induce cell wall-deficiency, so possibly the holin-endolysin enzymes could be a cue for other nearby bacteria to shed their cell wall and therefore be protected from the released phages.

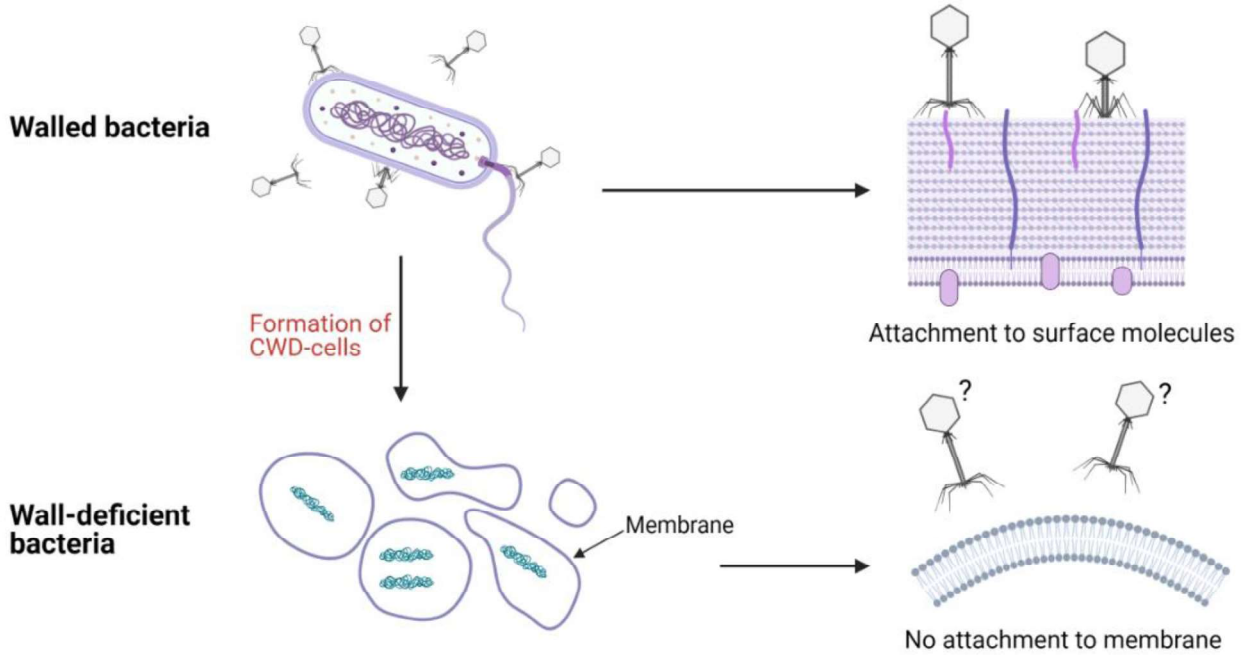

Figure 3. Cell wall-deficiency as an escape mechanism for phage infection. Walled bacteria are susceptible to phage infection, since phages can recognize molecules located on the cell surface or bind to structures such as pili and flagella. Several bacteria can shed their wall and form wall-deficient cells. We hypothesize that phages can no longer recognize its host in this wall-deficient state, which therefore stays uninfected. Created with BioRender.com.

Wall-deficient cells of Actinomycetes that revert back to filamentous growth often show a wide range of phenotypically different colonies, which can be explained by gross genetic changes [11, 74]. Such mutations can sometimes lead to the evolution of beneficial traits, such as phage-resistance [75]. Many phages can infect members of the bacterial Actinobacteria phylum and for most bacteria, even multiple phages are known [76]. There is rich literature on phages that can infect Actinobacteria but, to our knowledge, no phage is currently known to infect *Kitasatospora viridifaciens*, which easily makes CWD cells. In fact, one of the features by which *Kitasatospora* species are classified in their unique genus is their resistance to the most common *Streptomyces* phages [77, 78]. Perhaps *K. viridifaciens* has accumulated a specific set of mutations during many switches of CWD cells to the mycelial mode of growth in nature, resulting in broad resistance against most common *Streptomyces* phages. Nevertheless, this resistance to phages can also be explained by our hypothesis that the formation of wall-deficient cells is an escape mechanism by itself, although both possibilities are not mutually exclusive. On the other hand, switching to a wall-less state may not only be beneficial for the bacteria, but also for the bacteriophage. A recent study demonstrated that T4-like phages could be adsorbed by *E. coli* L-forms, which however did not result in lysis of these CWD bacteria [79]. These results imply that cell wall-deficiency could not only be an escape mechanism for the bacterial host, but the phage may also profit from this situation, as they could switch to a pseudolysogenic lifestyle within CWD cells. Taken together, these examples demonstrate the advantages of switching to a CWD lifestyle during the possibility of phage attack.

Concluding remarks and outlook

Our knowledge about the biology of bacteriophages and their bacterial host have increased significantly over the last few decades. However, the understanding of CWD cells and their ecological role in association with phages is largely unexplored territory. The hypothesis that cell wall-deficiency could be a new and underexplored mechanism for phage evasion raises several interesting research options. The most interesting one would be to investigate if phages indeed cannot recognize their usual host and whether this is due to the absence of molecules in the cell wall. On the other hand, if phages are still able to recognize their host without a cell wall, to which molecule(s) do they attach and can they eject their genome?

Perhaps CWD cells are currently one step ahead in the ongoing evolutionary arms race between phages and their host. If we assume this to be true, would there already be a sign of coevolution between the phage's RPBs and the CWD surface-associated molecules? Most research about CWD bacteria, such as mycoplasma, protoplasts and L-forms, and their interaction with phages, date from the pre-molecular era [80-82]. It would be interesting to explore their interaction with more modern technologies, such as cryo-EM, next-generation sequencing or genome editing. Apart from exploring possible phage–host interactions and defense mechanisms in CWD bacteria, improving our understanding on bacterial and phage biology may provide biotechnological advances in, for example, phage therapy. In this case, specific phages are used as an alternative for antibiotics to treat bacterial infections [83]. Phage therapy therefore seems like a suitable strategy to treat recurrent infections and chronic diseases caused by CWD bacteria, as they are insensitive to wall-targeting antibiotics and phages can selectively kill pathogenic bacteria without harming the host or its microbiome. However, the use of bacteriophages for treating stubborn infection might be restricted if phages do not recognize wall-deficient pathogenic bacteria. In addition, clinically administered antibiotics can trigger the formation of CWD cells, which could be an unwanted consequence that limits the use of bacteriophage treatment afterwards. If phages are unable to recognize the CWD bacteria, a mixture of different phages should be considered for phage

therapy or the genomes of bacteriophages could be genetically modified [84, 85]. Further studies should continue to contribute valuable insights on phage infections of CWD cells and phage therapy.

Chapter 3

Genome sequencing and characterization of *Streptomyces* phage Pablito, representing a new species within the genus *Janusvirus*

Véronique Ongenae, Joana Azeredo, Andrew M. Kropinski, Daniël Rozen, Ariane Briegel and Dennis Claessen

This chapter was published as:

Ongenae, V., Azeredo, J., Kropinski, A. M., Rozen, D., Briegel, A., & Claessen, D. (2022). Genome sequence and characterization of Streptomyces phage Pablito, representing a new species within the genus Janusvirus. *Scientific Reports*, *12*(1), 17785.

Abstract

Streptomycetes are ubiquitous soil bacteria. Here we report the complete and annotated genome sequence and characterization of *Streptomyces* phage Pablito, isolated from a soil sample in Haarlem, the Netherlands using *Streptomyces lividans* as host. This phage was able to infect a diverse range of *Streptomyces* strains, but none belonging to the sister genus *Kitasatospora*. Phage Pablito has double-stranded DNA with a genome length of 49,581 base pairs encoding 76 putative proteins, of which 26 could be predicted. The presence of a serine integrase protein indicated the lysogenic nature of phage Pablito. The phage remained stable over a wide range of temperatures (25-45 °C) and at pH ≥ 7.0, but lost infectivity at temperatures above 55 °C or when the pH dropped below 6.0. This newly isolated phage is closely related to *Streptomyces* phage Janus and Hank144 and considered a new species classified in the genus *Janusvirus*, within the subfamily *Arquattrovirinae*.

Introduction

Streptomyces spp. are Gram-positive, spore-forming bacteria that thrive in almost all soil environments. They are well-known for their ability to produce a wide array of clinically-relevant antibiotics, such as streptomycin, neomycin, chloramphenicol and many more [86-88]. Most research has been focused on the industrial use of these bacteria and their secretion of secondary metabolites [89, 90]. However, it remains largely unknown how bacteriophages can recognize, attach and infect these multicellular bacteria. *Streptomyces* have an unusual lifecycle, which starts when spores encounter a favorable environment. This triggers germination and outgrowth into a so-called vegetative mycelium. After a period of vegetative growth, aerial hyphae are formed that can develop into chains of spores. These spores can be dispersed to more favorable environments to establish new colonies. Previous research has shown that *Streptomyces* phages can only infect young vegetative mycelia, but are unable to infect spores [15, 16]. However, most bacteriophage research has been focused on unicellular bacteria, while the interactions and underlying mechanisms of bacteriophages infecting multicellular bacteria, like *Streptomyces,* remains largely unexplored. Besides the phage growth limitation system [91, 92] , chemical defense [51] and recently discovered cell wall-deficiency [93], many more defense mechanisms against phage attack might be present in *Streptomyces*.

In addition, relatively few *Streptomyces* phages have been properly sequenced and characterized in comparison to other genera. Therefore, it is important to isolate new phages infecting multicellular bacterial species, allowing us to expand our knowledge about the immense viral diversity.

In this paper, we describe a newly discovered Actinobacteriophage, called *Streptomyces* phage Pablito, which was isolated from a soil sample in the Netherlands. This phage belongs to the genus *Janusvirus*, within the subfamily *Arquattrovirinae*. Phage Pablito is a temperate phage with an icosahedral capsid head of 56.1 ± 1.3 nm and a long non-contractile tail of 163.5 ± 0.4 nm. Finally, we provide a whole genome analysis of this newly

identified phage. Together, these results shed light on phage taxonomy and can expand the knowledge on phage-*Streptomyces* interactions in the future.

Material and methods

Bacteriophage isolation

Phage Pablito was isolated from a soil sample obtained from the National Park Zuid-Kennemerland in the Netherlands (N52°23′31″, E4°34′49″). To this end, 0.5 g soil was mixed with spores from the host *S. lividans* strain 1326 in 10 ml Difco Nutrient Broth (DNB) (BD Biosciences) supplemented with 0.5% glucose and 4 mM $Ca(NO_3)_2$ and incubated overnight at 30 °C, while shaking at 130 RPM. After 24 h, the culture was centrifuged for 10 min at 4000 g and the supernatant containing phages was filtered through a 0.22 µm filter (Millipore). The supernatant was subsequently spread onto a DNB agar plate, followed by applying an overlay (in DNB soft agar) containing 10^3 spores ml^{-1} from *S. lividans*. The plate was incubated at 30 °C for 24-48 h before plaque formation was assessed. Single plaques were purified by streaking them twice to a fresh double agar overlay plate containing the bacterial host. High titre single viral stocks were obtained by picking purified plaques and incubating them with *S. lividans* in DNB medium for 10 min before plating on double-agar overlay DNB plates. Viral lysates were collected by flooding the plate with 24 ml DNB and gently rocking the plate for 2 h. The supernatant was filtered through a 0.22 µm filter. Collected phages were stored at 4 °C.

Host range analysis

The host range of phage Pablito was determined using serial dilutions on double agar overlay plates. In short, 3 µl of the phage dilution was spotted in duplicate on a bacterial lawn of different *Streptomyces* and *Kitasatospora* strains from the Microbial biotechnology (MBT) collection at Leiden University [94], which represents an in-house collection of isolated actinomycetes. The plates were incubated at 30 °C for at least 24 h before lysis was observed. The presence of a lysis zone was scored as a positive result. The efficiency of plating (EOP) for a given strain was calculated relative to the host strain *S. lividans* when plaques were observed.

Stability of phage Pablito

A one step-growth curve analysis was performed in triplicate to calculate the latent period and phage burst size [95]. In short, 10^5 spores ml^{-1} of *S. lividans* were allowed to germinate in 10 ml DNB medium at 30 °C for 5 h. At T = 0, the culture was infected with phage Pablito at Multiplicity of Infection (MOI) = 0.01 and 100 µl was sampled at 10 min intervals up to 180 min. The samples were filtered, diluted and immediately plated on double agar plates. Burst size was calculated using the following formula:

$$\text{Burst size} = \frac{(\text{total phages after burst (T = 80 and T = 90)} \,/\, \text{total phages before burst (T = 0 to T = 70)}}{\text{number of phages at T = 0}}$$

The thermal stability of phage Pablito was determined by incubating 1 ml of lysate (10^6 PFU ml^{-1}) at 25, 30, 37, 45, 55 and 65 °C. The samples were filtered after 1 h of incubation and immediately plated on double agar plate to determine the phage titre. For pH stability, 10 µl of a phage Pablito suspension (10^6 phages ml^{-1}) was added to 990 µl DNB medium adjusted to different pH values (2–9) using 6 M HCl or 1 M NaOH. The tubes were then incubated at 30 °C for 1 h before the samples were filtered through a 0.22 µm filter and plated using the double agar overlay method. All measurements were performed in triplicate.

DNA extraction and phylogenetic analysis

DNA of phage Pablito was isolated using the Phage DNA Isolation Kit from Norgen (Thorold, Canada) according to the manufacturers protocol. After isolation, multiple samples were pooled and DNA was concentrated using the Concentrator Plus (Eppendorf) for 20 min. Whole-genome sequencing and de novo assembly of phage Pablito was performed by BaseClear using Illumina NovaSeq PE150 sequencing with a mean coverage of 118.21 (Leiden, the Netherlands). The complete genome sequence of *Streptomyces* phage Pablito was deposited at GenBank under accession number OK412919. A linear map of the genome was constructed by Geneious Prime 2020.1.2 and PhageTerm was used to determine genome ends [96].

Phylogenetic analysis was performed using the putative protein sequence of the major capsid head protein. The protein sequences of *Streptomyces* phage Janus, Hank144, Pablito and Joe were acquired from NCBI and aligned using MUSCLE [97]. A Maximum Likelihood phylogenetic tree was constructed through Molecular Evolutionary Genetics Analysis Version X (MEGAX) using 100 bootstrap replicates to estimate the genus of Phage Pablito.

Electron microscopy

Two liquid cultures of *S. lividans* infected with phage Pablito were filtered, combined and precipitated overnight with 5 × PEG solution (20% PEG8000 in 2.5 M NaCl) at 4 °C and centrifuged for 70 min at 3500 g after which the supernatant was discarded. Of the remaining pellet, 3 µl was placed on a glow discharged 200 mesh carbon coated copper grid (EMS) and allowed to set for 30 s before excess sample solution was removed by filter paper. The phages were stained with 2% uranyl acetate for 45 s and air-dried for an additional 30 min. The grids were observed using a single tilt specimen holder inside a 120 kV Talos L120C TEM with a Lab6 electron source and Ceta detector at the Netherlands Center for Nanoscopy (NeCEN, Leiden).

Results

Morphology and host range determination of Pablito

Bacteriophage Pablito produced clear small plaques on the *S. lividans* host strain using the double agar overlay method (Fig. 1a). Transmission electron microscopy (TEM) was used to reveal the morphology of phage Pablito. This demonstrated that phage Pablito has an icosahedral capsid head of 56.1 ± 1.3 nm ($n = 3$) and a long non-contractile tail of 163.5 ± 0.4 ($n = 3$) (Fig. 1b). The long, flexible tail together with the icosahedral capsid head were the first indication that this phage is a siphovirus belonging to the class *Caudoviricites*, which was further confirmed by whole-genome sequencing (see below).

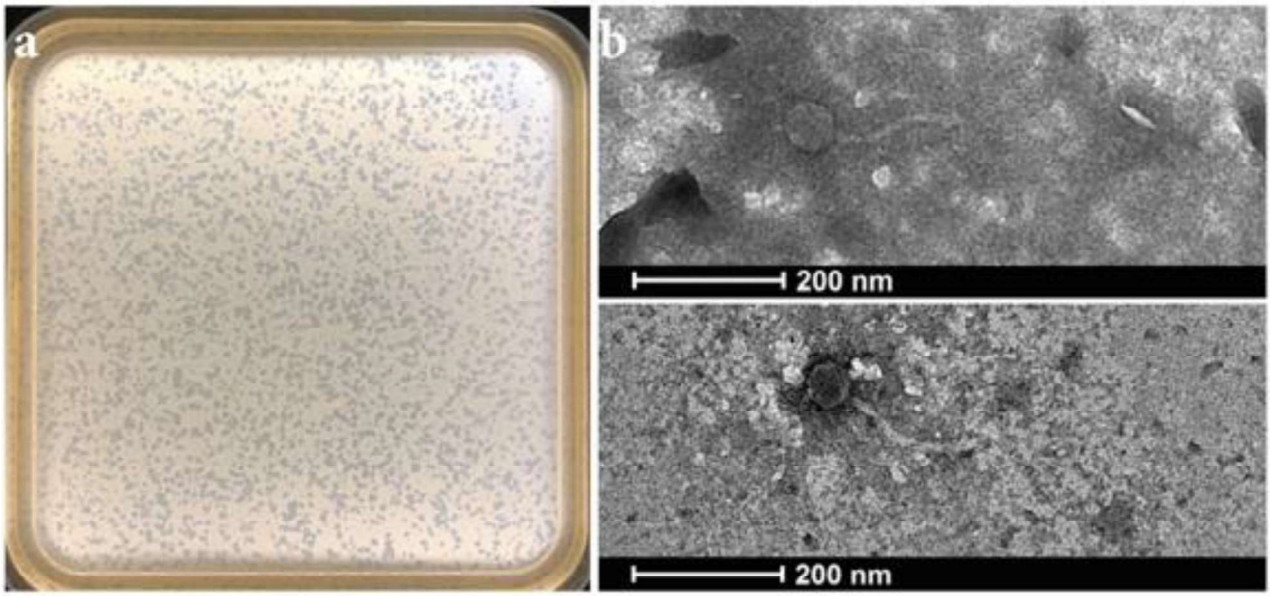

Figure 1. Morphology of phage Pablito. (**a**) Plaque morphology of phage Pablito after 24 h of infection in *S. lividans* using the DNB double agar overlay plate. (**b**) Representative TEM images of phage Pablito. Phage particles were stained with 2% uranyl acetate.

A host range assay on 10 actinomycetes revealed that all eight *Streptomyces* strains tested could be infected by phage Pablito (Table 1). Depending on the host strain, some lysis zones showed a turbid morphology, which is common for several *Streptomyces* phages [98], and was the first indication that phage Pablito might be a temperate phage. The EOP for a strain relative to the host strain *S. lividans* from which the phage was isolated, is given when plaques were countable. On the contrary, the two species that remained uninfected (i.e. MBT66 and *K. viridifaciens*) belong to the sister genus *Kitasatospora,* members of actinomycetes which are morphologically similar to *Streptomyces* but generally classified by their resistance against *Streptomyces* phages [77, 78].

Table 1. Susceptibility of actinomycete strains to infection by phage Pablito as determined by plaque assays.

Bacterial strain	Origin	Infectivity	Lysis zone morphology	EOP
Streptomyces lividans	MBT collection	+	Clear	1
Streptomyces coelicolor	MBT collection	+	Turbid	
Streptomyces griseus	MBT collection	+	Turbid	
Streptomyces venezuelae	MBT collection	+	Turbid	
Streptomyces albus	MBT collection	+	Clear	0.3
Kitasatospora virifidaciens	DSM40239	-	None	
MBT13	MBT collection	+	Turbid	
MBT61	MBT collection	+	Turbid	
MBT66	MBT collection	-	None	
MBT86	MBT collection	+	Clear	1.5

Genomic analysis

Whole genome sequencing and de novo assembly of phage Pablito revealed a double-stranded DNA genome of 49,581 base pairs. While its host *S. lividans* has relatively high G + C content of 72%, *Streptomyces* phage Pablito has a G + C content of 66.4% and a 3′-cohesive termini of CGCCGTGTCTT (Fig. 2). The genome contains 76 potential coding sequences (CDSs), of which 50 encode for hypothetical proteins, while the function of 26 CDSs could be predicted. The latter were categorized as morphogenesis proteins, nucleotide metabolism and DNA replication proteins, lysogenic module and a bacterial lysis protein as indicated in Figure 2.

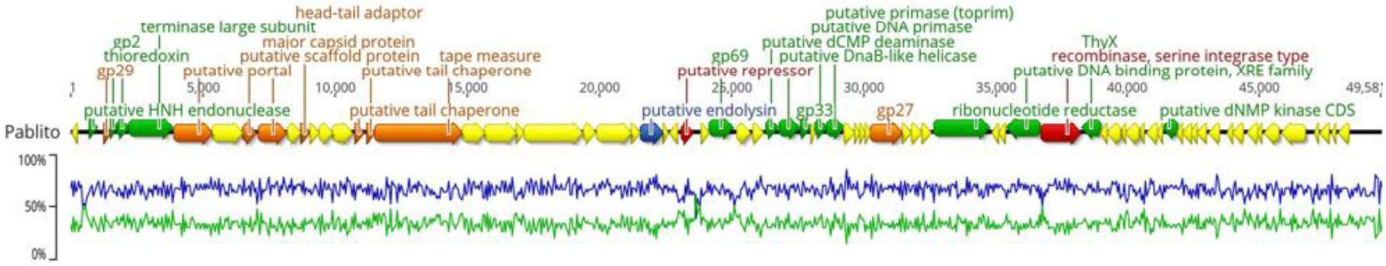

Figure 2. Schematic representation of the dsDNA genome of *Streptomyces* phage Pablito. Arrowheads are indicated in the direction of the CDS. Hypothetical proteins are displayed in yellow and the color code for predicted proteins is as follows: green for nucleotide metabolism and DNA replication, orange for morphogenesis, red for lysogeny and dark blue for bacterial lysis. The green line represents AT content, while the blue line represents GC content. The genome map was generated through Geneious Prime 2020 1.2.

Phylogenetic analysis (Fig. 3a) based on the putative major capsid head protein revealed that *Streptomyces* phage Pablito is similar to *Streptomyces* phage Janus and *Streptomyces* phage Hank144, while *Streptomyces* phage Joe is more distantly related. Based on the criteria from the Bacterial Viruses Subcommittee, 70% nucleotide identity is established as the cut-off for genera, while 95% identity assigns phages to the same species [99]. As calculated by the intergenomic distance calculator VIRIDIC [100], *Streptomyces* phage Pablito shows 70.0 and 72.5% relatedness to *Streptomyces* phages Janus and Hank144, respectively (Fig. 3b). Since the relatedness of *Streptomyces* phage Pablito is lower than 95%, this phage is considered a new species according to the International Committee on Taxonomy of Viruses (ICTV) [100]. Because *Streptomyces* phage Janus and *Streptomyces* phage Hank144 are both temperate phages and whole genome sequencing revealed the presence of a serine integrase protein in *Streptomyces* phage Pablito, we conclude that phage Pablito is a temperate phage as well [101]. Together, these data indicate that *Streptomyces* phage Pablito is a newly discovered species that can be included in the genus *Janusvirus*. A taxonomic proposal has been submitted to ICTV to officially recognize phage Pablito as part of the genus *Janusvirus* as a new species called "*Janusvirus Pablito*". The Actinobacteriophage Database (https://phagesdb.org/) places phage Pablito in Cluster BD, Subcluster BD2. In addition, phage Pablito is peripherally

related to two prophages found in *Streptomyces finlayi* strain NBSH44 and *Streptomyces venezuelae* strain ATCC 14583.

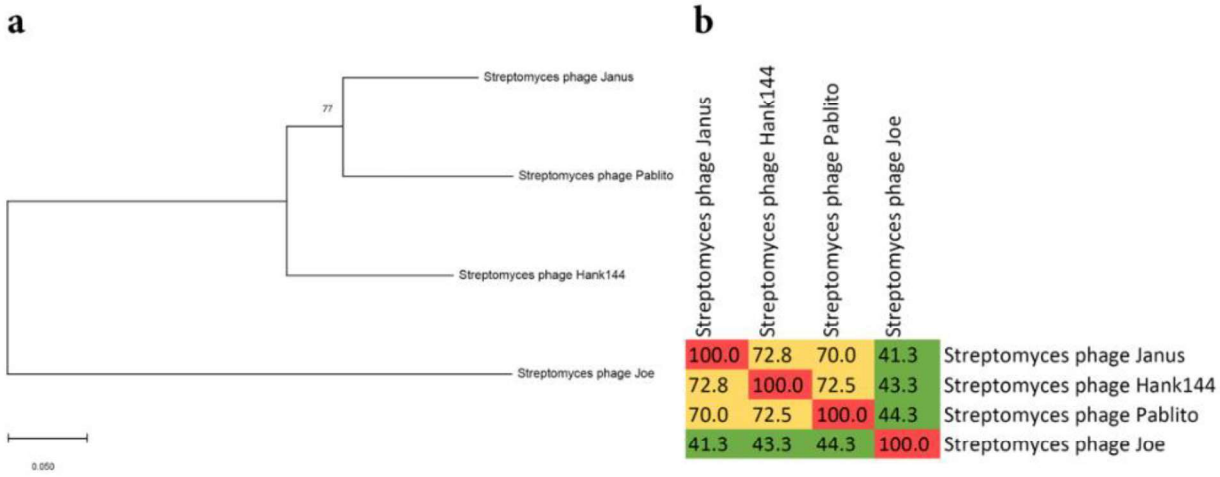

Figure 3. *Streptomyces* phage Pablito belongs to the subfamily *Arquattrovirinae*, genus *Janusvirus*. (**a**) Evolutionary history of phage Pablito based on the major capsid head protein. Total of 100 bootstraps replicates were used to calculate the Maximum-Likelihood tree in MEGA.X. (**b**) Heatmap calculated by VIRIDIC to show pairwise intergenomic distance/relatedness amongst phage genomes. Genomes of *Streptomyces* phage Janus (NC_054660.1) and *Streptomyces* phage Hank144 (NC_054661.1) were used to show relatedness, while the genome of *Streptomyces* phage Joe (NC_054674.1) was used as an outlier.

One-step growth curve

Streptomyces phage adsorption was found to be maximal for germlings [98]. We therefore incubated *S. lividans* spores first for 5 h in DNB medium before infecting the culture with bacteriophages. The one-step growth curve of phage Pablito showed a relatively long latent period of 80 min, with a burst size of 22 virions per cell (Fig. 4). However, another rise of viral titer was observed around 150 min, which can happen when multiple phages bind to one germinated spore, as a sign of delayed adsorption or as an indication of a lysogenic infection cycle [102]. The highest titre obtained was around 10^6 PFU ml^{-1} after 24 h. A different range of MOI, longer incubation periods and even flooding of a confluent plaque plate did not result in an increase of the total number of phages ml^{-1}.

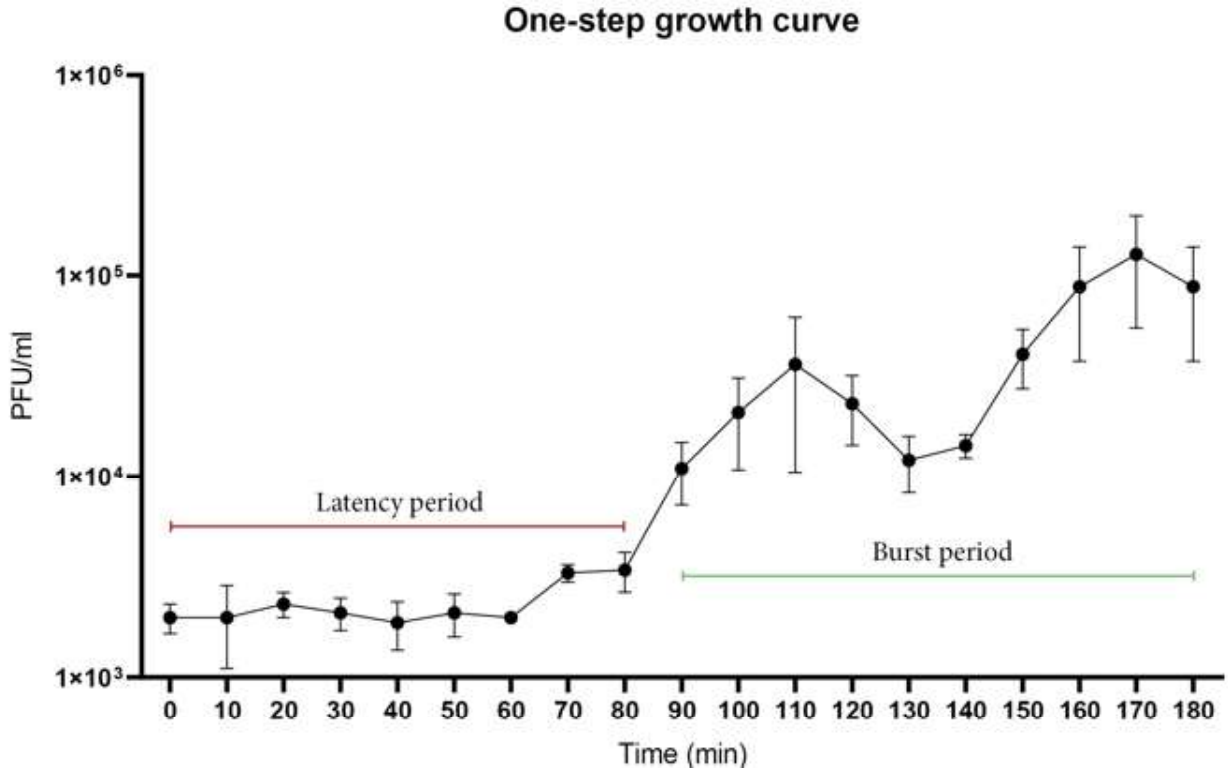

Figure 4. One-step growth curve. At MOI = 0.01, phage Pablito had a latent period of 80 min and a second burst at 150 min with a total burst size of 22 virions per cell.

Phage stability

We also assessed the effect of temperature and pH on phage viability. Phage Pablito was stable up to 45 °C without a reduction in viability (Fig. 5a). However, the infectivity significantly decreased when the phage was incubated for an hour at 55 °C or higher. Phage Pablito was relatively stable at pH 7.0–9.0, while infectivity steeply declined when the pH was lower than 6.0 (Fig. 5b). No plaques were found when the pH was below 4.0, while only a small amount of activity was retained at pH 5.0 and pH 6.0.

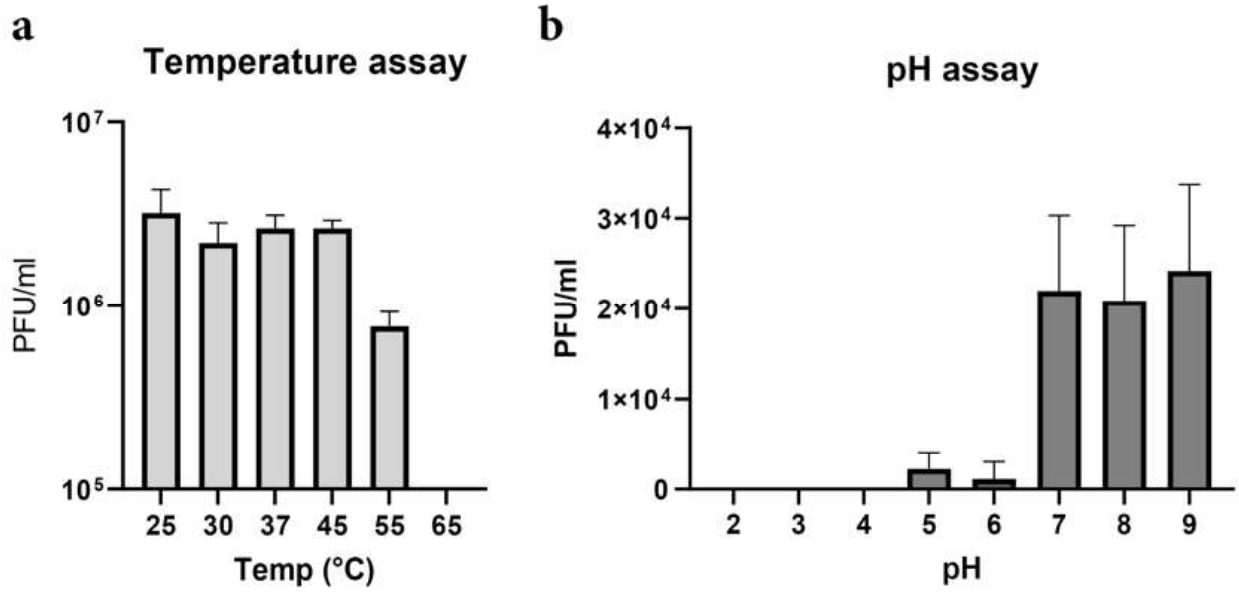

Figure 5. Stability of phage Pablito. (**a**) Phage Pablito remains relatively stable at temperatures ranging from 25 to 45 °C, but decreased stability is observed at higher temperatures. (**b**) Phage stability was optimal at pH of 7.0 and higher. A significant drop in PFU's was observed at pH ≤ 6.0.

Conclusion

This study presents *Streptomyces* phage Pablito as a temperate siphophage being able to infect diverse *Streptomyces* strains. Genomic analysis and TEM images showed that this phage could be classified as a new species in the genus *Janusvirus* within the subfamily *Arquattrovirinae*. Members of this subfamily/genus have long non-contractile tails and icosahedral capsid heads. Phage Pablito showed a burst size of 22 virions per cell and was stable at temperatures ranging from 25 to 45 °C and a pH between 7.0 and 9.0. This phage can be used in future studies to shed new light on bacteriophage-*Streptomyces* interactions and disclose how this phage affects soil community.

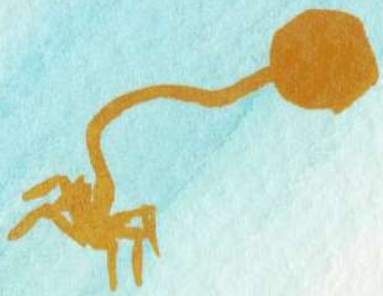

Chapter 4

Genome sequencing and characterization of *Streptomyces* phage Vanseggelen and Verabelle, representing two new species within the genus *Camvirus*

Véronique Ongenae, Annabel Kempff, Vera van Neer, Helena Shomar, Florian Tesson, Daniël Rozen, Ariane Briegel and Dennis Claessen

This chapter was published as:

Ongenae, V., Kempff, A., van Neer, V., Shomar, H., Tesson, F., Rozen, D., Briegel, A. & Claessen, D. (2023). Genome sequence and characterization of Streptomyces phages Vanseggelen and Verabelle, representing two new species within the genus Camvirus. *Scientific Reports*, *13*(1), 20153.

Abstract

Despite the rising interest in bacteriophages, little is known about their infection cycle and lifestyle in a multicellular host. Even in the model system *Streptomyces*, only a small number of phages have been sequenced and well characterized so far. Here, we report the complete characterization and genome sequences of *Streptomyces* phages Vanseggelen and Verabelle isolated using *Streptomyces coelicolor* as a host. A wide range of *Streptomyces* strains could be infected by both phages, but neither of the two phages was able to infect members of the closely related sister genus *Kitasatospora*. The phages Vanseggelen and Verabelle have a double-stranded DNA genome with lengths of 48,720 and 48,126 bp, respectively. Both phage genomes contain 72 putative genes, and the presence of an integrase encoding protein indicates a lysogenic lifestyle. Characterization of the phages revealed their stability over a wide range of temperatures (30–45 °C) and pH values (4–10). In conclusion, *Streptomyces* phage Vanseggelen and *Streptomyces* phage Verabelle are newly isolated phages that can be classified as new species in the genus *Camvirus,* within the subfamily *Arquattrovirinae.*

Introduction

Streptomyces are Gram-positive, spore-forming bacteria, with a relatively high G + C-content [103]. Their multicellular morphology and lifecycle are unique within the bacteria realm. Furthermore, *Streptomyces* are well-known for their ability to produce natural products with a wide range of biological activities [104]. These include, for example, metabolites that can act as anti-fungals, anti-virals, anti-tumor agents and many clinically relevant antibiotics [87]. However, the production of these metabolites from *Streptomyces* can be negatively influenced by bacteriophage contaminations, which can result in huge economic losses [105]. Bacteriophages, or phages for short, are viruses that can infect bacteria. Yet, it remains largely unknown how bacteriophages can recognize, attach and infect these multicellular bacteria and more detailed descriptions of new phage species will be beneficial for following research [17, 93].

All known *Streptomyces* phages belong to the class *Caudoviricetes,* which are tailed bacterial and archaeal viruses with icosahedral capsid heads and double-stranded DNA genomes [106]. The phages within this class are divided into three morphotypes: long contractile tails (myoviruses), long non-contractile tails (siphoviruses) or short non-contractile tails (podoviruses). Of all characterized *Streptomyces* phages, 91% have long non-contractile tails and are therefore siphoviruses [107]. Compared to other genera, relatively few *Streptomyces* phages have been properly characterized and sequenced. According to The Actinobacteriophage Database [108], only 340 *Streptomyces* phages have been sequenced to date, while there are over 2700 *Escherichia coli* phage genomes deposited in Genbank [109, 110].

Here, we describe two newly discovered Actinobacteriophages, which we name *Streptomyces* phage Vanseggelen and *Streptomyces* phage Verabelle. These temperate phages belong to the genus *Camvirus*, within the subfamily *Arquattrovirinae*. Vanseggelen has an icosahedral capsid head of 53.7 ± 7.9 nm and a long non-contractile tail of 228.7 ± 7.5 nm, while Verabelle has an icosahedral capsid head of 63.2 ± 1.2 nm and a long non-contractile

tail of 200.4 ± 1.5 nm. Furthermore, we provide a complete genomic analysis of these newly identified phages. Together, these results will hopefully increase our knowledge on phage-host dynamics in *Streptomyces* in the future and expanded the list of available, sequenced and characterized *Streptomyces* phages.

Material and methods

Bacteriophage isolation

Streptomyces phages Vanseggelen and Verabelle were isolated from a soil sample obtained from the National Park Zuid-Kennemerland in the Netherlands (N52° 23′ 31″, E4° 34′ 49″) using *Streptomyces coelicolor* as the host. Details on isolation procedures are reported previously in detail [111]. The collected phage stock solutions were stored at 4 °C.

Host range analysis

The host range of Vanseggelen and Verabelle was determined by using serial dilutions on double agar overlay plates. The phage stock solutions were serial diluted with Difco Nutrient Broth (DNB) (BD biosciences) supplemented with 4 mM $Ca(NO_3)_2$ and 0.5% w/v glucose. Droplets of 3 µl of the phage dilutions were spotted in duplicate on a bacterial lawn of nine different *Streptomyces strains* and one *Kitasatospora* strain from the Microbial Biotechnology (MBT) collection at Leiden University [94]. *Streptomyces* strains MBT13, MBT61 and MBT86 are new species and have not been taxonomically classified yet. The plates were incubated at 30 °C for at least 24 h before lysis was observed, after which the presence of a lysis zone was scored as a positive result. The efficiency of plating (EOP) for a given strain was calculated relative to the host strain *S. coelicolor*, only when distinct clear individual plaques were observed.

Morphology analysis

The plaque morphology of Vanseggelen and Verabelle was determined by using serial dilutions on double agar overlay plates on the host *S. coelicolor.*

Representative images of the phages were made using transmission electron microscopy (TEM). For a single grid preparation, 3 µl of the phage lysates (Vanseggelen = 10^6 PFU/ml and Verabelle = 10^7 PFU/ml) was placed on a glow-discharged 200 mesh carbon coated copper grid (EMS) and allowed to set for 30 s before excess sample solution was removed by filter paper. The phages were stained with 2% uranyl acetate for 45 s after which excess liquid was removed and the samples were air-dried for an additional 30 min. The grids were observed using a single tilt specimen holder inside a 120 kV Talos L120C TEM with a Lab6 electron source and Ceta detector at the Netherlands Center for Nanoscopy (NeCEN, Leiden).

Stability analysis

A one-step growth curve analysis was performed in triplicate to determine the latent period and burst size of both phages [95]. Since *Streptomyces* phage adsorption was found to be maximal for germlings [112], 10^8 spores ml^{-1} of *S. coelicolor* were allowed to germinate in 10 ml DNB medium at 30 °C while shaking at 200 rpm. After approximately 5 h, the culture was infected with Vanseggelen or Verabelle at Multiplicity of Infection (MOI) of 0.01 and 100 µl was sampled at 10 min intervals up to 180 min. The samples were filtered with a 0.20 µm filter, serial diluted with DNB medium and immediately plated on double agar overlay plates. The burst size was calculated using the following formula:

$$\text{Burst size} = \frac{(\text{total phages after burst (x)} \,/\, \text{total phages before burst (y)})}{\text{number of phages at T} = 0}$$

The thermal stability of Vanseggelen and Verabelle was determined by adding 100 µl of phage suspension (Vanseggelen = 10^5 PFU/ml and Verabelle = 10^7 PFU/ml) to 900 µl DNB medium and incubating the phages at 25, 30, 37, 45, 55 and 65 °C. The samples were filtered with a 0.20 µm filter after 1 h of incubation. A serial dilution was made with DNB medium, which was immediately spotted on double agar overlay plates to determine the phage titers. To assess viability at common storage temperatures, the phages were incubated in DNB medium without glycerol at -80, -20 and 4 °C for seven days. To determine pH stability, 100 µl of the phage suspensions was added

to 900 µl DNB medium that was pH adjusted using 1 M HCl or 1 M NaOH. The samples were incubated at 30 °C for 1 h before filtration. A serial dilution was made with DNB medium, which was immediately spotted on double agar overlay plates to determine the phage titer. All the phage stability measurements were performed in triplicate. All statistical analyses were performed with a Student's *t*-test.

DNA extraction and phylogenetic analysis

DNA isolation, whole genome sequencing and de novo assembly of Vanseggelen and Verabelle were performed by the Institute Pasteur using Illumina NovaSeq PE150 sequencing (Paris, France). The complete genome sequences of Vanseggelen and Verabelle were deposited at GenBank under accession number OQ970438 and OQ970439, respectively. Linear maps of the genomes were constructed by Geneious Prime 2022.1.1 (https://www.geneious.com) and genomes were de novo assembled using SPAdes v3.15.5 and aligned starting by the phage terminase [113].

A viral proteomic phylogenetic tree and a genomic alignment based on the whole genome sequences of *Streptomyces* phages Alsaber, Amela, Endor1, Endor2, Hydra, Indigo, Joe, Pablito, phiCAM, Saftant, Sitrop, Verse and Yosif were constructed using ViPtree: the Viral Proteomic Tree version 3.5 [114]. The genome sequences of these phages were acquired from the National Center for Biotechnology Information (NCBI). Pairwise genome comparisons of phages within the *Camvirus* genus were visualized and performed with clinker [115]. A heatmap to determine intergenomic relatedness was constructed with the use of VIRIDIC [100].

Results

Morphology and host range

Two novel phages infecting *Streptomyces* have been isolated from soil samples in the Netherlands. Both phages produced small, clear plaques on the host strain *S. coelicolor* while using the double agar overlay method (Fig. 1a). TEM images revealed that Vanseggelen has an icosahedral capsid

head of 53.7 ± 7.9 nm (n = 5) and a long non-contractile tail of 228.7 ± 7.5 nm (n = 4). Verabelle has an icosahedral capsid head of 63.2 ± 1.2 nm (n = 3) and a long non-contractile tail of 200.4 ± 1.5 nm (n = 3) (Fig. 1b).

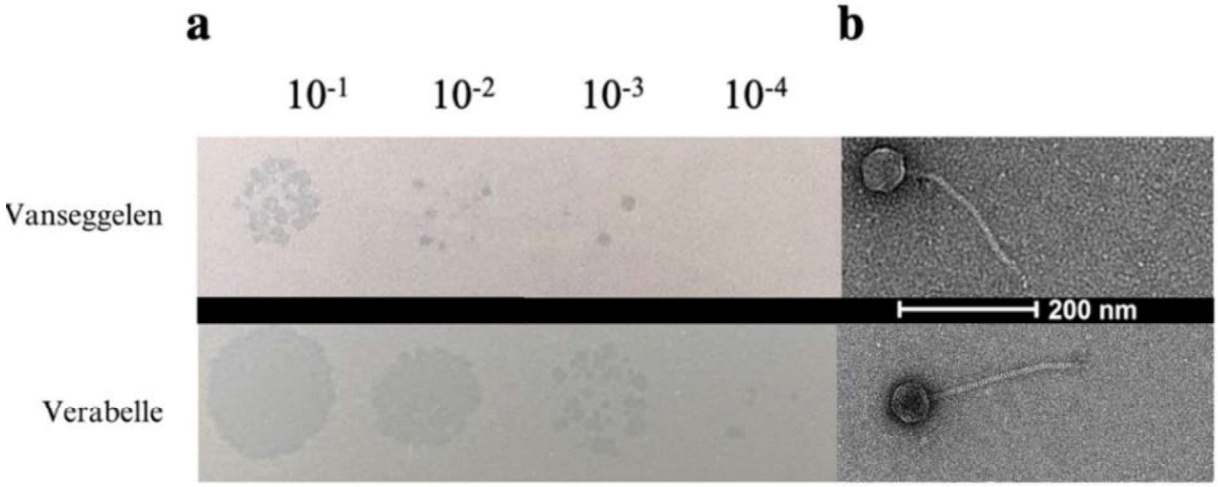

Figure 1. Morphology of Vanseggelen and Verabelle. (**a**) Plaque morphology after 24 h of infection in *S. coelicolor*, using a serial dilution with the DNB double agar overlay method. (**b**) Representative TEM images of Vanseggelen and Verabelle stained with 2% uranyl acetate.

A host range analysis of Verabelle performed on ten different actinomycetes strains revealed that all nine *Streptomyces* strains could be infected, and the phage produced clear as well as turbid lysis zone morphologies depending on the host (Table 1). Vanseggelen was not able to infect *Streptomyces griseus*, *Streptomyces lividans* and MBT13, but could infect the other six *Streptomyces* strains tested (Table 2). However, both phages were unable to infect *K. virifidaciens*. When distinct clear individual plaques were visible in a given strain, the efficiency of plating (EOP) was determined relative to the original host *S. coelicolor.*

Table 1. Host range determination of *Streptomyces* phage Verabelle.

Bacterial strain	Origin	Infectivity	Lysis zone morphology	EOP
Streptomyces coelicolor	MBT collection	+	Clear	1
Streptomyces albus	MBT collection	+	Clear	40.9
Streptomyces cattleya	MBT collection	+	Clear	4.1
Streptomyces griseus	MBT collection	+	Turbid	
Streptomyces lividans	MBT collection	+	Turbid	
Streptomyces venezuelae	MBT collection	+	Turbid	
Kitasatospora viridifaciens	DSM40239	-	None	
MBT13	MBT collection	+	Turbid	
MBT61	MBT collection	+	Clear	9.5
MBT86	MBT collection	+	Clear	2.2

Table 2. Host range determination of *Streptomyces* phage Vanseggelen.

Bacterial strain	Origin	Infectivity	Lysis zone morphology	EOP
Streptomyces coelicolor	MBT collection	+	Clear	1
Streptomyces albus	MBT collection	+	Clear	3.2
Streptomyces cattleya	MBT collection	+	Clear	1.7
Streptomyces griseus	MBT collection	-	None	
Streptomyces lividans	MBT collection	-	None	
Streptomyces venezuelae	MBT collection	+	Turbid	
Kitasatospora viridifaciens	DSM40239	-	None	
MBT13	MBT collection	-	None	
MBT61	MBT collection	+	Clear	3.2
MBT86	MBT collection	+	Clear	1.5

One-step growth curve

The one-step growth curve of Vanseggelen shows a latent period of 140 min, with a burst size of 17 virions per bacterial cell (Fig. 2a). The one-step growth curve of Verabelle also shows a latent period of 140 min, but with a burst size of 8 virions per bacterial cell (Fig. 2b). The latent period of both phages is relatively long compared to other *Streptomyces* phages [98, 111].

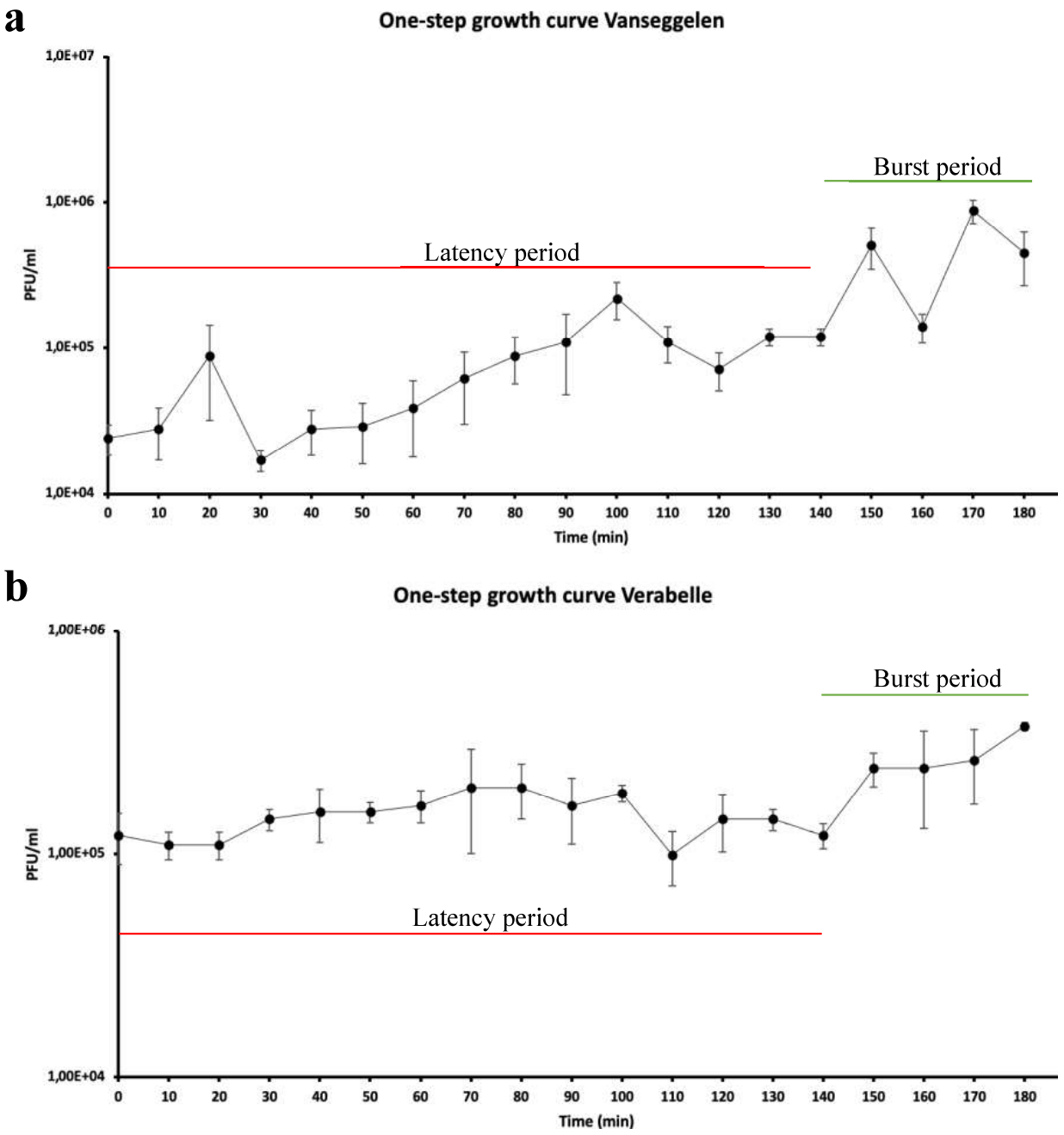

Figure 2. One-step growth curves of Vanseggelen and Verabelle at MOI = 0.01. (**a**) Vanseggelen had a latent period of 140 min and a total burst size of 17 virions per cell. (**b**) Verabelle had a latent period of 140 min and a total burst size of 8 virions per cell.

Phage stability

Vanseggelen and Verabelle were stable up to 45 °C without a significant reduction in viability (Fig. 3). The absence of plaques at 65 °C indicates that Vanseggelen was not viable after incubation at 65 °C for 1 h. In addition, Vanseggelen made significantly less plaques after storing the phage samples at − 80 °C for one week (Fig. 4a), while Verabelle could be incubated at temperatures of − 80, − 20 and 4 °C without loss in viability (Fig. 4b). The optimal pH range for Vanseggelen was between pH 6.0–10.0, from which a decreasing trend in viability was visible at both lower and higher acidity (Fig. 5a). Verabelle remained relatively stable at pH values from 4.0 to 10.0 and no viability was detected at pH values of 3.0 and 11.0 (Fig. 5b).

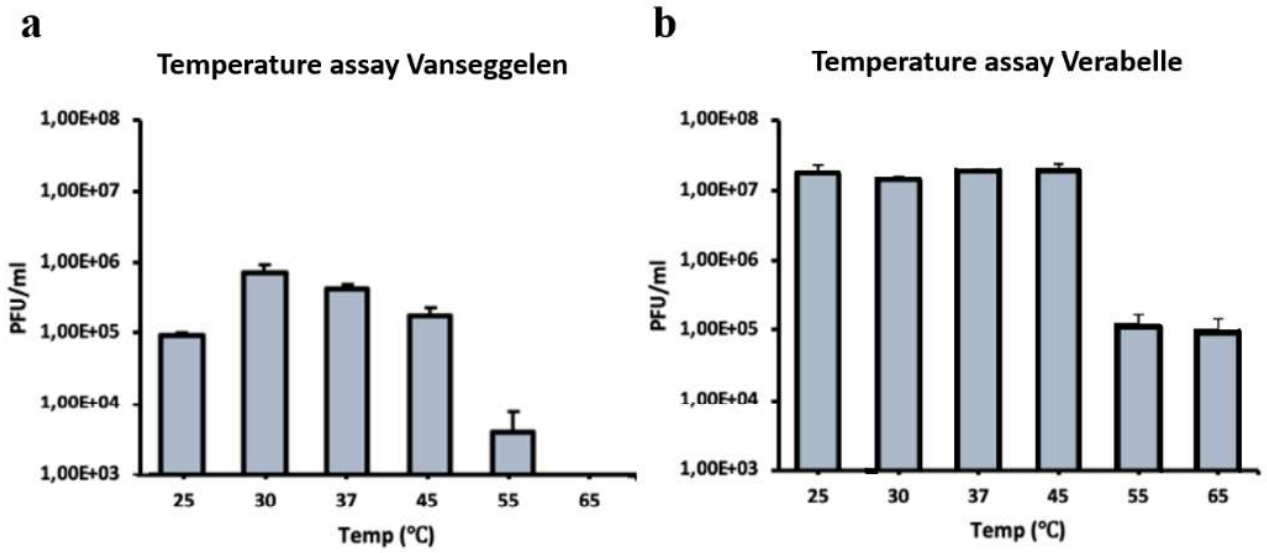

Figure 3. Temperature stability of Vanseggelen and Verabelle. (**a**) Vanseggelen was stable from 30 up to 45 °C without a reduction in viability. However, the infectivity significantly decreased when the phage was incubated for one hour at 55 °C or higher. (**b**) Verabelle remains stable between temperatures ranging from 25 to 45 °C, but the viability significantly decreased at higher temperatures.

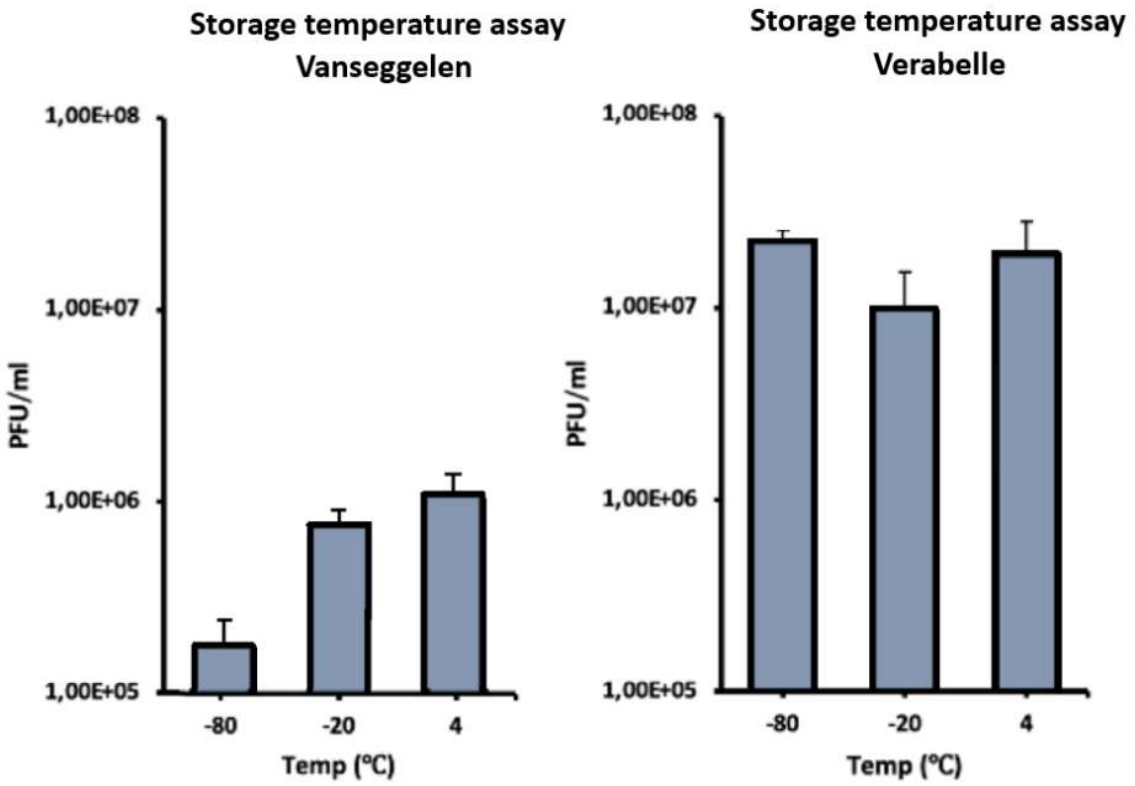

Figure 4. Storage stability of Vanseggelen and Verabelle. (**a**) Vanseggelen retains its viability when stored at − 20 or 4 °C (**b**) Verabelle remains viable at all storage temperatures.

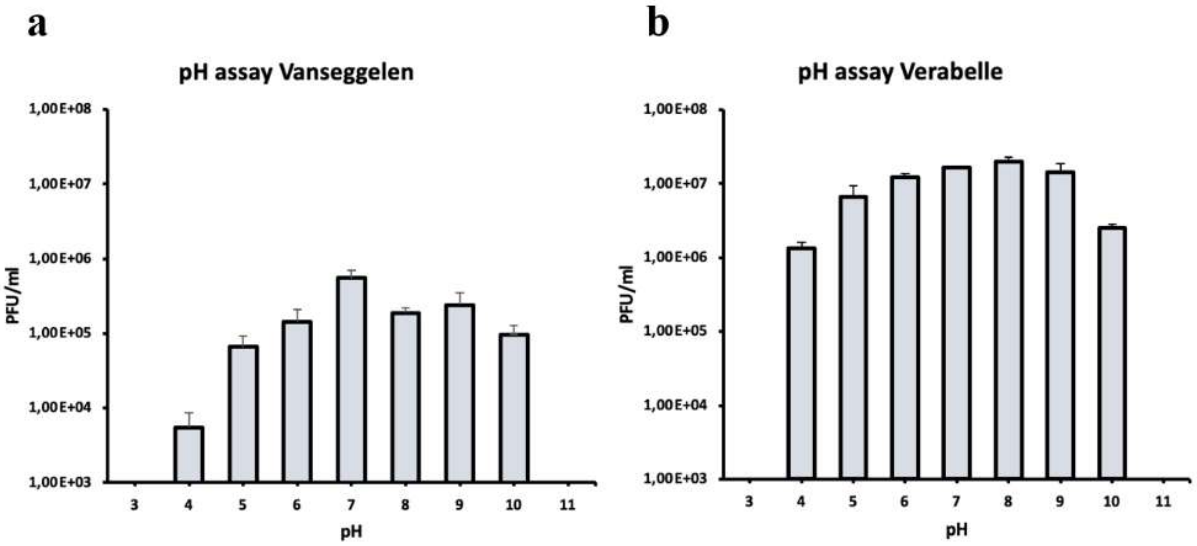

Figure 5. pH stability of Vanseggelen and Verabelle. (**a**) Vanseggelen remains relatively stable at pH values 5.0–10.0. (**b**) Verabelle remains relatively stable at pH values 4.0–10.0 and shows no viability at pH values 3.0 and 11.0.

Genomic analysis

Whole genome sequencing and de novo assembly of *Streptomyces* phage Vanseggelen revealed a double-stranded DNA genome of 48,720 base pairs with a G + C content of 65.6% and a 3′-cohesive termini of CGGTACGTGAT. This genome contains 72 potential coding sequences (CDSs), of which 37 encode for hypothetical proteins and the function of 35 CDSs could be predicted (Fig. 6a). Verabelle revealed a slightly smaller double-stranded DNA genome of 48,126 base pairs with G + C content of 65.0% and a 3′-cohesive termini of CGTACCGTCAT. Again, the genome contains 72 potential CDSs, of which 40 are hypothetical proteins and the function of 32 CDSs could be predicted (Fig. 6b). The three additional CDSs that could be predicted in Vanseggelen are an additional minor tail protein, an RNA-polymerase sigma factor and a nucleoid associated Lsr2-like protein. Both genomes possess a putative integrase, indicating the capability of a temperate lifestyle. The Actinobacteriophage Database places both phages in Cluster BD, Subcluster BD3 [108]. Although the genomes of both phages are similar, there are some sequence variations that result in differences at the protein level (Fig. 7).

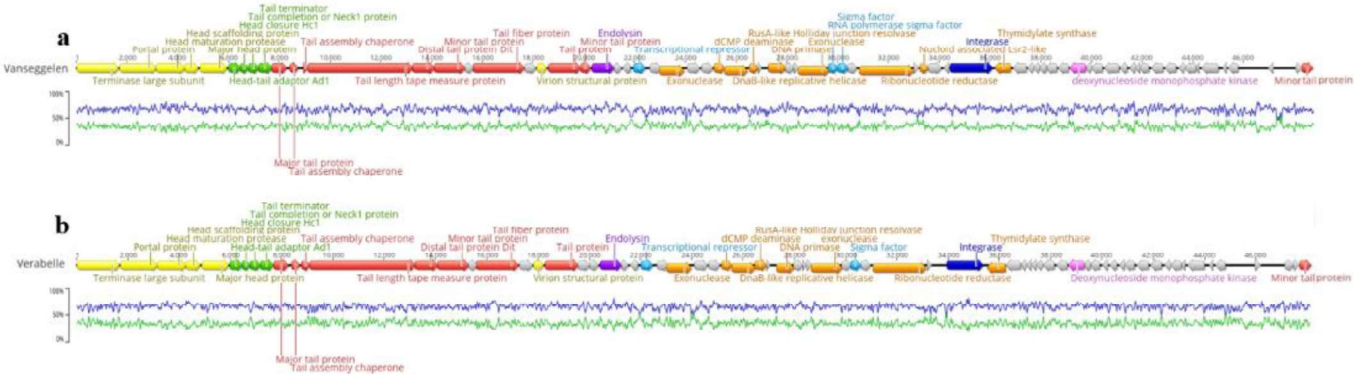

Figure 6. Schematic representation of the double-stranded DNA sequence of Vanseggelen and Verabelle. (**a**) Overview of the linear genome of Vanseggelen. (**b**) Overview of the linear genome of Verabelle. (**a**)/(**b**) Arrowheads are indicated in the direction of the coding sequence (CDS). Hypothetical proteins are displayed in grey and the predicted proteins are color coded as follows: yellow for head and packaging, red for tail, orange for DNA, RNA and nucleotide metabolism, green for connector, purple for lysis, light blue for transcription regulation, dark blue for integration and excision and pink for other. The blue line represents the GC content, while the green line represents the AT content. The genome maps were generated through Geneious Prime 2022.1.1. (https://www.geneious.com).

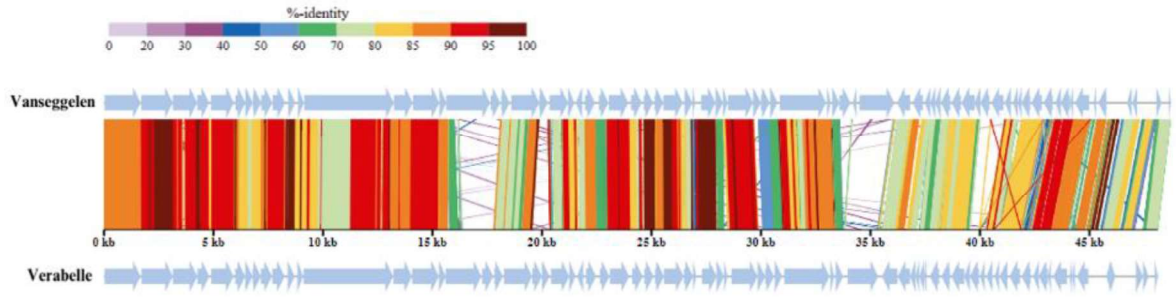

Figure 7. Genomic alignment of Vanseggelen and Verabelle. The predicted genes are indicated and the colored vertical blocks between the genomes indicate the level of nucleotide similarity. The genome alignment was generated through ViPTree [114].

Phylogenetic analysis (Fig. 8a) based on the whole genome sequences of the closest-related phages, revealed that Vanseggelen is most closest related to *Streptomyces* phage Endor2 and Verabelle is most closely related to *Streptomyces* phage Sitrop. They are more distantly related to *Streptomyces* phages Pablito, Hydra and Yosif, which belong to different genera. These results indicate that both phages belong to the same genus, namely *Camvirus*. The genomic alignment of all phages within the *Camvirus* genus (Fig. 8b) show that phage Vanseggelen shares a similar tail fiber protein with phage Endor2, phiCAM, Alsaber, Amela and Endor2, while Verabelle shares a similar tail fiber protein with phage Sitrop, Saftant and Joe. The lack of genome similarity in tail fiber proteins between phage Vanseggelen and Verabelle might explain their difference in host range as seen in Tables 1 and 2. Additionally, phage Vanseggelen and Verabelle have a different integrase protein, indicating that they will likely integrate at different places in their host.

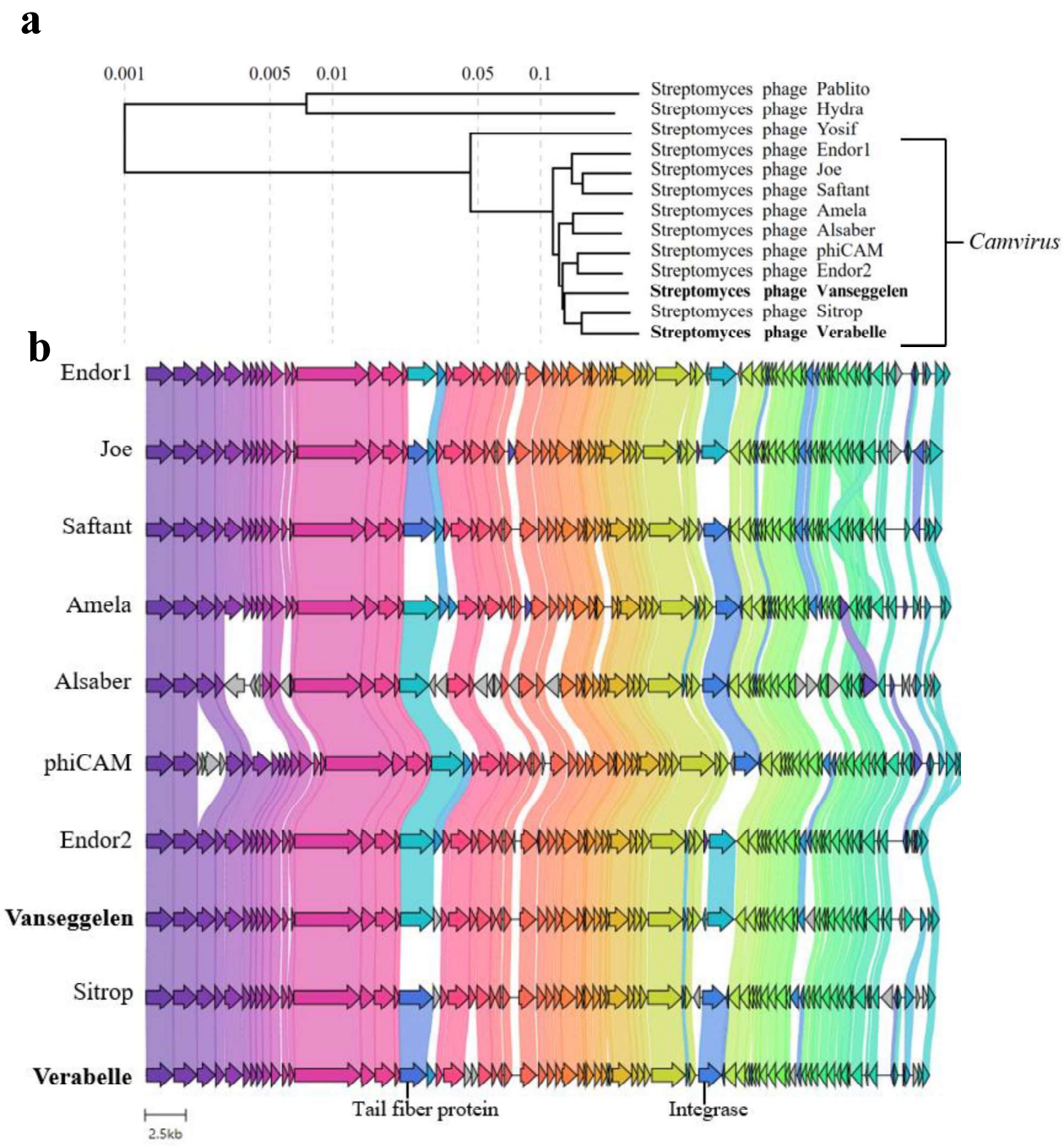

Figure 8. Phylogeny and genome similarity of Vanseggelen and Verabelle based on the whole genome sequences. (**a**) *Streptomyces* phages Vanseggelen and Verabelle belong to the genus *Camvirus*, within the subfamily *Arquattrovirinae*. The viral proteomic tree was generated through ViPTree [114]. (**b**) Genome alligment of all phages within the *Camvirus* genus starting at the terminase. Vanseggelen and Verabelle don't share similarity in the tail fiber protein and integrase as indicated by light blue arrowheads in Vanseggelen and dark blue in Verabelle.

Next, a heatmap of the intergenomic relatedness (Fig. 9) was made. The two phages show a relatedness of 75.0 to each other and Vanseggelen is most related to phage Endor2 with a relatedness of 82.4, while Verabelle is most related to phage Sitrop with 77.8. The Bacterial Viruses Subcommittee of the International Committee on Taxonomy of Viruses (ICTV) has determined that if a phage exhibits ≥ 70% and < 95% nucleotide relatedness, the phage belongs to a new species in an undefined or existing genus. A sequence similarity of ≥ 95% is the cut-off for identifying a phage as a new species. Since the relatedness of Vanseggelen and Verabelle is lower than 95% compared to the top ten most similar *Streptomyces* phages, these phages are both considered as new species according to ICTV [24]. A taxonomic proposal has been submitted to ICTV to officially recognize Vanseggelen and Verabelle as part of the genus *Camvirus,* as a new species called "*Camvirus vanseggelen*" and "*Camvirus verabelle*".

Streptomyces phage Pablito	Streptomyces phage Hydra	Streptomyces phage Yosif	Streptomyces phage Alsaber	Streptomyces phage Amela	Streptomyces phage Endor2	**Streptomyces phage Vanseggelen**	Streptomyces phage Endor1	Streptomyces phage phiCAM	Streptomyces phage Joe	Streptomyces phage Saftant	Streptomyces phage Sitrop	**Streptomyces phage Verabelle**	
100.0	50.6	47.2	46.4	47.5	45.3	45.3	44.3	46.9	44.7	44.9	45.9	46.5	Streptomyces phage Pablito
50.6	100.0	52.9	57.3	58.2	55.1	53.5	55.6	56.8	53.2	54.3	53.9	52.9	Streptomyces phage Hydra
47.2	52.9	100.0	62.1	63.1	62.4	62.4	61.5	61.2	57.9	58.8	59.4	59.7	Streptomyces phage Yosif
46.4	57.3	62.1	100.0	84.0	79.2	77.8	77.0	76.2	74.6	76.8	79.3	73.5	Streptomyces phage Alsaber
47.5	58.2	63.1	84.0	100.0	79.5	76.9	75.9	78.3	73.5	72.9	77.7	73.2	Streptomyces phage Amela
45.3	55.1	62.4	79.2	79.5	100.0	82.4	78.7	80.4	77.1	73.0	77.2	75.7	Streptomyces phage Endor2
45.3	53.5	62.4	77.8	76.9	82.4	100.0	75.8	74.4	75.0	70.9	75.6	75.0	**Streptomyces phage Vanseggelen**
44.3	55.6	61.5	77.0	75.9	78.7	75.8	100.0	76.7	81.5	76.0	71.4	70.4	Streptomyces phage Endor1
46.9	56.8	61.2	76.2	78.3	80.4	74.4	76.7	100.0	71.6	72.2	74.2	74.3	Streptomyces phage phiCAM
44.7	53.2	57.9	74.6	73.5	77.1	75.0	81.5	71.6	100.0	81.7	74.5	72.8	Streptomyces phage Joe
44.9	54.3	58.8	76.8	72.9	73.0	70.9	76.0	72.2	81.7	100.0	77.1	71.7	Streptomyces phage Saftant
45.9	53.9	59.4	79.3	77.7	77.2	75.6	71.4	74.2	74.5	77.1	100.0	77.8	Streptomyces phage Sitrop
46.5	52.9	59.7	73.5	73.2	75.7	75.0	70.4	74.3	72.8	71.7	77.8	100.0	**Streptomyces phage Verabelle**

Figure 9. Intergenomic relatedness. Genomes of the top ten most similar *Streptomyces* phages Alsaber, Amela, Endor2, Endor1, phiCAM, Joe, Saftant and Sitrop were used to show relatedness. The genomes of *Streptomyces* phages Pablito, Hydra and Yosif are classified in different genera as shown in green. The heatmap was calculated by VIRIDIC [100].

Discussion

In this study, the newly isolated *Streptomyces* phages Vanseggelen and Verabelle have been fully characterized and sequenced. These results increase our insights on phage-host dynamics in *Streptomyces* and expand available, sequenced and characterized *Streptomyces* phages. TEM images showed that both phages have a long, flexible non-contractile tail with an icosahedral capsid head typical for siphoviruses. Both phages belong to the class *Caudoviricetes,* which was confirmed by whole genome sequencing. Since the majority of the sequenced *Streptomyces* phages have a long non-contractile tail, this tail morphotype is possibly necessary for effectively penetrating the thick peptidoglycan layer of Gram-positive bacteria. The host range analysis showed that both phages can form lysis zones with a turbid morphology with some host strains, indicating that Vanseggelen and Verabelle are likely able to switch from a lytic to a lysogenic lifecycle. Indeed, since all other phages belonging to the genus *Camvirus* are temperate phages and whole genome sequencing revealed that both genomes contain an integrase protein, we can conclude that Vanseggelen and Verabelle are temperate phages as well [101].

Of all sequenced *Streptomyces* phages available in the Actinobacteriophage database [76], we have calculated that the average genome length is 73,556 bp with a G + C content of ~ 61%, which is relatively high, and could be explained by the relatively high G + C-content of their bacterial hosts. Both Vanseggelen and Verabelle have a double-stranded DNA with a genome length of 48,720 bp and 48,126 bp, which is a bit smaller than average. Both phages were able to infect several different *Streptomyces* strains, but could not infect *K. virifidaciens. Kitasatospora* is the sister genus of *Streptomyces* that also belongs to the phylum *Actinobacteria.* Their morphology and lifecycle are similar to *Streptomyces* bacteria,

but *Kitasatospora* is usually identified by the fact that they cannot be infected by *Streptomyces* phages [77, 78]. Possibly, because of the difference in cell wall composition, since the cell wall of *Kitasatospora* strains contain both LL- and meso-diaminopimelic acid [116]. It would be interesting to isolate and characterize phages on *Kitasatospora* species in the future to dissect differences in infectivity between *Streptomyces* and *Kitasatospora* phages.

Despite the high degree of nucleotide similarity between the genomes of Vanseggelen and Verabelle, there were sequence variations that resulted in differences at the protein level, which could also account for the differences in host range. *Streptomyces* phage Verabelle showed a slightly broader host range infectivity than Vanseggelen, which could be explained by potential phage specific defense mechanisms or the difference in tail fiber proteins. Additionally, a different integrase protein was found, which suggest that both the tail fiber protein and integrase are a common source of variation in closely related phages within the *Camvirus* genus.

The one-step growth curve of Vanseggelen and Verabelle showed a long latent period of 140 min and a relatively low burst size, even when compared to other *Streptomyces* phages [98, 111]. The low burst size could be the result of the morphological complexity of *Streptomyces* [98]. The meaning of MOI loses its significance once spores have germinated and a mycelium is formed as multiple phages are able to attach, but the mycelium would still be counted as one colony forming unit [112, 117]. This notion of MOI in *Streptomyces*-phage dynamics complicates quantitative experiments and could explain the low burst sizes shown in this study.

Temperature plays a fundamental role in phage attachment, penetration, multiplication, and the length of the latent period, and is therefore a crucial factor for phage viability [118]. Both phages remain stable at temperatures ranging from 30 to 45 °C while phage viability decreases at higher temperatures. These results are consistent with a previous study that shows that phages most likely lose their DNA from the capsid head between temperatures of 50 and 60 °C due to the tail complex breaking of the capsid

head [119]. This results in the marked loss of infectivity and structural changes in the capsid proteins. It is suspected that denaturation of DNA and proteins within the capsid head only occurs at temperatures above 80 °C [120]. Another important factor for phage viability is the acidity of the environment in which the phage persists. *Streptomyces* strains can grow well between a pH range of 5.5–11.5 [119]. However, both Vanseggelen and Verabelle remain stable at pH values from 4.0 to 10.0. Although the exact effect of acidity on the capsid head or tail has not been clearly elucidated yet, a previous study showed that extreme pH values, such as highly acidic or highly alkaline conditions, can result in the denaturation or structural changes to phage capsid head proteins [121].

The *Streptomyces* phages described in this study can help to discover new insights in the interactions between *Streptomyces* bacteria and bacteriophages. More fundamental research is needed to study the attachment, lifecycle and infection of phages targeting multicellular bacteria, like *Streptomyces.* Since *Streptomyces* are producing a wide range of clinically relevant antibiotics, such studies become increasingly important in order to keep exploiting *Streptomyces*' antimicrobial potential and abolish phage infection in various industries like biotechnology, agriculture and medicine.

Chapter 5

Reversible bacteriophage resistance by shedding the bacterial cell wall

Véronique Ongenae, Adam Sidi Mabrouk, Marjolein Crooijmans, Daniël Rozen, Ariane Briegel and Dennis Claessen

This chapter was published as:

Ongenae, V., Mabrouk, A. S., Crooijmans, M., Rozen, D., Briegel, A., & Claessen, D. (2022). Reversible bacteriophage resistance by shedding the bacterial cell wall. *Open Biology*, *12*(6), 210379.

Abstract

Phages are highly abundant in the environment and pose a major threat for bacteria. Therefore, bacteria have evolved sophisticated defense systems to withstand phage attacks. Here, we describe a previously unknown mechanism by which mono- and diderm bacteria survive infection with diverse lytic phages. Phage exposure leads to a rapid and near-complete conversion of walled cells to a cell wall-deficient state, which remains viable in osmoprotective conditions and can revert to the walled state. While shedding the cell wall dramatically reduces the number of progeny phages produced by the host, it does not always preclude phage infection. Altogether, these results show that the formation of cell wall-deficient cells prevents complete eradication of the bacterial population and suggest that cell wall-deficiency may potentially limit the efficacy of phage therapy, especially in highly osmotic environments or when used together with antibiotics that target the cell wall.

Introduction

Bacteria are routinely exposed to a wide range of stresses in their environment, such as changes in temperature, pH, salt concentration or nutrient limitation. To withstand such fluctuating conditions, almost all bacteria are enveloped by a stress-bearing cell wall. Another serious threat are bacteriophages, which outnumber bacteria in the environment by a factor of 10 [19]. Phages recognize their host by interacting with specific receptors, especially sugars and proteins, present in the cell wall or exposed on the cell surface. Following binding and infection, lytic phages will kill their host, while lysogenic phages persist as prophages inside the bacterium [122, 123]. In order to counteract phage attack, bacteria have evolved multiple highly specific escape mechanisms, such as restriction-modification, abortive infection, or CRISPR/Cas systems, among many others [45-47, 53, 124-129]. Another common and effective strategy to overcome phage attack is by modifying or masking surface-associated phage receptors [59-61]. However, these strategies are permanent and often effective only against specific phages.

Here, we present a robust response that occurs when diverse lytic phages infect bacterial hosts in osmoprotective environments. We show that upon phage exposure, the bacteria transiently shed their cell wall, leading to the formation of viable cell wall-deficient (CWD) cells that increase survival of the bacterial population.

Material and methods

Strains, bacteriophage isolation and sequencing

Bacterial strains and phages used in this work are listed in electronic supplementary material, table S1. Actinobacteriophages were isolated from soil samples collected in the Netherlands at longitude 52°23′31″ N and latitude 4°34′49″ E. The soil samples were collected at a depth of three cm and stored at 4 °C before processing. Actinobacteriophage isolation was performed as described before using *Streptomyces lividans* (phage LA7 and LD10), *Streptomyces coelicolor* (phage CE2 and CE10) and *Streptomyces*

griseus (phage GA3) as bacterial hosts in Difco Nutrient Broth (DNB) [95]. High viral titre stocks were obtained by picking streak purified plaques until confluent lysis was observed. Plates were flooded with DNB broth and lysates were filtered through a 0.22 µm filter. Concentration and activity of these lytic phages was confirmed using a spot assay. Phages were serial diluted and 3 µl was spotted on a DNB double agar overlay plate containing the host strain. After 24 h, PFU's were quantified. Genomic material of bacteriophage LA7 was isolated using the Phage DNA Isolation Kit from Norgen (Thorold, Canada) according to the manufacturers protocol. Whole-genome sequencing of phage LA7 followed by *de novo* assembly was performed by BaseClear (Leiden, The Netherlands) and the sequencing data are available on NCBI (GenBank accession no. OK412919). Phage LA7 was later named Pablito, an unclassified phage in the genus *Arequatrovirus* [24].

Characterization of bacteria-phage interactions

L-phase broth (LPB) was used to identify if *Streptomyces*, *Escherichia coli* and *Bacillus subtilis* were able to form CWD cells after phage infection. LPB is an osmoprotective medium, which consists of a mixture of TSBS and YEME (1 : 1v/v) supplemented with 25 mM $MgCl_2$ [11]. For Streptomyces strains, 10^6 spores ml^{-1} were inoculated in 10 ml LPB medium with 1000 phages ml^{-1}. OD_{600} was measured after 24 h of incubation at 30 °C, 200 RPM. To test if *E. coli* and *B. subtilis* could form CWD cells, an overnight culture was diluted to OD = 0.01 in LPB and incubated at 30 °C until OD = 0.5 was reached. Subsequently, phages T4 or *φ*29 were added at a MOI of 2.0. The culture was incubated for 24 h at 30 °C, 200 RPM before imaging.

To produce protoplasts, MBT86 was grown in a mixture of TSBS and YEME (1 : 1 v/v) supplemented with 5 mM $MgCl_2$ and 0.5% glycine for 48 h at 30 °C, 100 RPM. Protoplasts were prepared by incubating the mycelial pellet in 10 mg ml^{-1} lysozyme solution for one hour [130]. The culture was filtered through an EcoCloth filter, centrifuged at 1000 g for seven minutes and resuspended in one ml P+ buffer [130]. Protoplasts of *B. subtilis* were produced using an overnight culture that was diluted to OD = 0.01 in LPB medium supplemented with 25 mM $MgCl_2$, 1.2 mg ml^{-1} penicillin G sodium from Duchefa Biochemie

(Haarlem, The Netherlands) and 8 mg ml^{-1} lysozyme, and grown for 24 h at 30°C. For *E. coli* spheroplasts, an overnight culture was diluted to OD = 0.01 in LPB medium supplemented with 25 mM $MgCl_2$ and 0.4 mg ml^{-1} penicillin G sodium, and was grown for 24 h at 30 °C. Subsequently, MBT86 protoplasts were inoculated with 1000 phages ml^{-1}, while *E. coli* spheroplasts and *B. subtilis* protoplasts were inoculated with phages T4 or *φ*29 at a MOI of 1.0 and incubated for 24 h at 30 °C, 200 RPM before imaging.

To determine if proteins extruded after phage infection can initiate the formation of CWD cells, an overnight *B. subtilis* culture was inoculated in LPB medium until OD = 0.5 and subsequently infected with *φ*29 at a MOI of 10. The medium was filtered after 24 h using an Amicon ultra-15 centrifugal filter unit (30 kDa, Millipore) and the supernatant was added to a fresh overnight grown *B. subtilis* culture at OD = 0.5. After 24 h, CWD cell formation was assessed.

Viability after phage infection

To verify the viability of the CWD cells from MBT86 observed after phage infection, 100 µl of the phage-infected culture in DNB or LPB medium was plated in triplicate on MYM medium [131]. The plates were grown for 3 days at 30 °C before analysing morphology. CFU's of *E. coli* and *B. subtilis* were determined using serial dilution of the phage infected culture on LB plates. After one day of growth at 30 °C, CFUs were calculated. To calculate the concentration of phages after infection, 1 ml of a phage-infected culture (triplicates) was filtered through 0.22 µm, serial diluted and PFU's were quantified with a spot assay.

Microscopy

The Zeiss Axio Lab A1 upright Microscope, equipped with an Axiocam 105 colour (resolution of 5 megapixel) or Axiocam MRc (resolution of 64.5 nm $pixel^{-1}$) camera was used to take bright field images. The Zeiss Axio observer Z1 microscope was used to visualize stained bacteria on a thin layer of LPB soft agar covering the glass slide. All stains (Molecular Probes) were added directly to 25 µl of liquid culture. The membrane dye FM5–95 was used at a

final concentration of 0.02 mg ml^{-1} and the nucleic acid dye SYTO-9 at 0.5 µM. Peptidoglycan was visualized using 0.02 mg ml^{-1} Wheat Germ Agglutinin (WGA) Oregon. SYTO-9 and WGA Oregon were excited using a 488 nm laser and monitored in the region between 505–600 nm, while FM5–95 was excited at 561 nm and detected using a 595 nm long pass filter. Images were adjusted using OMERO software [132].

Fluorescent labelling of *φ*29 phages was accomplished by adding 475 µl phage with 25 µl Alexa Fluor 488 NHS-Ester (Thermo Fisher) at a final concentration of 0.05 mg ml^{-1} (10 mM). The labelled phages were gently shaken at room temperature for 3 h and washed with an Amicon ultra-0.5 centrifugal filter unit (100 kD, Millipore) in phage storage buffer (100 mM NaCl, 10 mM $MgSO_4$, 10 mM Tris-HCl and 1 mM EDTA) and stored at 4 °C until use.

The OrganoPlate 2-lane 96 wells plate was used to visualize phage-host interaction over time. An overnight grown culture of MBT86, *E. coli* and *B. subtilis* was inoculated in 0.5% DNB or LB soft agar, while greater than 10^6 phages ml^{-1} were inoculated on the other side of the PhaseGuide to allow free interaction between the channels. Time lapses were recorded using the Lionheart FX Automated Microscope with temperature set at 30 °C for at least 48 h. Images were analysed using Gen5 software. These movies were used to quantify CWD cell formation. To exclude rod-shaped bacteria, only particles with a circularity of 0.8–1.00 were included and every image was checked to prevent that rod-shaped bacteria were included in the analysis.

Cryo-electron microscopy

E. coli spheroplasts and *B. subtilis* protoplasts were produced as described before. After 24 h, the cultures were centrifuged at 300 RPM for 30 min and the pellet was resuspended with 10 nm gold fiducial markers (Cell Microscopy Core, UMC Utrecht) at a 1 : 10 ratio. After 10 min of incubation, approximately 10^8 to 10^{10} phages were added to visualize initial interaction. Of this sample, 3 µl was added to a glow-discharged R2/2 200 mesh holey carbon EM grid (Quantifoil) for 30 s and the sample was blotted for 1 s, after which the grid was plunged in liquid ethane using the Leica GP automated freeze-plunger. The vitrified samples were observed at the Netherlands Center for Nanoscopy

(NeCEN, Leiden). Tilt series of *E. coli* were collected with the 300 kV Titan Krios 2 TEM (Thermo Fisher Scientific) using a X-FEG electron gun and Gatan K2 Summit DED (Gatan Pleasanton). The tilt series ranged from −60 to +60 with a two-degree increment, had a defocus of 8, a pixel size of 4.4 Å and a cumulative dose of 100 electrons per $Å^2$. Tilt series of *B. subtilis* were collected with the 300 kV Titan Krios 1 TEM (Thermo Fisher Scientific) using a S-FEG electron gun and K3 bioquantum (Gatan Pleasanton). The tilt series settings are the same as for *E. coli*. Tomography software (Thermo Fisher Scientific) was used to record the data and IMOD software [133] to reconstruct tomograms.

Results

Filamentous actinobacteria can switch to a CWD state after phage infection

Many filamentous actinobacteria have a natural ability to form CWD cells in response to environmental stressors, after which they can revert to filamentous growth upon the removal of stress [11, 12, 74]. As part of our work to understand the functions of the transition to CWD cells, we focused on *Streptomyces* strain MBT86, a natural isolate from the Qinling mountains, China [94], which has previously been shown to readily produce CWD cells [11]. When bacteria were grown in osmoprotective conditions (LPB medium) in the presence of phage LA7 for at least 24 h, we observed that all remaining cells are CWD after lysis of the dominant mycelial population (Fig. 1a,b; electronic supplementary material, Fig. S1, movie S1). These cells lacked most of their peptidoglycan-based cell wall and were only enveloped by their cell membrane (Fig. 1c,d). Quantification revealed that the number of CWD cells after 24 h was more than 34 times higher in the presence of phage LA7 (204 ± 125 CWD cells, $n = 3$) compared to samples without the phage (6 ± 5 CWD cells $n = 3$). When phage LA7 was added to MBT86 in DNB medium (without osmoprotectants), no CWD cells were found (Fig. 1e; electronic supplementary material, Fig. S1A). Consistent with this observation, the optical density (OD_{600}) of MBT86 culture decreased to undetectable levels within 24 h after addition of the phage, while cultures of MBT86 grown in

osmoprotective LPB medium with phage reached significantly higher densities (OD_{600} = 0.285 ± 0.05 after 24 h). CWD cells were also observed when pre-grown mycelium was exposed to LA7 (electronic supplementary material, Fig. S1C). Viability of CWD cells after phage infection was assessed by determining the number of colony forming units (CFU) after plating mixtures of liquid cultures that still contained the phages. On average 4.1×10^3 CFU ml^{-1} were observed. This translated to approximately 4% of the expected CFU's based on the initial number of spores. As seen in Fig. 1f,g, more bacteria could survive phage infection in osmoprotective LPB medium compared to DNB medium. Furthermore, these colonies consisted of filamentous cells, indicating that the CWD cells had reverted to the canonical mycelial mode-of-growth. Importantly, this demonstrates that a considerable fraction of the population survives phage attack. Moreover, fewer new phages were produced in osmoprotective LPB medium compared to DNB medium with the same starting concentration of approximately 1000 phages ml^{-1} (Fig. 1h). Taken together, these results show that osmoprotective conditions provide MBT86 with a survival mechanism against phage attack, coinciding with a drop in the number of new progeny phages that are produced.

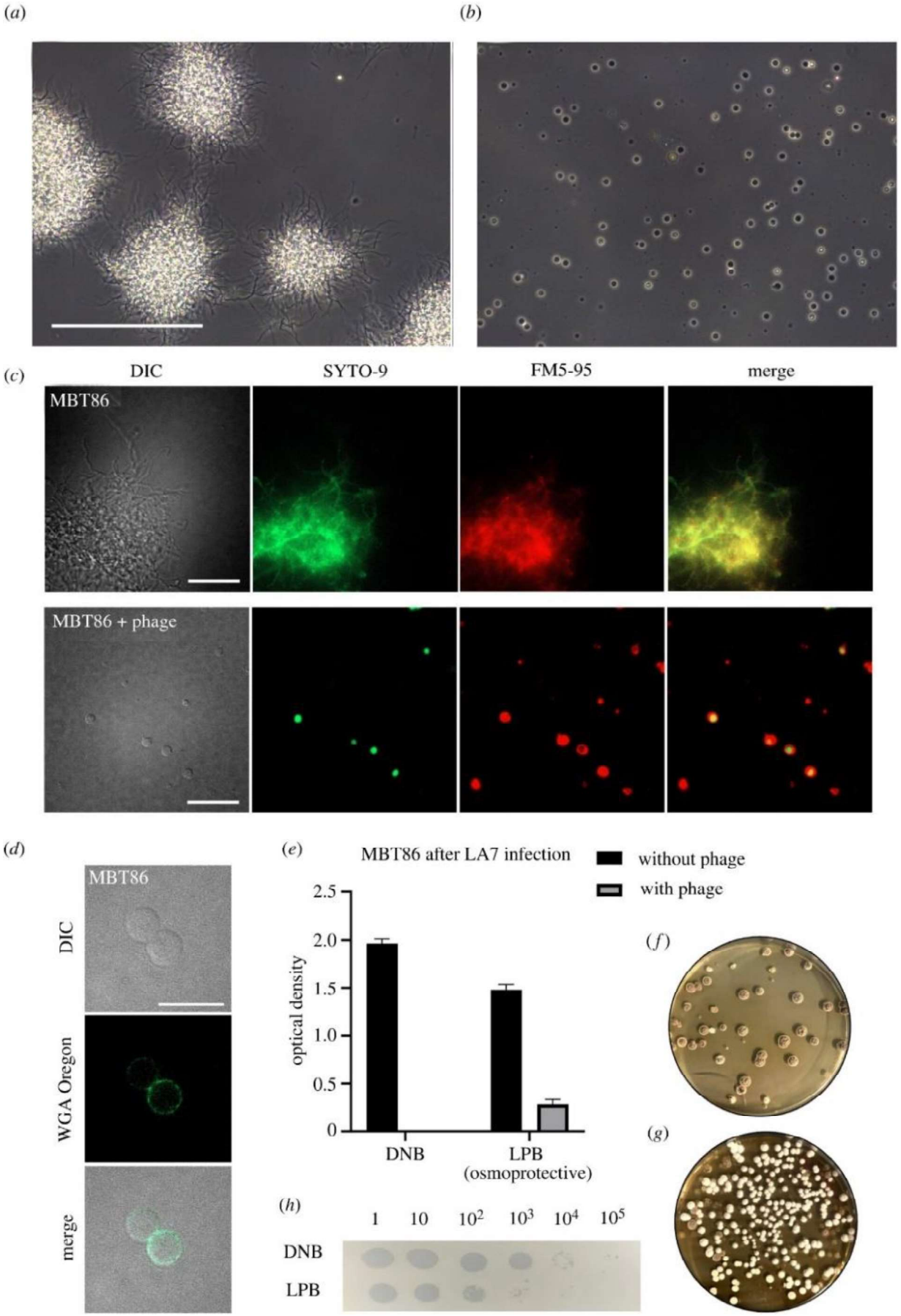
(a)
(b)
(c)
DIC
SYTO-9
FM5-95
merge
MBT86
MBT86 + phage
(d)
MBT86
DIC
WGA Oregon
merge
(e)
MBT86 after LA7 infection
without phage
with phage
optical density
2.5
2.0
1.5
1.0
0.5
0
DNB
LPB
(osmoprotective)
(f)
(g)
(h)
1
10
10^2
10^3
10^4
10^5
DNB
LPB

Figure 1. Formation of CWD cells after phage infection in the actinomycete MBT86. (*a*) Morphology of MBT86 after 48 h in LPB medium. Scale bar represent 100 µm. (*b*) Morphology of MBT86 in LPB medium 24 h after phage LA7 infection. (*c*) Morphology of MBT86 with and without phage LA7 24 h after infection. Cells were stained with the DNA dye SYTO-9 (green) and FM5-95 (red) to dye membranes. Intensity of fluorescence was adjusted for visualization purposes. Scale bars represent 20 µm. (*d*) After 24 h of phage LA7 infection, the resulting CWD cells of MBT86 were stained with the peptidoglycan stain WGA Oregon. Some cells already start to rebuild their peptidoglycan layer. Scale bar represent 10 µm. (*e*) OD_{600} measurement 24 h after phage LA7 infection in DNB medium and LPB medium. The experiment was performed in triplicates with standard deviation presented as error bars. In LPB medium after phage infection, the OD_{600} was still 0.285 ± 0.05. (*f*) Regrowth of MBT86 after phage infection in DNB medium. Note that small mycelial fragments grew back into colonies. (*g*) Regrowth of MBT86 CWD cells after phage infection in LPB medium. Note that these colonies have developmental defects, as seen by a mixture of white and grey colonies. (*h*) Plaque assay showing PFUs of LA7 on DNB and osmoprotective LPB medium. Images were taken 24 h after LA7 infection.

To determine if the response of MBT86 was specific to LA7, we exposed this strain to three other lytic phages to which MBT86 was susceptible (CE2, CE10 and LD10). In all cases, we observed a qualitatively similar response and a marked increase in CWD cells (Fig. 2a,b). However, exposure to phage LA7 yielded more CWD cells compared to exposure to the other phages CE2, CE10 and LD10. This difference might be explained by a variance of virulence between the phages. A lower population size of LA7 phages was observed after 24 h (Fig. 2c), which implies that the bacteria probably had more time to grow into longer mycelial filaments that subsequently resulted in more CWD cells. Next, we tested whether other *Streptomyces* strains than MBT86 would also behave similarly to phage exposure. Notably, the number of CWD cells increased after phage infection in all other tested species (Fig. 2d; electronic supplementary material, Fig. S1D).

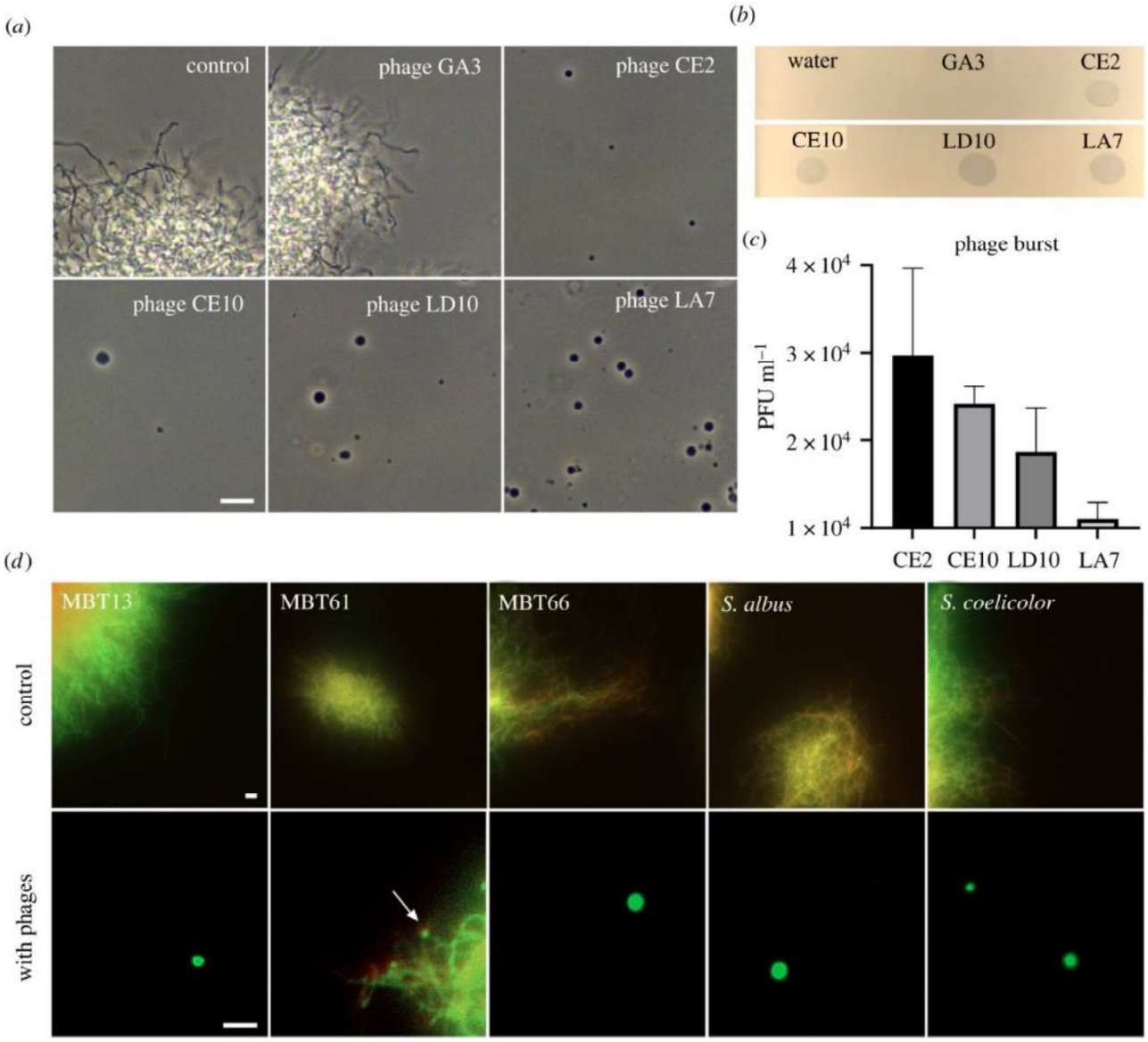

Figure 2. Formation of CWD cells after phage infection is independent of bacteriophage and common in actinomycetes. (*a*) Morphology of MBT86 24 h after infection with phages GA3 (non-susceptible), CE2, CE10, LD10 and LA7 in LPB medium. Phages LD10 and LA7 provoke more CWD cell formation compared to phages CE2 and CE10. Scale bar represents 10 µm. (*b*) Spot assay of the five phages used in panel A. Plaques indicate susceptibility to the host strain MBT86. (*c*) Phage burst measured 24 h after MBT86 infection in DNB medium. (*d*) Morphology of CWD cells after phage infection of *Streptomyces albus, Streptomyces coelicolor* and several actinomycetes from our culture collection (referred to with the prefix MBT). Cells were stained with the DNA dye SYTO-9 (green) and FM5-95 (red) to dye membranes. Note that here, the merged image is shown. Scale bars represent 10 µm.

Exposure to phages leads to CWD *Escherichia coli* and *Bacillus subtilis* cells

Since the formation of CWD cells after phage infection was observed in different *Streptomyces* strains, we wanted to test if this behaviour is also found in other genera. Therefore, we extended our studies to the phylogenetically distant species *Bacillus subtilis* and *Escherichia coli*, which split from *Streptomyces* roughly three billion years ago [134]. Both species were inoculated in osmoprotective LPB medium and exposed to the lytic phages *φ*29 and T4, respectively. 24 h after the addition of the phage, both cultures contained CWD cells, which did not appear to proliferate (Fig. 3). To quantify CWD cell formation after phage infection in soft agar (another osmoprotective environment), samples with and without the addition of phages were analysed. We observed that all *B. subtilis* cells embedded in soft agar adopted a CWD lifestyle approximately 12 h after *φ*29 phage infection (Fig. 4a; electronic supplementary material, movie S2). Without addition of the phage, no CWD cells were observed. A comparable response was observed with *E. coli,* where almost 93% of the surviving cells had adopted a wall-deficient state after 24 h (Fig. 5a; electronic supplementary material, movie S3). To explore whether the formation of CWD cells was due to endolysins extruded by lysed bacteria, a phage infected *B. subtilis* culture in LPB was filtered and only the supernatant was added to a fresh bacterial culture in LPB. However, this did not give rise to CWD cells, suggesting there are insufficient free lytic agents secreted in the medium to induce this response.

Artificially produced CWD cells survive phage infection

To test whether artificially produced CWD cells were susceptible to phage infection, the cell wall was stripped away using lysozyme and/or antibiotics. These cells are referred to as protoplasts for monoderm bacteria and spheroplasts for diderm bacteria, and they do not proliferate without their cell wall. Protoplasts of MBT86 and *B. subtilis* as well as spheroplasts of *E. coli* were seemingly unaffected by phage infection and did not disappear from the culture after exposure to phages LA7, *φ*29 and T4, respectively (electronic supplementary material, Fig. S2). These results provide direct evidence that wall-deficiency provides protection against lytic phages. Interestingly, phages were found near artificially produced spheroplasts of *E. coli* (electronic supplementary material, Fig. S3A). This raised the question whether the phages could attach and maybe even eject their genomic material into wall-deficient cells.

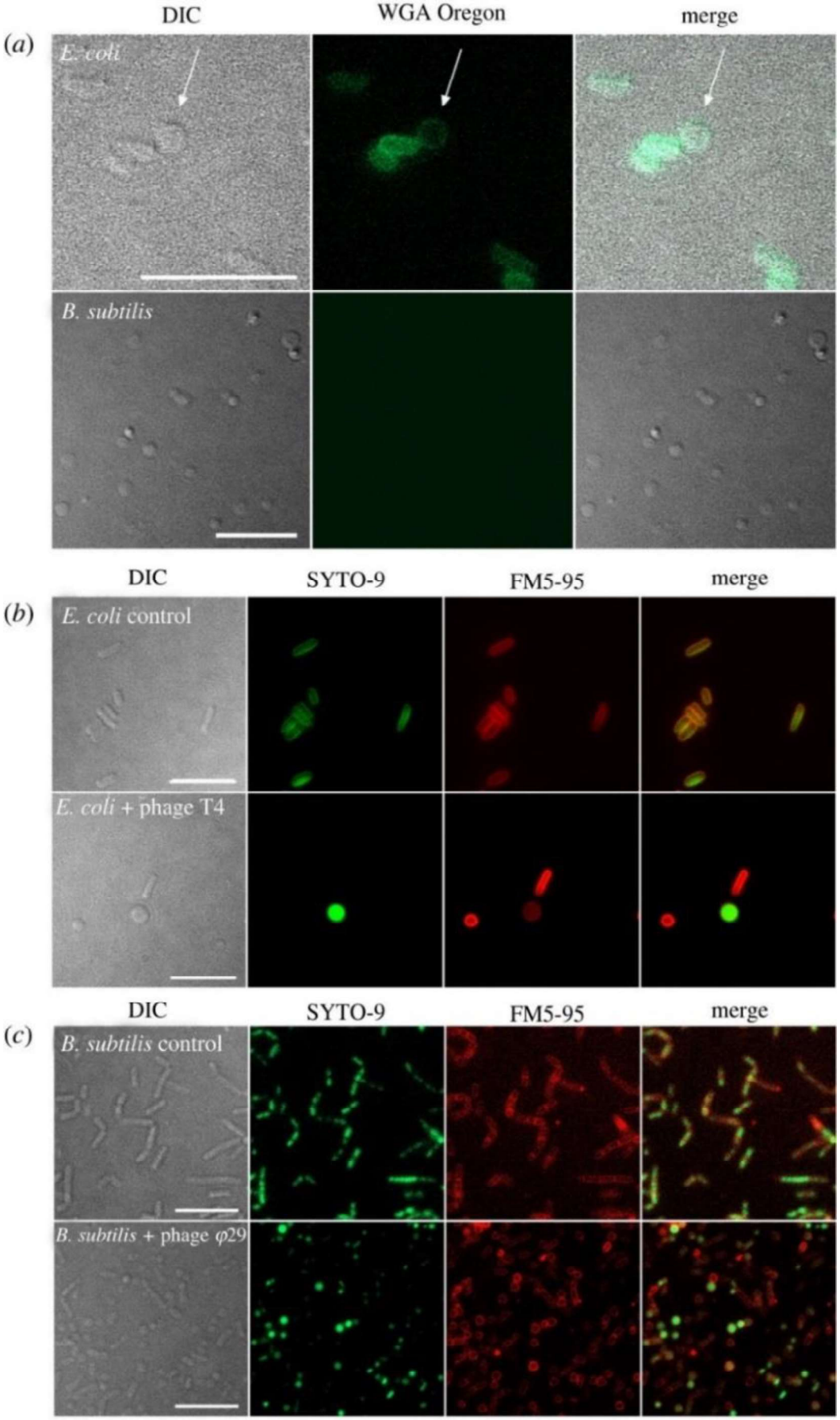
(a)
DIC
WGA Oregon
merge
E. coli
B. subtilis
(b)
DIC
SYTO-9
FM5-95
merge
E. coli control
E. coli + phage T4
(c)
DIC
SYTO-9
FM5-95
merge
B. subtilis control
B. subtilis + phage φ29

Figure 3. Formation of CWD cells after phage infection of *E. coli* and *B. subtilis* in LPB medium. (*a*) *E. coli* and *B. subtilis* were inoculated in LPB medium for 24 h with phages T4 and φ29, respectively. CWD cells were stained with WGA Oregon to visualize peptidoglycan. Note that *E. coli* CWD cells still have some peptidoglycan, while *B. subtilis* cells have none. (*b*) Morphology of *E. coli* with and without phage T4 after 24 h in LPB medium. Cells were stained with the DNA dye SYTO-9 (green) and FM5-95 (red) to dye membranes. (*c*) Morphology of *B. subtilis* with and without phage φ29 after 24 h in LPB medium. Cells were stained with the DNA dye SYTO-9 (green) and FM5-95 (red) to dye membranes. Scale bars represent 10 µm. Note that CWD cells from *B. subtilis* are smaller than CWD cells from *E. coli* and MBT86.

Phages cannot attach to CWD cells of *E. coli* but can attach and propagate in *B. subtilis* CWD cells

To address this question, we used cryo-electron tomography (cryo-ET). The resulting three-dimensional data of *E. coli* spheroplasts with phage T4 revealed a highly heterogeneous sample with an inconsistent appearance of CWD cells and outer membrane vesicles (electronic supplementary material, Fig. S3B-C, movie S4). However, no phage attachment was observed for any of the CWD cells or cell fragments that were imaged. Interestingly, cryo-ET data of *B. subtilis* showed that bacteriophage φ29 was not only able to attach to protoplasts of *B. subtilis* (figure 4*b*) but could also eject DNA into the cells and propagate. We observed attached phages with filled as well as empty capsid heads (indicating DNA ejection). Furthermore, we detected filaments inside some protoplasts that were surrounded by phages (Fig. 4c; electronic supplementary material, Fig. S4, movie S5). These filaments strongly resemble p1 proteins that are associated with φ29 DNA replication [135].

In both *B. subtilis* and *E. coli*, significantly more bacteria survived a phage infection in the osmoprotective LPB medium compared to LB medium (Fig. 4d and 5b). In addition, *B. subtilis* grown in LPB medium and pre-made protoplasts produced similar amounts of φ29 progeny, in contrast to LB medium, where a significantly higher phage titre was observed over time (Fig. 4e). When the same experiment was performed with *E. coli*, we again noticed increased levels of phage T4 in LB medium and significantly fewer T4 progeny in LPB medium over time, as opposed to spheroplasts, that did not produce any progeny at all (Fig. 5c). These results are in line with our cryo-ET data showing that phage φ29 was able to attach and propagate in protoplasts of *B.*

subtilis, while phage T4 was not observed in association with any *E. coli* spheroplasts remnants (Fig. 5d,e).

Altogether, our results imply that transiently lacking or shedding a cell wall is a common and general escape mechanism against phage attack.

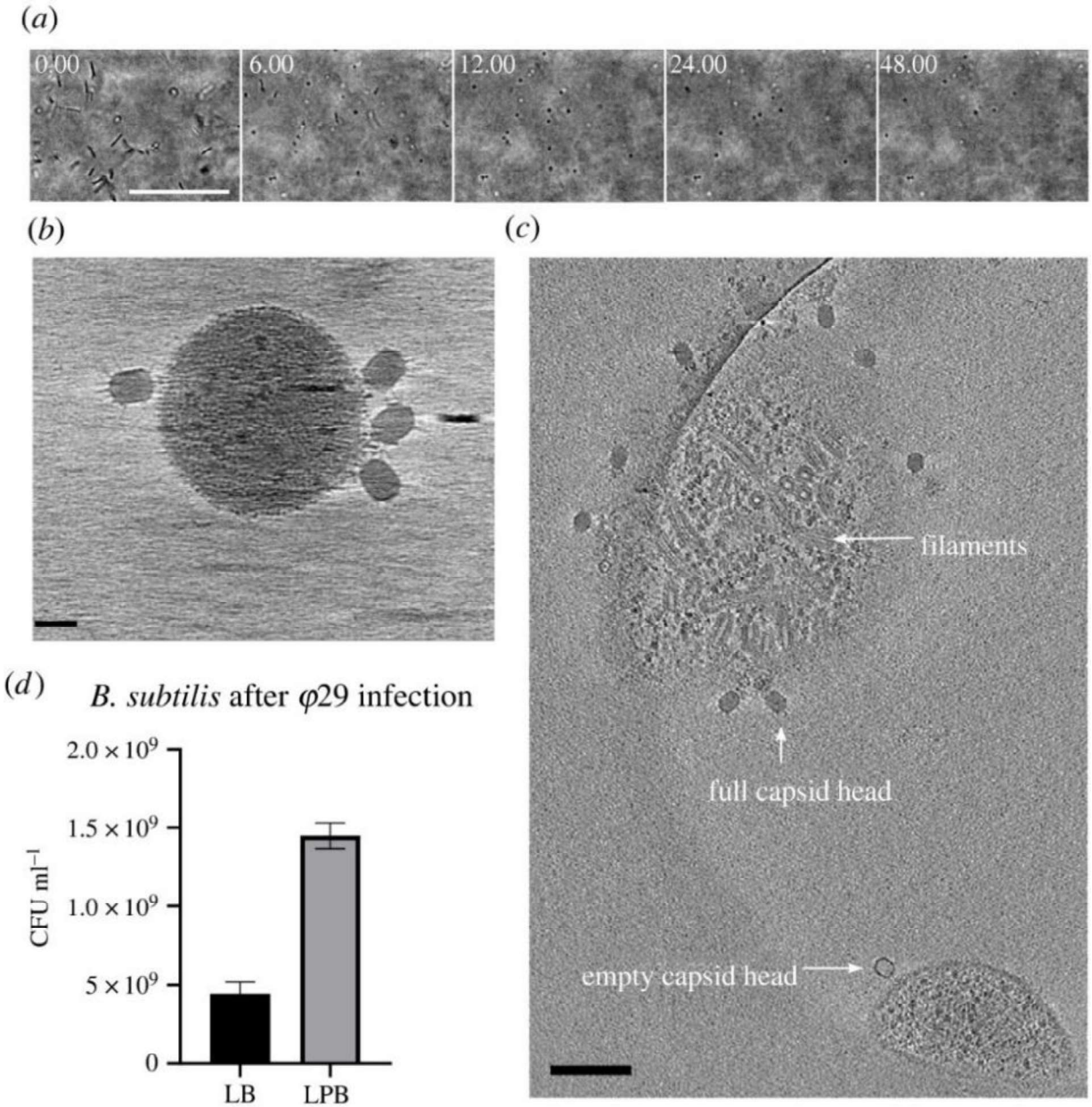
(a)
0.00
6.00
12.00
24.00
48.00
(b)
(c)
filaments
full capsid head
empty capsid head
(d)
B. subtilis after φ29 infection
2.0 × 10^9
1.5 × 10^9
1.0 × 10^9
5 × 10^9
0
CFU ml^−1
LB
LPB
(e)
φ29 phage production
10^11
10^10
10^9
10^8
10^7
10^6
10^5
10^4
PFU ml^−1
0 2 4 6 8 10 12 14 16 18 20 22 24
h
LB
LPB
protoplasts

Figure 4. Growth, cryo-ET and infection rate of *B. subtilis* after *φ*29 phage infection. (*a*) Time lapse of *B. subtilis* after *φ*29 phage infection followed for 48 h. Individual micrographs were taken from electronic supplementary material, movie S1. Scale bars represent 50 µm. (*b*) Four *φ*29 phages with full capsid heads attaching to the membrane of a CWD *B. subtilis* cell. Scale bar represents 30 nm. (*c*) A tomography snapshot of *B. subtilis* protoplasts with *φ*29, see electronic supplementary material, movie S3 for the full tomography. On the bottom is an empty phage attaching to a protoplast, while on top there is a protoplast filled with filaments associated with phage *φ*29 DNA assembly. Scale bar represents 100 nm. (*d*) CFUs of *B. subtilis* 24 h after phage infection with *φ*29 in LB medium and LPB medium. Significantly more cells survive in LPB medium ($p < 0.0001$). (*e*) Phage *φ*29 production measured in plaque forming units (PFU)/ml in LB and LPB media with protoplasts as a negative control. The *φ*29 production in LB media compared to LPB media is significantly different ($p < 0.027$) at $t = 24$. Statistical analysis was performed with a Student's *t*-test.

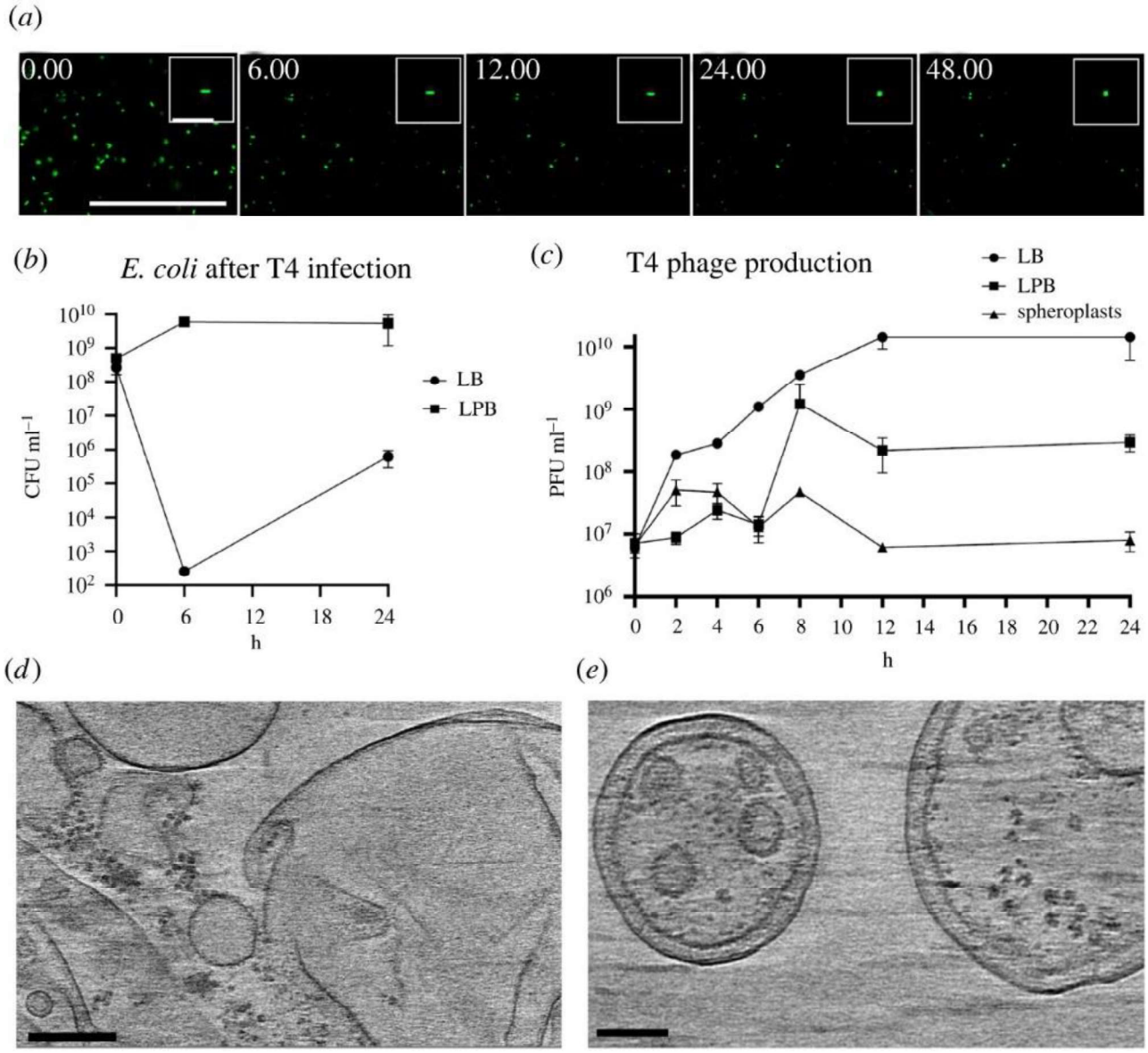

Figure 5. Growth and infection rate of *E. coli* after T4 phage infection. (*a*) Time lapse of green fluorescence *E. coli* after T4 phage infection followed for 48 h. Individual micrographs were taken from electronic supplementary material, movie S1, in which more details are visible. Scale bars represent 100 µm and 10 µm for the inlays. (*b*) CFUs of *E. coli* over time after phage infection with T4 in LB medium and LPB medium. More cells survive after 24 h in LPB medium ($p = 0.09$). (*c*) T4 phage production measured in PFU ml^{-1} in LB and LPB media with spheroplasts as a negative control. The T4 production in LB media compared to LPB media is significantly different ($p < 0.05$) for each timepoint after $t = 0$. All statistical analysis was performed with a Student's *t*-test. (*d*) Typical view of *E. coli* tomography data showing empty vesicles and outer membrane fragments. No attached phages were observed in any of the datasets. (*e*) Spheroplasts with both an inner and outer membrane, without phages in proximity. Scale bars represent 200 nm.

Discussion

The arms race between bacteria and bacteriophages has resulted in the evolution of many antiphage-defense mechanisms, which we recently started to uncover [49, 136]. In this study, we have discovered a yet unknown general escape mechanism against phage attack for both the diderm model organism *E. coli*, the monoderm *B. subtilis*, and various filamentous actinomycetes. By contrast to L-forms, the CWD cells produced after phage infection are not able to proliferate and will switch back to the walled mode-of-growth in favourable conditions [11, 137]. Besides the species tested here, many more bacteria may be capable of surviving phage infection in osmoprotective medium. In standard hypotonic cultivation media without high levels of osmolytes, phages produce endolysins that degrade the bacterial cell wall and cause lysis. For *B. subtilis* it has been shown that prophage-encoded endolysins in LB medium resulted in the release of membrane vesicles that immediately burst [138]. However, our results show that the addition of spent media from cultures exposed to phages did not result in the formation of CWD cells in LPB medium. We hypothesize that the concentration of endolysins in the supernatant is either not high enough to initiate the conversion to CWD cells, or these wall-deficient cells are simply a result of the initial attachment or DNA ejection of phages in supportive medium. However, the exact mechanism behind the phenomena of bacteria shedding their cell wall in response to bacteriophages in osmoprotective medium remains to be uncovered. In nature, bacteria may encounter such osmoprotective environments, such as inside eukaryotic host cells, plant sap with high levels of osmolytes or in soil after rain [22, 66, 139-141].

Cryo-ET allowed us to observe the distinct interaction between bacteriophages and CWD cells. To our knowledge, this is the first time the interaction of CWD cells and bacteriophages was captured in detail. We showed that φ29 was able to attach, eject DNA and even produce new progeny phages in *B. subtilis* protoplasts, as indicated by the observed filaments inside protoplasts [135]. Phage φ29 normally binds to glycosylated teichoic acid in the cell wall [142], but can sporadically also attach to fragments of lipoteichoic acids in the membrane of protoplasts [143, 144]. For CWD *E.*

coli cells, it was hypothesized that T4 could recognize OmpC and lipopolysaccharide on the remaining outer membrane [30]. However, three-dimensional cryo-ET imaging revealed that T4 phages were not attached to remnants of *E. coli* spheroplasts. On the other hand, a recent paper from Petrovic Fabijan *et al.* showed that T4 was able to eject DNA in L-forms of *E. coli*, but no cells were lysed [79]. Perhaps the difference in attachment of phages could be explained by the fact that L-forms are able to proliferate, whereas spheroplasts cannot. However, no new progeny phages were produced in either L-forms or spheroplasts of *E. coli* and we observed an increased survivability in both forms of CWD cells. Not only *E. coli*, but also MBT86 and *B. subtilis* have a significantly higher survival after phage attack in osmoprotective medium by adopting a CWD state, compared to walled cells in normal medium.

Phage therapy is considered a promising alternative to treat antibiotic-resistant infections [66]. However, in this study, we have shown that both diderm and monoderm bacteria can escape phage attack by adopting a cell-wall-deficient lifestyle. These CWD cells can arise in osmoprotective environments in nature, or in the presence of cell wall targeting antibiotics. Whereas commonly known phage defense mechanisms like restriction modification or CRISPR/Cas can protect bacteria against specific phages, CWD cells might be resistant to a broad range of phages, which warrants a careful analysis of the interaction between phages and their host.

Supplementary data

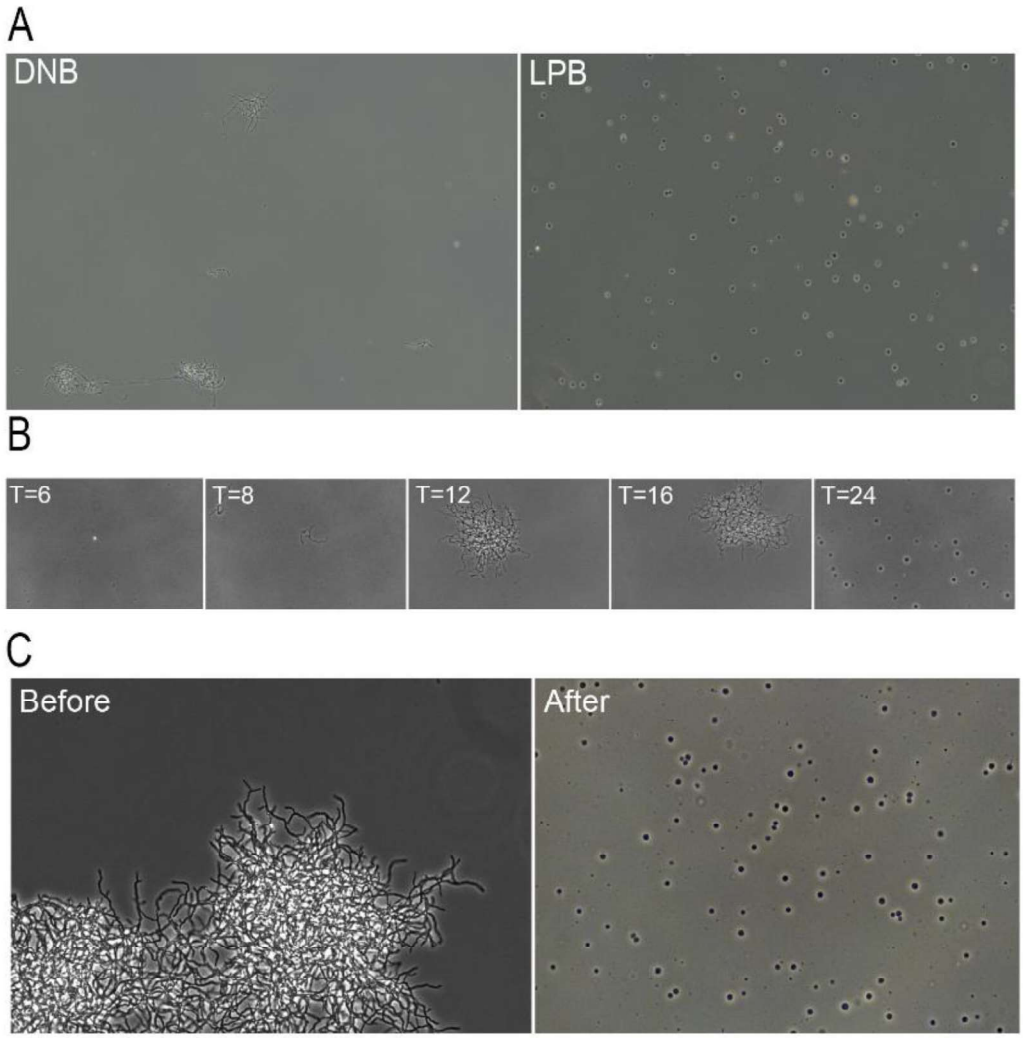

Figure S1. Morphology of actinomyces after phage infection. (A) Morphology of MBT86 after 24 hours of phage infection with LA7 in DNB medium and LPB medium. (B) MBT86 spores and phage LA7 were inoculated simultaneously in LPB medium at T=0. After approximately 8 hours, the spores start to form mycelial fragments that turned into CWD cells after 24 hours. (C) MBT86 spores were pre-grown for 24 hours to form mycelium in LPB before phage LA7 was added. After another 24 hours, only CWD cells were observed. (D) CWD cells were counted with an hemacytometer in duplo of several *Streptomyces* strains in LPB with and without phages.

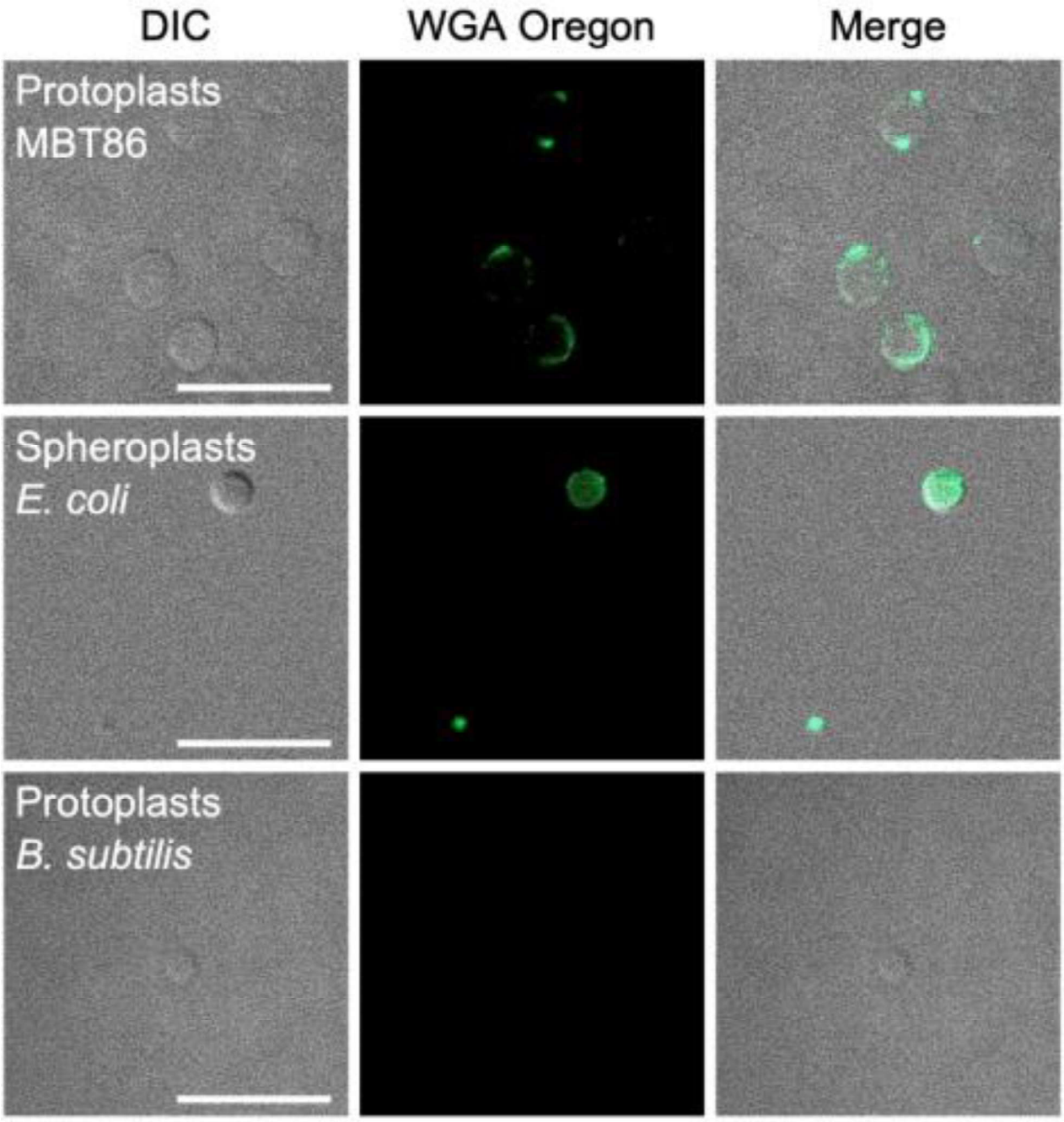

Figure S2. Artificially produced CWD cells survive phage infection. MBT86 protoplasts (first panel), *E. coli* spheroplasts (second panel) and *B. subtilis* protoplasts (third panel) were grown in LPB medium with either phage LA7, T4 or φ29 and imaged after 24 hours. Cells were stained with WGA Oregon to visualized peptidoglycan. Protoplasts of *B. subtilis* have no peptidoglycan, similar to *B. subtilis* CWD cells formed after phage infection. Scale bars represents 10μm.

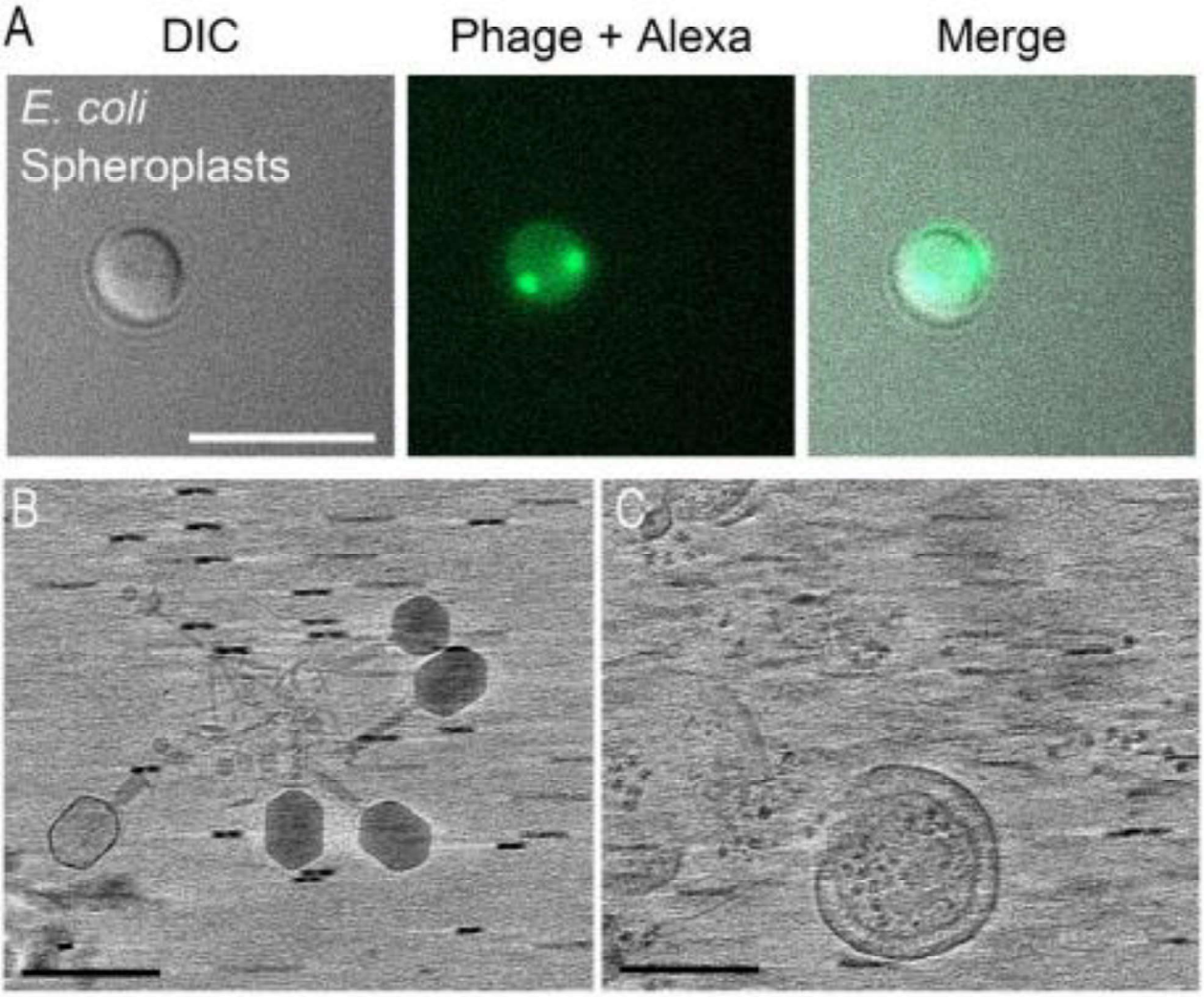

Figure S3. Heterogeneous appearance of *E. coli* spheroplasts with phage T4. (A) *E. coli* strain ET8 spheroplasts were imaged 24 hours after inoculation with phage T4 that were previously dyed with Alexa Fluor™ 488 NHS-Ester. The CWD cells did not lyse and phages surrounded the cells as indicated by fluorescent green dots. Scale bars represents 10μm. (B) Four unattached phages with a full capsid head and one with an empty capsid head. (C) Image of spheroplast fragments taken from the same tomogram as panel B. Phages were in close proximity to these fragments but not attached. Scalebars represent 200 nm.

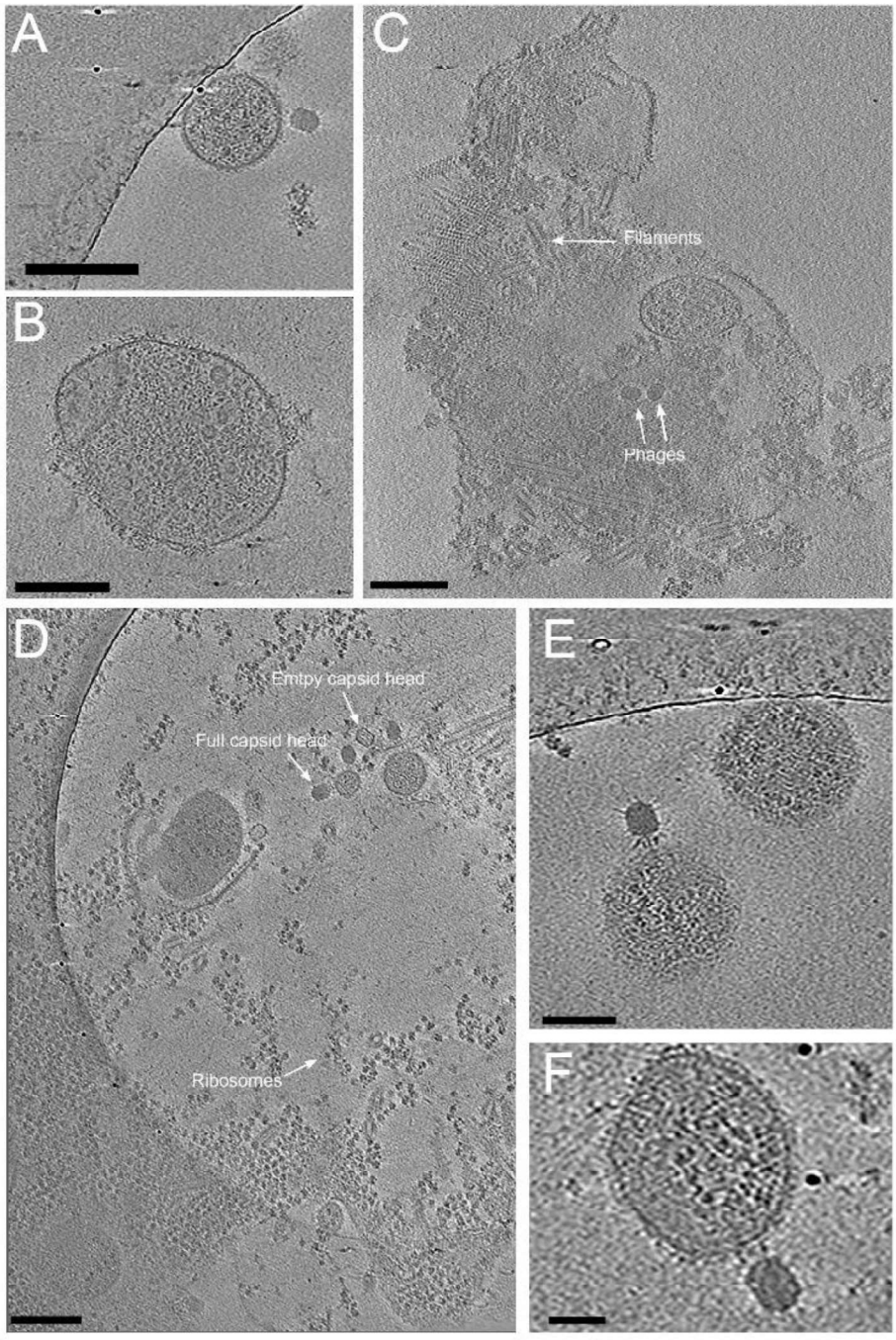

Figure S4. Phage Φ29 can attach to *B. subtilis* protoplasts and produce progeny. (A) One φ29 phage attaching to a *B. subtilis* protoplasts. (B) A protoplast with ribosomes and filaments inside. (C) An exploding protoplast extruding phages, filaments and cell debris in the environment. (D) A protoplast exploding at the bottom and phages with full and empty capsid heads attaching to CWD cells at the top. (E) Phage φ29 with a retracted sheet in the process of ejecting DNA inside a protoplast. (F) Phage φ29 attaching to a protoplast. Scale bars represent 70 nm (panel A), 50 nm (panel E and F) and 200 nm (panel B, C and D).

Table S1. Strains used in this study

Strains	Genotype	Reference
Bacterial strains		
E. coli RP437	*thr-1 araC14 leuB6(Am) fhuA31 lacY1 tsx-78 λ- eda-50 hisG4(Oc) rfbC1 rpsL136(strR) xylA5 mtl1 metF159(Am) thiE1*, with pBTOK-sfGFP	Lab collection
E. coli ET8	Wildtype	Lab collection
Bacillus subtilis	Type strain 110NA	Franklin Norbrega, DSMZ
Streptomyces coelicolor (A3)2 M145	Wildtype	Lab collection
Streptomyces albus G. ATCC 25426	Wildtype	Lab collection
Streptomyces lividans 1326	Wildtype	Lab collection
Streptomyces sp. MBT13	Wildtype	Lab collection
Streptomyces sp. MBT61	Wildtype	Lab collection
Streptomyces sp. MBT66	Wildtype	Lab collection
Streptomyces sp. MBT86	Wildtype	Lab collection
Phages		
T4	Wildtype, host: *E. coli*	Lab collection
Φ29	Wildtype, host: *B. subtilis*	Franklin Norbrega
Phage CE2	Wildtype, host: *Streptomyces coelicolor*	This work
Phage CE3	Wildtype, host: *Streptomyces coelicolor*	This work
Phage CE10	Wildtype, host: *Streptomyces coelicolor*	This work
Phage GA3	Wildtype, host: *Streptomyces griseus*	This work
Phage LA7	Wildtype, host: *Streptomyces lividans*	This work
Phage LD10	Wildtype, host: *Streptomyces lividans*	This work

Movie S1. Time laps of MBT86 mycelium embedded in 0.5% DNB soft agar followed for 48 hours after LA7 infection. The mycelium is losing density over time and starts to produce CWD cells after approximately 12 hours. Images were acquired automatically every 30 minutes for at least 48 hours.

Movie S2. Time laps of *B. subtilis* embedded in 0.5% LB soft agar followed for 48 hours after φ29 infection. After 12 hours, all rod-shaped cells have switched to a spherical morphology. Images were acquired automatically every 30 minutes for at least 48 hours.

Movie S3. Time laps of green fluorescent *E. coli* embedded in 0.5% LB soft agar induced with 20ng/ml anhydrotetracycline followed for 48 hours after T4 infection. Most bacteria lyse within 6 hours, but some persistent CWD cells survive. Images were acquired automatically every 20 minutes for at least 48 hours.

Movie S4. Tomogram of *E. coli* spheroplasts with five phages that did not attach to the cells.

Movie S5. Tomogram of *B. subtilis* protoplasts filled with filaments associated with phage DNA assembly and φ29 attaching to the membrane with full capsid heads and on the bottom a phage with an empty capsid head.

Chapter 6

YidC2 is required for insertion of the holin-endolysin system during phage infection in *Streptomyces coelicolor*

Véronique Ongenae, Xiaobo Zhong, Bas Leemburg, Chiara Foini, Livia Pietrow, Koen Bruijn, Jorrit Boekel, Daniël Rozen, Gilles P. van Wezel, Ariane Briegel and Dennis Claessen

Abstract

Bacteriophage infection has been extensively studied, but the molecular mechanism of a successful infection cycle remains largely unknown. Here, we show that phage CF3 needs the host membrane protein insertase YidC2 to successfully complete its infection cycle in *Streptomyces coelicolor*. Adsorption assays and cryo-electron microscopy revealed that phage CF3 could attach and inject its DNA in a strain lacking YidC2, but was unable to subsequently induce lysis of the bacteria. Additionally, robust interactions between the holin-endolysin system of the phage and the YidC2 protein of *S. coelicolor* were observed and the block in phage release in the *yidc2* mutant could be overcome by Sec-dependent endolysin secretion. Therefore, we propose that the holin-endolysin system of phage CF3 exploits the membrane insertase YidC2 to complete the phage infection cycle. Additionally, our findings suggest that YidC2 is critical for maintenance of cell wall-deficiency following phage infection. Altogether, our work contributes to a deeper understanding of the intricate dynamics between bacteria and bacteriophages, shedding light on the molecular mechanisms of phage infections.

Introduction

Bacteriophages, or phages in short, are viruses that can infect bacteria. They represent the most abundant biological entities in nature and play an instrumental role in all ecosystems [19]. The interaction between phages and their hosts has been extensively studied, but mostly in unicellular model organisms like *Escherichia coli*, *Bacillus subtilis* and *Pseudomonas aeruginosa* [13, 14, 145-147]. The molecular mechanism behind the phage infection cycle in non-model bacteria remains largely unknown. The multicellular lifestyle of *Streptomyces* is unique in the bacterial realm and starts when a spore enters a favorable environment. This causes spores to germinate, leading to the formation of vegetative hyphae. These hyphae elongate and branch, forming a dense interconnected network of filaments, called a mycelium. Upon nutrient scarcity, *Streptomyces* undergoes a process of differentiation, which involves the formation of specialized hyphae that grow into the air to form spores again [4]. Concomitant with this morphological differentiation, chemical differentiation is initiated, leading to the production of antibiotics and other specialized metabolites [104, 148-150]. Previous research has shown that phages cannot infect spores, while young germinating spores are the most vulnerable developmental stage for phage infection [112]. In addition, recent research showed that aerial hyphae and spores are formed in response to phage infection to suppress further spread of phages [17].

Most research on *Streptomyces*-phage interactions has been focused on the characterization of defense systems against phage attack, like chemical defenses [51, 151], the phage-growth limitation system [91] and many more [152]. One recently discovered escape mechanism against phage attack is the ability of *Streptomyces* to become cell wall-deficient (CWD) [93]. Without their cell wall, the usual receptor molecules like peptidoglycan, teichoic acids or proteins associated with the cell wall are lost and bacteriophages can no longer infect the bacterial cell. After evasion of phage predation, the cell wall-deficient cells of *Streptomyces* can revert to their canonical mycelial mode-of-growth [93, 153].

During lytic phage infection, the host cell's metabolism is exploited and directed towards supporting the production of new progeny phages. Phages

can encode their own proteins to carry out key cellular functions, or rely on the host metabolism to complete their infection cycle [154]. A critical step following the assembly of new phages is lysis of the host to release progeny phages in the environment. Therefore, phages use so-called holins that are inserted in the bacterial membrane. These holins enable the passage of endolysins across the membrane that subsequently cleave the peptidoglycan layer. Especially in multicellular bacteria, little is known about the host machinery required for phage production and bacterial lysis. However, if a phage is fully dependent on host proteins, the host might mutate or eliminate proteins that the phage requires, to prevent successful phage reproduction.

Here, we show that YidC2 of *Streptomyces coelicolor* plays a key role during infection of phage CF3, which is a temperate phage classified in the genus *Camvirus*. YidC2 is predicted to be a membrane protein insertase required for inserting proteins into the membrane [155, 156]. We found that phage CF3 was unable to complete its infection cycle in a Δ*yidc2* mutant. Adsorption assays and cryo-electron microscopy revealed that phage CF3 could still attach and infect *S. coelicolor* Δ*yidC2*, but progeny phages remained stuck inside the bacteria. Additionally, we found interactions between the holin-endolysin system and the YidC2 protein with bioinformatics and a bacterial two-hybrid assay. Notably, the block in phage release in the Δ*yidc2* mutant could be overcome by secretion of additional endolysins in a Sec-dependent manner. Altogether, we hypothesize that the holin-endolysin system of phage CF3 requires YidC2 for proper insertion in the bacterial membrane to complete the phage infection cycle and subsequently, lyse the bacteria.

Material and methods

Strains and growth conditions

All bacterial strains and phages used in this study are described in Table S1. *Streptomyces* strains were grown for five days on Soy Flour Mannitol (SFM) at 30 °C to collect spores. For growth of *Streptomyces* in liquid, Difco Nutrient Broth (DNB) or L-phase broth (LPB) were used [11].

Construction of *S. coelicolor* Δ*yidC2*

All plasmids and primers used in this study are listed in Table S2 and Table S3, respectively. To delete *yidC2* in *S. coelicolor*, PCR targeted mutagenesis was performed [157]. In short, *Escherichia coli* BW25113/pIJ790 containing cosmid E20 (containing *yidC2,* SCO2851) was transformed with an integrating PCR product carrying an apramycin resistance cassette. This PCR product was generated by using primers E20_KOF and E20_KOR. After introduction of the PCR product and recombination, *E. coli* colonies with the mutated cosmid were selected by being resistant to both apramycin and kanamycin. The mutated cosmid was isolated and transformed into *E. coli* ET12567/pUZ8002, which was then used for conjugation to *S. coelicolor*. Ex-conjugants that were apramycin resistant and kanamycin sensitive were picked and verified by southern hybridization for loss of the *yidC2* gene [158].

Construction of Sec-endolysin and Sec-eGFP secretion strains

Genomic DNA of *Streptomyces coelicolor* M145 or phage CF3 and plasmids pCB-1 [159] or pGWS758 [160] were used as templates to amplify coding sequence of Sec signal peptides (SPs)/YidC2, the coding sequence of the holin-endolysin of phage CF3, the cumate-inducible promoter and the coding sequence of eGFP, respectively. All genes were expressed using the integrative plasmid pIJ82Cu harboring a cumate-inducible promoter. To create pIJ82Cu, the promoter region of pCB-1 was amplified using primers IDProm-F and IDProm-R creating a 5' NdeI restriction enzyme site. The amplified product was then inserted into the plasmid pIJ82 that has been linearized with BamHI via Gibson assembly.

To create *S. coelicolor* strains expressing Sec-secreted variants of the endolysin of phage CF3 and eGFP, both genes were placed behind the sequence encoding the N-terminal SP of SCO5376 [161] under control of the cumate-inducible promotor [162]. Therefore, primer pairs SecGFP-F1/SecGFP-R1 and SecGFP-F2/TatGFP-R2 primers were used to amplify the SP of SCO5376 and eGFP, respectively. For creation of the Sec-secreted endolysin variant, primer pairs SecGFP-F1/SecEndo-R1 and SecEndo-F2/TatEndo-F2 were used to amplify the SP of SCO5376 and endolysin, respectively. Subsequently, Gibson assembly was use to insert the amplified product pairs into plasmid pIJ82Cu that had been linearized with NdeI digestion, generating plasmids, pIJ82Cu-SecGFP and pIJ82Cu-SecEndo.

To express the endolysin and eGFP signal sequence under the control of the cumate-inducible promoter, both genes were amplified with GFP-F/TatGFP-R2 and Endo-F/TatEndo-F2, respectively. The amplified products were subsequently inserted into pIJ82Cu that has been linearized with NdeI digestion via Gibson assembly, yielding pIJ82Cu-GFP and pIJ82Cu-Endolysin, respectively. Conjugation [130] and heat-shock transformation [163] were used to introduce plasmids into *Streptomyces* and *E. coli* cells, respectively.

Bacteria-phage interactions

Phage stocks were isolated as described previously [111]. Briefly, bacteriophages were added to DNB cultures containing *S. coelicolor* spores at Multiplicity of Infection (MOI) = 0.1. After overnight incubation at 30 °C (200 RPM), phages were filtered through a 0.22 µm filter for phage stocks of ~10^7 phages ml^{-1}.

Plaque assays were used to determine if phages could infect the *S. coelicolor* mutant strains. To this end, phages were serial diluted in DNB medium and 3 µl was spotted in duplicate on a DNB double agar overlay plate containing the strain of interest. After overnight incubation at 30 °C, individual plaques were quantified. To test the interaction in liquid, bacteria and phages were inoculated at MOI=1 in 10 ml DNB or LPB and incubated overnight at 30 °C, while shaking at 200 RPM. To test whether *S. coelicolor* Δ*yidC2* could make chemically induced CWD cells, 0.2 mg ml^{-1} lysozyme or 0.5 mg $µl^{-1}$ mitomycin C was added to the spores in LPB medium.

Bacterial two-hybrid assay

To assess protein interactions, a bacterial two-hybrid assay was used, which was essentially performed as described [164]. Interactions of LpmP and CslZ were used as the positive control [164]. Primer pairs ThYidC2-F/ThYidC2-R, ThHolin-F/ThHolin-R and ThEndo-F/ThEndo-R were used to amplify the genes encoding YidC2, holin and endolysin, respectively, using genomic DNA of *S. coelicolor* or phage CF3 as the template. Amplified products were ligated into either plasmids pKT25 or pUT18C using XbaI and EcoRI restriction enzyme sites, generating pKT25-YidC2, pKT25-Holin, pKT25-Endolysin, pUT18C-YidC2, pUT18C-Holin and pUT18C-Endolysin, respectively.

Conjugation [130] and heat-shock transformation [163] were used to introduce plasmids into *Streptomyces* and *E. coli* cells, respectively.

Membrane fluidity

Membrane fluidity was measured as previously described [165]. In short, three biological replicates of 20 ml of 16 hour-old mycelium were centrifuged for 10 minutes at 2,500 RPM and washed three times in 5 ml PBS buffer. The pellet was resuspended in 100 µl PBS containing 1 mM Laurdan (6-Dodecanoyl-N, N-dymethyl2-naphthylamine, Sigma) dissolved in dimethylformamide (DMF) and allowed to incubate in the dark for 10 minutes at 30 °C, 200 RPM. The stained mycelia were collected and washed twice in pre-warmed PBS with 1% DMF and subsequently resuspended in 100 µl pre-warmed PBS buffer. The dye was excited at 350 nm and fluorescence was measured at 435 and 490 nm using a Zeiss LSM900 Airyscan 2 microscope with the climate control chamber set at 30 °C. Images of the hyphal tips were used to calculate membrane fluidity with the corresponding generalized polarization (GP) value as described before [166]. Statistical analysis was performed using a Student's *t*-test.

Adsorption assay

To determine if phage CF3 could attach to the bacterial hosts, adsorption assays were performed. In short, 10^7 spores were inoculated in 10 ml DNB broth in triplicate and allowed to germinate for four hours for *S. coelicolor* and seven hours for *S. coelicolor* Δ*yidC2* at 30 °C, while shaking at 200 RPM. At timepoint zero, 10^5 phages ml^{-1} of phage CF3 were added to the cultures and every ten minutes, 100 µl samples were collected and immediately filtered through a 0.22 µm filter. Plaque assays were performed on strain MBT61 and after overnight incubation at 30 °C, plaque-forming units (PFU) were calculated and normalized to 100% free phages at timepoint zero. The effect of penicillin G (0.4 mg ml^{-1}), rifamycin (50 µg ml^{-1}), or lysozyme (0.2 mg ml^{-1}) on phage release in the *yidC2* mutant was evaluated by adding these compounds at T=0. The adsorption assay with the Δ*yidC2* Sec-endolysin strain was performed similarly, but after 60 minutes of infection with phage CF3, the release of endolysin through the Sec-secretion pathway was induced by adding 100µM of cumate.

Microscopy

To image the formation of cell wall-deficient cells, a Zeiss Axio Lab A1 upright microscope, equipped with an Axiocam 105 colour (resolution of 5 megapixel) camera was used to take bright field images. eGFP expression after cumate induction was imaged using a Zeiss LSM900 Airyscan 2 microscope at excitation and emission wavelengths of 488 nm and 509 nm, respectively. Images were adjusted using OMERO software [167].

To examine the morphology of phage CF3, transmission electron microscope (TEM) was used. To prepare a single grid, 3 µl of phage CF3 diluted in DNB medium (~10^4 phages ml^{-1}) was pipetted on a glow-discharged 200 mesh carbon coated copper grid (EMS). After 30 seconds, excess liquid was removed with filter paper. Next, the phages were stained with 2% uranyl acetate for 45 seconds, after which excess staining was removed and the grids were air-dried for 5 minutes. Negative staining images were recorded using a single tilt specimen holder inside a 120 kV Talos L120C TEM with a Lab6 electron source and Ceta detector at the Netherlands Center for Nanoscopy (NeCEN, Leiden).

Cryo-EM was used to investigate *S. coelicolor* Δ*yidC2* after infection with phage CF3. In short, spores were allowed to germinate for seven hours in DNB broth. Afterwards, the germlings were centrifuged for 10 minutes at 5,000 RPM and the bacterial pellet was dissolved in 100 µl lysate of phage CF3 (10^7 phages ml^{-1}). After 30 minutes of infection at room temperature, the culture was resuspended with 10 nm gold fiducial markers (Cell Microscopy Core, UMC Utrecht) at 1:25 ratio. Of this sample, 3 µl was added to a glow discharged R2/2 200 mesh holey carbon EM grid (Quantifoil). After 30 seconds of incubation, the sample was blotted for one second and immediately plunged in liquid ethane with the Leica GP automated freeze-plunger. The grids were observed inside the 120 kV Talos L120C TEM with a Lab6 electron source and Ceta detector at the Netherlands Center for Nanoscopy (NeCEN, Leiden).

Bioinformatic analysis

Protein structures and interactions between proteins were predicted by Alphafold 3.0 [168] and protein membrane topology and transmembrane domains were predicted by DeepTMHMM [169]. Sequence alignments were made with NCBI MSA sequence viewer [170].

Results

YidC2 plays an important role in phage infection

The molecular mechanism of phage infection in bacteria remains largely unknown. To identify host components required for successful completion of the phage infection cycle in *Streptomyces*, we systematically screened a large collection of *S. coelicolor* mutants for their susceptibility to our *Streptomyces* phage collection (Fig. S1). In short, 46 phages were spotted in duplicate on plaque assays with 28 different *S. coelicolor* strains lacking distinct cell wall-associated proteins. When lysis zones looked visually different compared to the WT plaque assay, serial dilutions were performed. Most phages did not show a difference in lysis zone formation in the mutants. However, when phage CF3 was serial diluted and spotted onto a lawn of *S. coelicolor* Δ*yidC2* in a double agar overlay assay (Fig. 1A), it was unable to form plaques. This suggests an interruption in the phage infection cycle. To validate these observations, we introduced phage CF3 to both the *yidC2* mutant and the parental strain in osmoprotective LPB medium, known to cause the formation of CWD cells during phage infection [93]. While the parental strain generated CWD cells following infection, the *yidC2* mutant persisted as mycelium (Fig. 1C), underscoring the necessity of YidC2 for completing the infection cycle.

Since *S. coelicolor* Δ*yidC2* could still be infected by phage CD8, we tested if this phage could still induce the shedding of the bacterial cell wall in LPB. However, *S. coelicolor* Δ*yidC2* did not form CWD cells after infection in osmoprotective medium with this phage. Interestingly, mitomycin C, a chemical that induces the lytic cycle of prophages in bacteria, could also not induce the formation of CWD cells in the *yidC2* mutant, unlike the parental strain that did produce CWD cells upon mitomycin C treatment. Notably, the *yidC2* mutant could produce CWD cells when treated with lysozyme (Fig. 1C). Taken together, these results show that YidC2 is required for completing the infection cycle as well as the formation of CWD cells upon phage infection.

YidC2 is a second paralogue of YidC, which acts as a protein membrane insertase in bacteria. *S. coelicolor* possesses two orthologues (YidC1 and YidC2) of *E. coli* YidC, which also shows significant homology to *B. subtilis* SpoIIIJ (Fig. S2). However, the C-terminus of YidC1 has an extension compared to YidC2, while YidC from *E. coli* has a relatively long N-terminal extension that is absent in YidC2. Additionally, YidC1 and YidC2 are highly divergent and only share around 23% amino acid sequence identity. Knocking-out YidC in *E. coli* results in a non-viable mutant, since the export of many proteins are dependent on this protein [155], but little is known about the function of YidC1 and YidC2 in *S. coelicolor*. Knocking-out YidC1 in *S.coelicolor* resulted in a non-viable mutant as well (data not shown), indicating that YidC1 is likely essential, in contrast to YidC2.

To predict the protein structure of YidC2 in *S. coelicolor*, Alphafold3 was used [168]. Additionally, membrane topology and transmembrane domains were predicted by InterPro [169]. As displayed in Figure 1B, YidC2 is predicted to have six transmembrane domains. Since depletion of YidC is in accordance with membrane-related defects in *E. coli* [171], we tested the difference in membrane fluidity between the *S. coelicolor* Δ*yidC2* and WT strain. The lipid dye $DiIC_{12,}$ with a high affinity for fluid membranes was used [172], but no differences in membrane fluidity were found between the both strains (Fig. S3). Additionally, no obvious differences in morphology between both strains could be found though visual inspection, but the *yidC2* mutant germinates approximately 3 hours slower in liquid compared to *S. coelicolor* (Fig. S4).

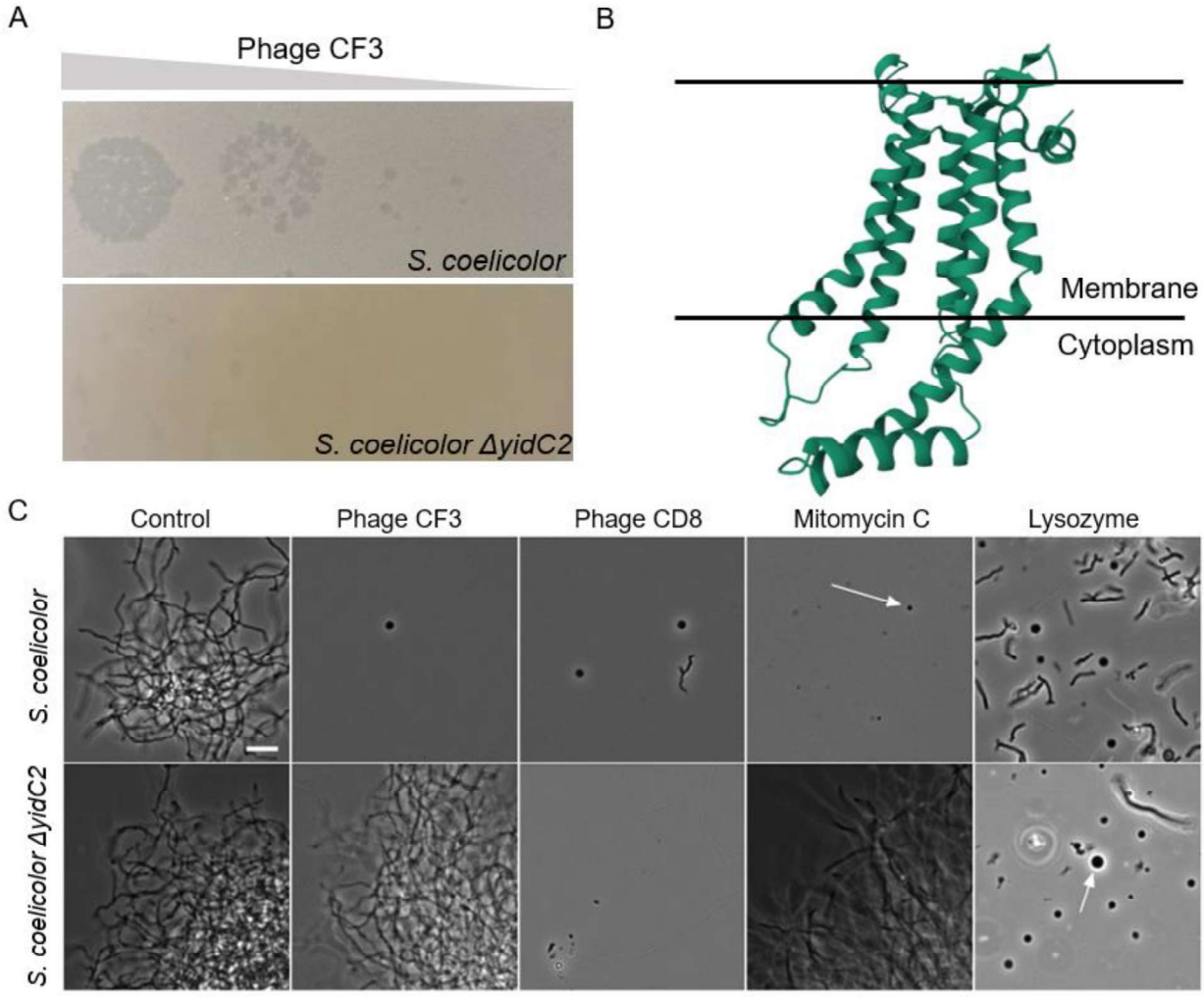

Figure 1. Phage CF3 cannot lyse *S. coelicolor* Δ*yidC2.* (A) Plaque morphology of serial diluted phage CF3 on *S. coelicolor* and *S. coelicolor* Δ*yidC2*. (B) Alphafold3 prediction of the structure of the YidC2 protein in *S. coelicolor*. The hypothetical membrane protein insertase YidC2 has six predicted transmembrane domains. (C) In osmoprotective medium, *S. coelicolor* forms CWD cells after infection with phage CF3, unlike the *yidC2* mutant that retains its mycelial morphology. In contrast, exposure of the *yidC2* mutant to phage CD8 leads to complete lysis without the formation of CWD cells. Mitomycin C, which induces the lytic cycle of prophages, can induce the CWD state in *S. coelicolor,* but not in *S. coelicolor* Δ*yidC2*. Interestingly, cell wall-deficiency can be induced by lysozyme in both strains.

YidC2 is required for the release of phages after infection

To examine the morphology of phage CF3, electron microscopy was used (Fig. 2A). This revealed that phage CF3 is morphologically classified as a siphovirus. Sequencing revealed that phage CF3 is a species in the genus

Camvirus, closely related to *Streptomyces* phage Vanseggelen [173]. These phages were previously shown to attach to the cell wall of *Streptomyces* via receptor proteins on their tail fibers. To test if phage CF3 could still adsorb to the *yidC2* mutant, an adsorption assay was performed. Since the *S. coelicolor* Δ*yidC2* has a reduced growth speed (Fig. S4), we allowed the mutant spores to germinate for seven hours, contrary to the spores of the parental strain, which were germinated for four hours. These different incubation times were selected, as they resulted in a comparable length of the germ tubes. Phage CF3 can adsorb to the parental strain and new progeny phages are released into the environment after 30 minutes (Fig. 2B). While the phages could still adsorb to the *yidC2* mutant as well, no new progeny phages were detected even after 90 minutes of infection. Since phages can adsorb to the parental and the mutant strain, it is unlikely that YidC2 serves as the receptor for CF3 or inserts the receptor in the bacterial membrane.

To gain further understanding of the specific stage at which the infection cycle was blocked, we infected 7-hour-old germlings of the *yidC2* mutant with phage CF3. Thirty minutes after the phage infection, we plunged the samples in liquid ethane and conducted imaging using cryo-EM. As seen in Figure 2C, we observed phages with both full and empty capsid heads inside the bacterium. The phages do not have a coherent size and capsid heads without DNA seem to gather at the cell membrane. This indicates that the phage successfully injected its DNA into the host and initiated the assembly of new phages. Consequently, it seems that the infection cycle was stalled during the release of the phage particles from the host.

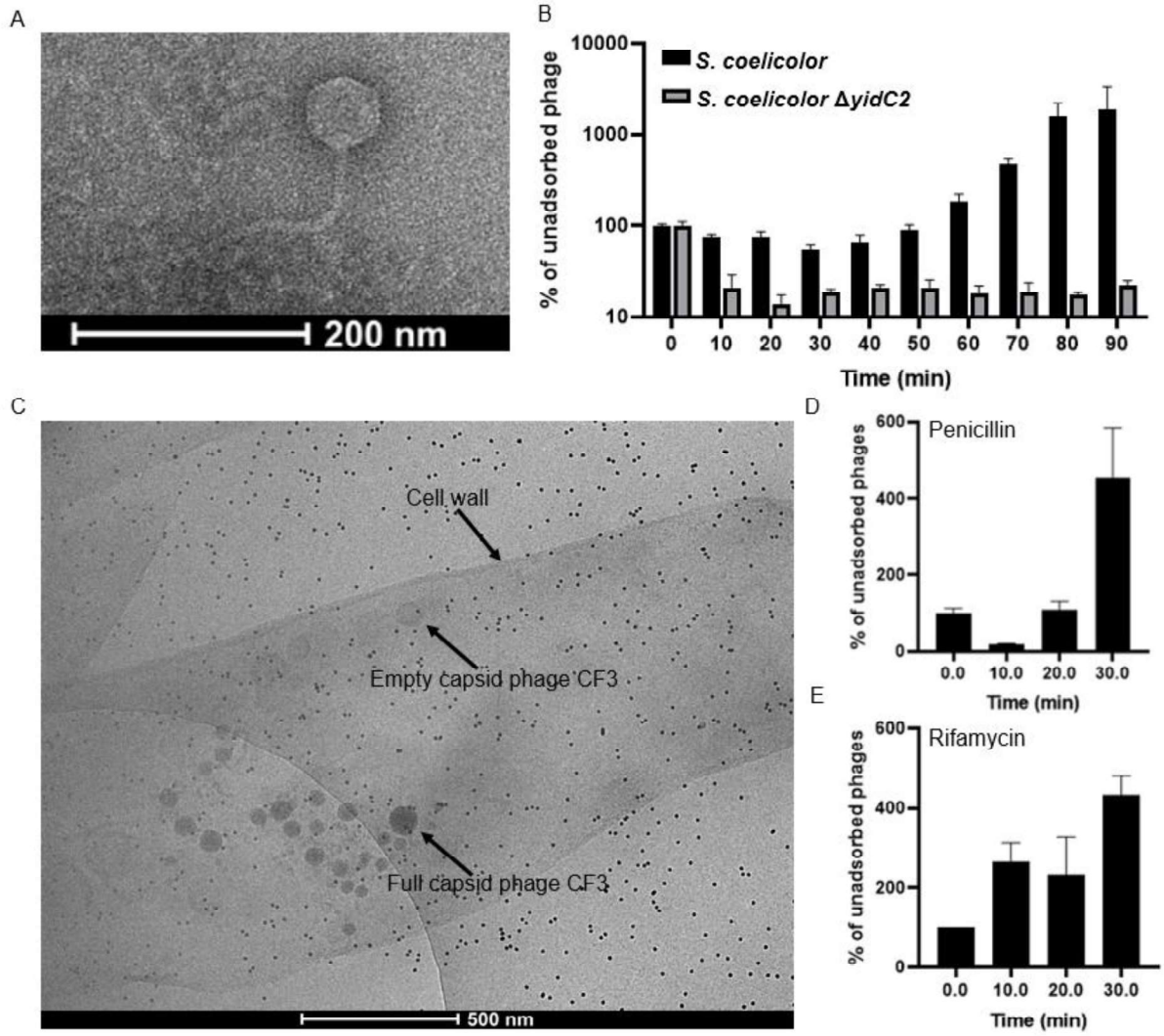

Figure 2. Phage CF3 cannot release progeny phages after infection in *S. coelicolor* Δ*yidC2*. (A) Representative TEM image of phage CF3 stained with 2% uranyl acetate. (B) Adsorption assay showing that phage CF3 can still adsorb and replicate in *S. coelicolor* but does not replicate in *S. coelicolor* Δ*yidC2*. Note that *S. coelicolor* Δ*yidC2* was allowed to germinate for seven hours instead of four hours, since this strain germinates slower. (C) Cryo-EM image of *S. coelicolor* Δ*yidC2* 30 minutes after infection with phage CF3. (D) Adsorption assay of phage CF3 with additional penicillin G in *S. coelicolor* Δ*yidC2* showing an increase in phage titer after 20 minutes. (E) Adsorption assay of phage CF3 with additional rifamycin in *S. coelicolor* Δ*yidC2* showing an increase in phage titer already after 10 minutes.

To verify if progeny phages were stuck inside the bacteria, we performed additional adsorption assays, while adding antibiotics that cause lysis of the host. When penicillin G, which inhibits cross-linking in the peptidoglycan [174], was introduced in the adsorption assay, we observed that progeny phages

were released into the medium of the *yidC2* mutant after 20 minutes (Fig. 2D). This aligns with our hypothesis that functional phages are assembled, but unable to exit the host. A similar response was observed with rifamycin (Fig. 2E), which leads to a suppression of RNA synthesis and ultimately cell death of the bacteria [175]. We also tested if lysozyme could lyse the bacteria from the outside to aid phage CF3 to get out of the bacteria, but phage CF3 could not survive an adsorption assay with additional lysozyme (Fig. S5).

YidC2 is predicted to interact with the holin-endolysin system of phage CF3

Since YidC2 is a predicted membrane protein insertase, we hypothesized that phage CF3 utilizes this host protein to putatively insert some of its own proteins in the membrane. One of the phage machineries that interacts with the bacterial membrane is the holin-endolysin system. The holin and endolysin of phage CF3 could be predicted by a BlastP search of all proteins of phage CF3 to the Actinobacteriophage database [108]. This holin is a type III holin, which has one transmembrane domain [176], and does not have a secretion peptide, indicating that it requires insertion into the membrane by another protein.

To predict whether YidC2 interacts with the holin-endolysin system of phage CF3, predicted aligned error (PAE) plots were made using Alphafold3 (Fig. 3). We observed a strong predicted interaction between YidC2 and the holin protein (Fig. 3A), while YidC2 is also predicted to interact with the N-terminus of the endolysin protein (Fig. 3B). The endolysin interacts strongly with itself, but also with the C-terminus of the holin protein (Fig. 3C). These results were partially confirmed with a bacterial two-hybrid assay in Figure 3D, but the strong interaction between YidC2 and the holin protein as predicted by Alphafold3 was not observed here. However, these results indicated that the holin-endolysin system of phage CF3 probably makes a robust interaction with the YidC2 protein from *S. coelicolor*.

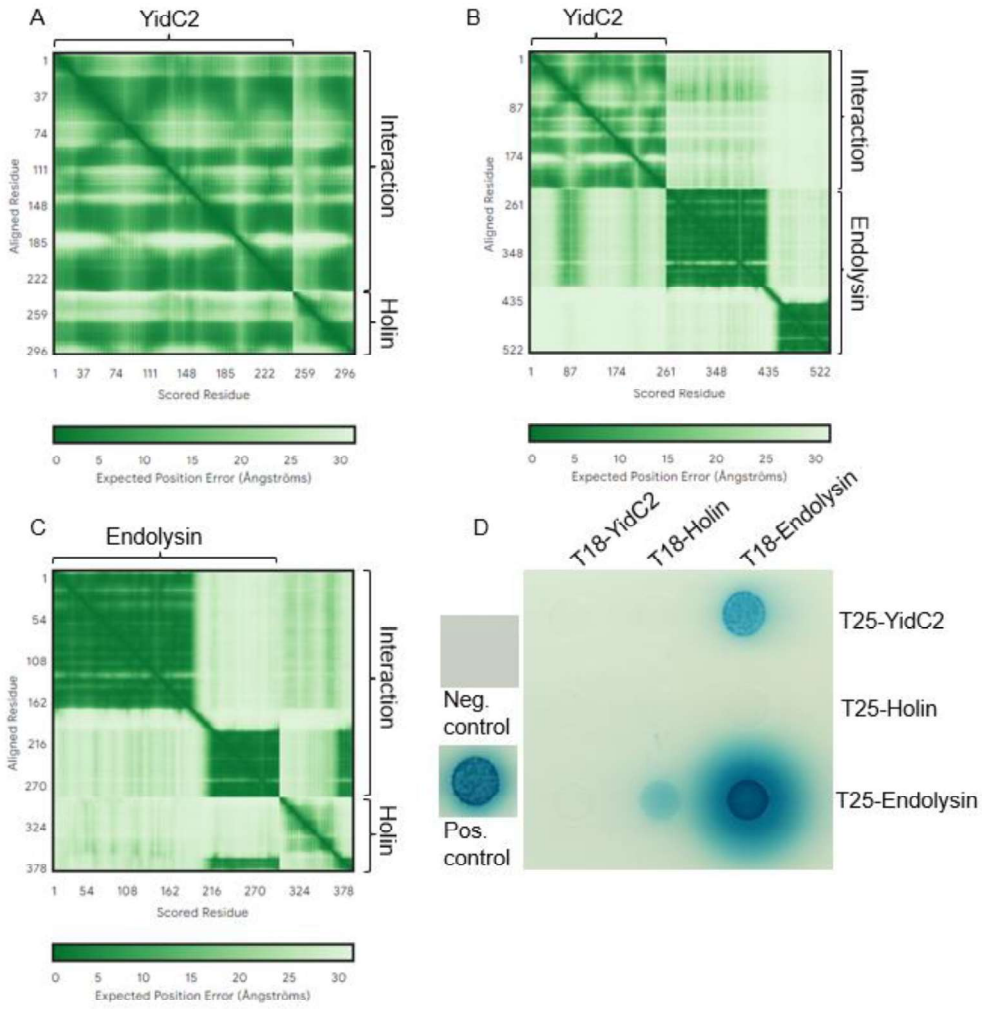

Figure 3. Predictions of holin, endolysin and YidC2 interactions. Predicted aligned error (PAE) plots made with Alphafold3, where a dark green color indicates higher confidence in an interaction between the two proteins. An interface predicted template modeling (ipTM) score <0.6 likely suggest a failed structure, and >0.8 represents confident high quality predictions, while a predicted template modeling (pTM) score >0.5 indicates that the overall predicted fold is highly similar to the true structure [168]. Note that TM scores are very strict for small proteins, like the holin protein. (A) PAE plot of the YidC2 protein with the holin protein from phage CF3. The dark green color in the interaction section indicates that an interaction between the two proteins over their entire length is highly likely. Scores of ipTM = 0.61 and pTM = 0.67. (B) PAE plot of the YidC2 protein with the endolysin protein of phage CF3. The endolysin is highly likely to interact with itself, and a weak interaction is predicted between YidC2 and the endolysin. Scores of ipTM = 0.21pTM = 0.42 (C) PAE plot of the endolysin protein and holin protein of phage CF3. An interaction is predicted between the C-terminal of the endolysin and the C-terminal of the holin protein. Scores of ipTM = 0.32 and pTM = 0.49. (D) Bacterial two-hybrid assay. Blue color indicates predicted interaction. Endolysin strongly interacts with itself, which was also seen in the Alphafold3 predictions. Additionally, the holin and endolysin of phage CF3 have a predicted weak interaction, and the endolysin interacts with the YidC2 protein.

All our data suggested that YidC2 may be required for the insertion of the holin-endolysin system of phage CF3 into the host membrane, facilitating the transport of endolysins across the membrane. To corroborate these findings, we engineered a strain with the endolysin protein placed behind a Sec-secretion signal and expressed from a cumate-inducible promotor. This setup ensures that upon cumate induction, endolysins are synthesized and secreted independent of the YidC2 protein. To test our setup, we first created a cumate inducible Sec-eGFP *S. coelicolor* strain, leading to secretion of eGFP to the exterior of the cell upon cumate induction. Indeed, as seen in Figure 4A, the eGFP signal is not retained inside *S. coelicolor* when the inducer was added to the Sec-eGFP strain, indicating that the Sec-secretion signal leads to efficient transport of eGFP across the membrane into the environment. When we infected the inducible Sec-endolysin parental and Δ*yidc2* strain with phage CF3, we observed clearer lysis zones upon cumate induction compared to the uninduced plaque assays (Fig. 4B). However, the efficiency of plating was still lower in the *yidc2* mutant compared to the wildtype. Therefore, an additional adsorption assay was performed using the Sec-endolysin Δ*yidc2* strain, to verify if phage CF3 could escape the bacteria after cumate induces the release of additional endolysins 60 minutes after phage infection (Fig. 4C). Importantly, we observe that phage CF3, upon induction, could escape from the bacteria after 120 minutes. These results show that the block in phage release in *S. coelicolor* Δ*yidc2* can be overcome by ectopic expression and Sec-dependent secretion of the endolysins.

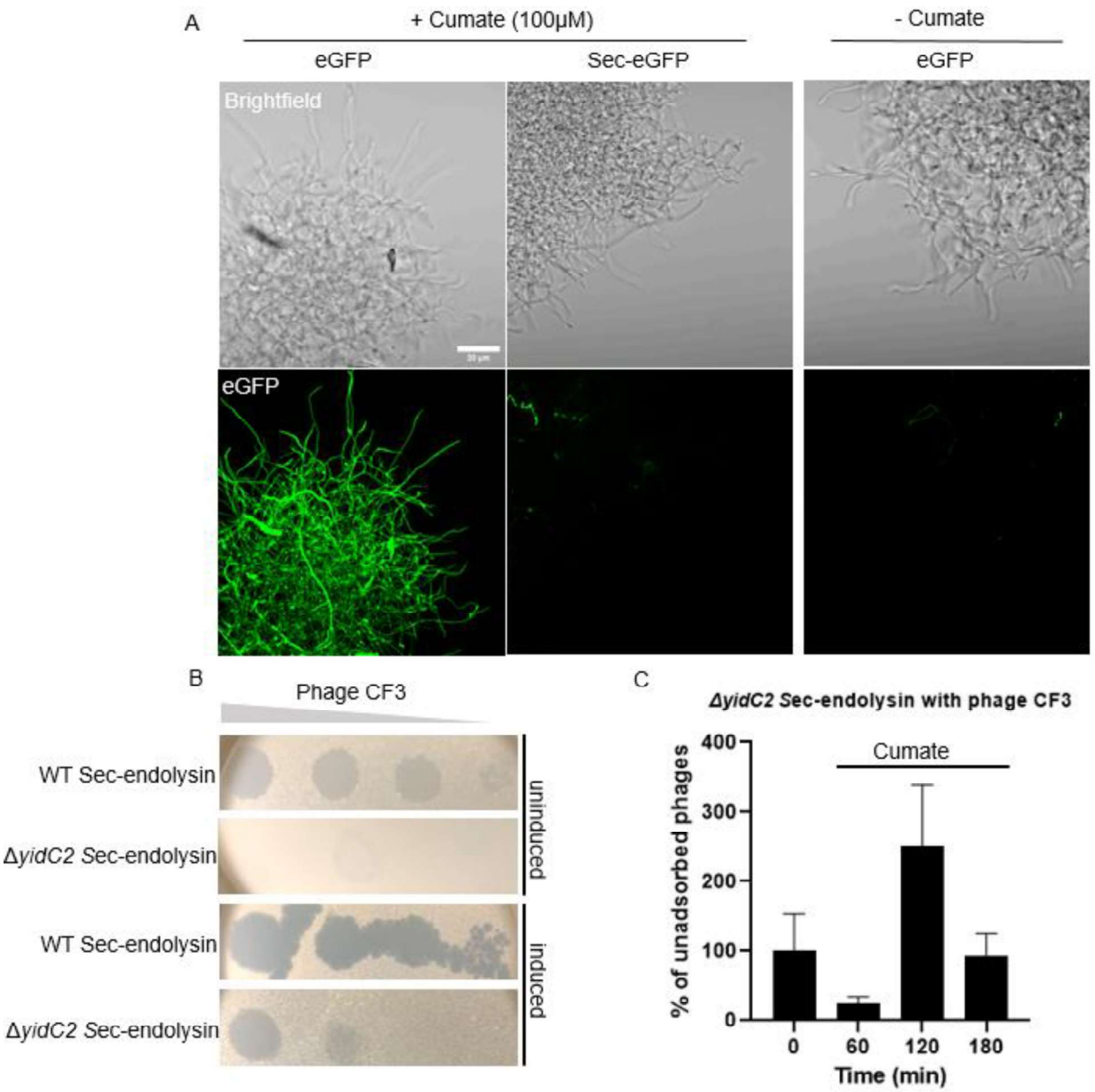

Figure 4. YidC2-independent secretion of the endolysin rescues release of phage CF3. (A) An inducible Sec-dependent eGFP protein is secreted outside of the cells after induction with 100µM cumate. Without cumate, the cells are not fluorescent. Scale bar is 20µm. (B) The WT and Δ*yidC2* strain with Sec-secreted endolysin proteins show clearer lysis zones when the bacterial strains are induced with 100µM cumate and infected with a serial dilution of phage CF3. (C) Adsorption assay of the Δ*yidC2* Sec-endolysin strain with phage CF3. Phage CF3 was added to young germlings at T=0 and after an hour of phage infection, the strain was induced with 100µM cumate to release endolysins in a Sec-dependent manner, which causes an increase in free phages after 120 minutes.

Summary and discussion

Our knowledge on the molecular mechanism of completing a successful phage infection is generally unknown. Once a phage has managed to eject its genome into a suitable bacterium, the phage has to redirect the metabolic activities of the host towards progeny phage production. Most phages depend on the host cell to supply essential amino acids, energy and machinery for replication. However, the strategies of a successful phage infection and thus a successful host-takeover are different for each particular phage-host pair [177]. After phage replication, holin proteins disrupt the bacterial membrane, allowing the fully-folded endolysin that accumulated in the cytosol to access the peptidoglycan, causing cell lysis and release of progeny phages [178]. Here, we showed that the membrane protein insertase YidC2 of *S. coelicolor* has a crucial interaction with the holin-endolysin system of phage CF3. Additionally, YidC2 might also be involved during cell wall shedding in these multicellular bacteria. Interestingly, these results could also be relevant for completion of the phage infection cycle in unicellular bacteria, as shown before [93].

Plaque assays and phage infection assays in liquid showed that *S. coelicolor* Δ*yidC2* was no longer susceptible to infection by phage CF3. Interestingly, no morphological differences were found between the wildtype and the *yidC2* mutant. Additionally, adsorption assays and cryo-EM revealed that phage CF3 could still attach and infect *S. coelicolor* Δ*yidC2*, but progeny phages could not lyse the host and accumulated inside the bacteria. Therefore, we hypothesized that the holin-endolysin system of phage CF3 interacts with the putative membrane protein insertase YidC2, which subsequently inserts the phages' holin protein in the bacterial membrane.

We predicted the interaction between the holin-endolysin system and the YidC2 protein with Alphafold3. Here, we showed that YidC2 has a strong predicted interaction with the holin protein and interacts with the N-terminus of the endolysin protein, while the holin interacts with the C-terminus of the endolysin. These results were also confirmed with an *in vivo* bacterial two-hybrid assay, suggesting an holin-endolysin interaction, an endolysin/YidC2 interaction and a strong dimerization of the endolysin protein. However, no interaction was observed between the holin and YidC2 protein in the bacterial

two-hybrid assay. The interaction interfaces of the holin could be blocked by the N- or C-terminal fusions or the holin protein could not fold properly during the assay, leading to a false-negative result [179]. When the endolysin protein of phage CF3 was synthesized and secreted independently of YidC2 in cumate-inducible Sec-endolysin Δ*yidC2* strain, we observed that the progeny phages could be released into the environment. Plaque assays showed clearer lysis zones when additional endolysins were induced from inside the Sec-endolysin Δ*yidC2* strain, but the infection could not be restored to the wildtype lysis zone morphology. Perhaps more proteins of phage CF3 rely on a functional YidC2 for release of healthy progeny phages. Since release of additional endolysins via the Sec-pathway is not enough to entirely restore the infection during plaque assays, perhaps lysis and subsequent progeny phage release is not completely holin-independent or the catalytic activity of the endolysins needs to be enhanced by holin interactions or various other processes [180, 181].

Notably, the term “holin” might be misleading, since not all holins form a hole or channel that let the endolysin pass through and many holins are uncharacterized at the molecular level [182]. Previous research has shown that phage-derived holins can be used for non-lytic endolysin translocation, by permeabilizing the bacterial cytoplasmic membrane and subsequent passage of secreted endolysins [183]. Correct insertion of the type III holin into the bacterial membrane exposes the C-terminus region, allowing the endolysin to associate. The membrane is then destabilized by multimeric patches of holins, resulting in local thinning of the membrane. The multimeric holin patches are triggered by an interaction with the single transmembrane helix and the holin flips irreversibly in a transmembrane orientation, moving the associated endolysin through the membrane. The endolysin will be released from the holin by the unstable transmembrane-oriented transition state. Subsequently, it will enzymatically degrade the peptidoglycan layer of the host bacterium [183]. Interestingly, this might also explain why we see the formation of CWD cells in WT *S. coelicolor* after phage infection, since the holins do not form the typical pore, and therefore the membrane remains intact in osmoprotective medium (Fig. 5).

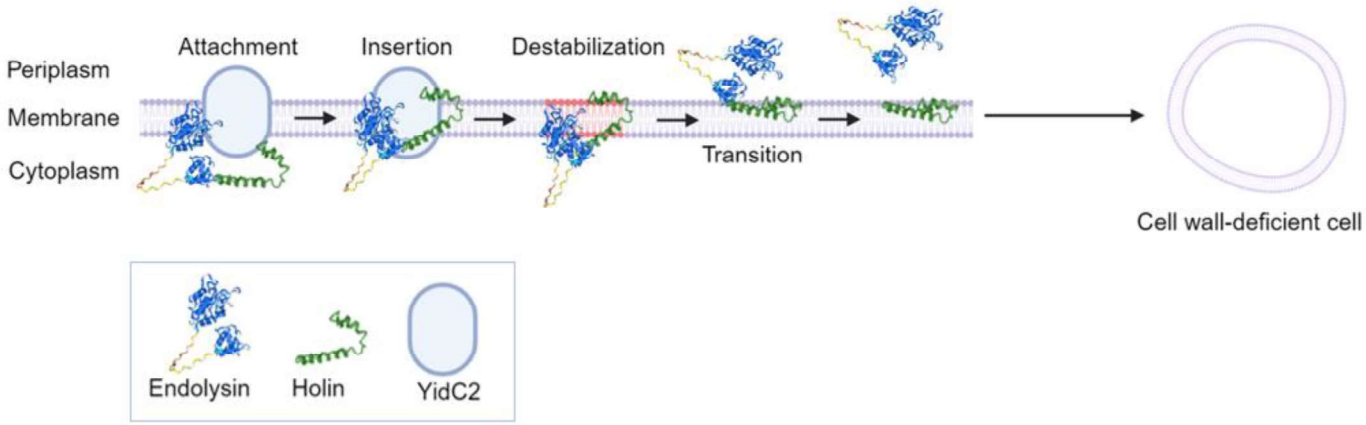

Figure 5. Hypothetical model of the function of YidC2 during infection with phage CF3. In *S. coelicolor*, YidC2 is a predicted membrane protein that integrates the phages' holin into the membrane. The endolysin interacts with the YidC2 protein, while the holin interacts with the C-terminus of the endolysin and probably also with YidC2. Then the endolysin switches conformation by interacting with itself and the holin is integrated in the membrane by YidC2. The holin destabilizes the membrane and switches to a transition state, subsequently "flipping" the endolysin through the membrane, so it can break down the peptidoglycan layer. Since the holin does not make a pore, the membrane remains intact, allowing the cell to shed the cell wall and switch to a CWD state. When YidC2 is knocked-out, the phage's endolysin cannot interact with YidC2 and the holin cannot be properly inserted in the membrane. Therefore, the progeny phages remain "stuck" inside the bacteria. Created with BioRender.com.

Taken together, this work suggests a molecular interaction between the holin-endolysin system of phage CF3 and the bacterial protein YidC2 from *S. coelicolor*. This further expands our knowledge on how phages takeover and manipulate the hosts metabolism. Additionally, we discovered that YidC2 plays a role during shedding of the bacterial cell wall after phage infection in *Streptomyces*. Altogether, these results form the basis to further explore the molecular mechanism of phage infection in *Streptomyces*, that are often used for antibiotic production in industry.

Supplementary data

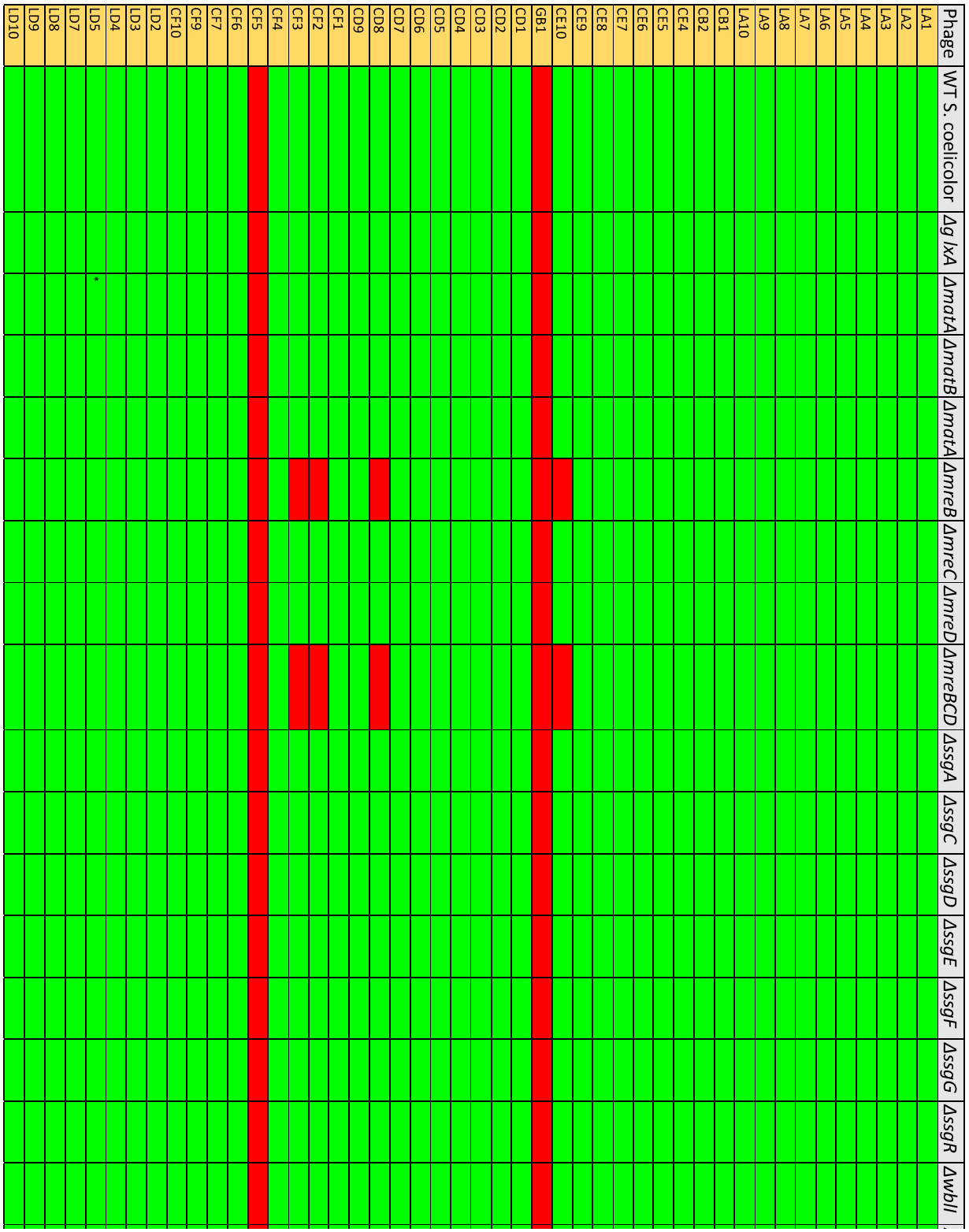

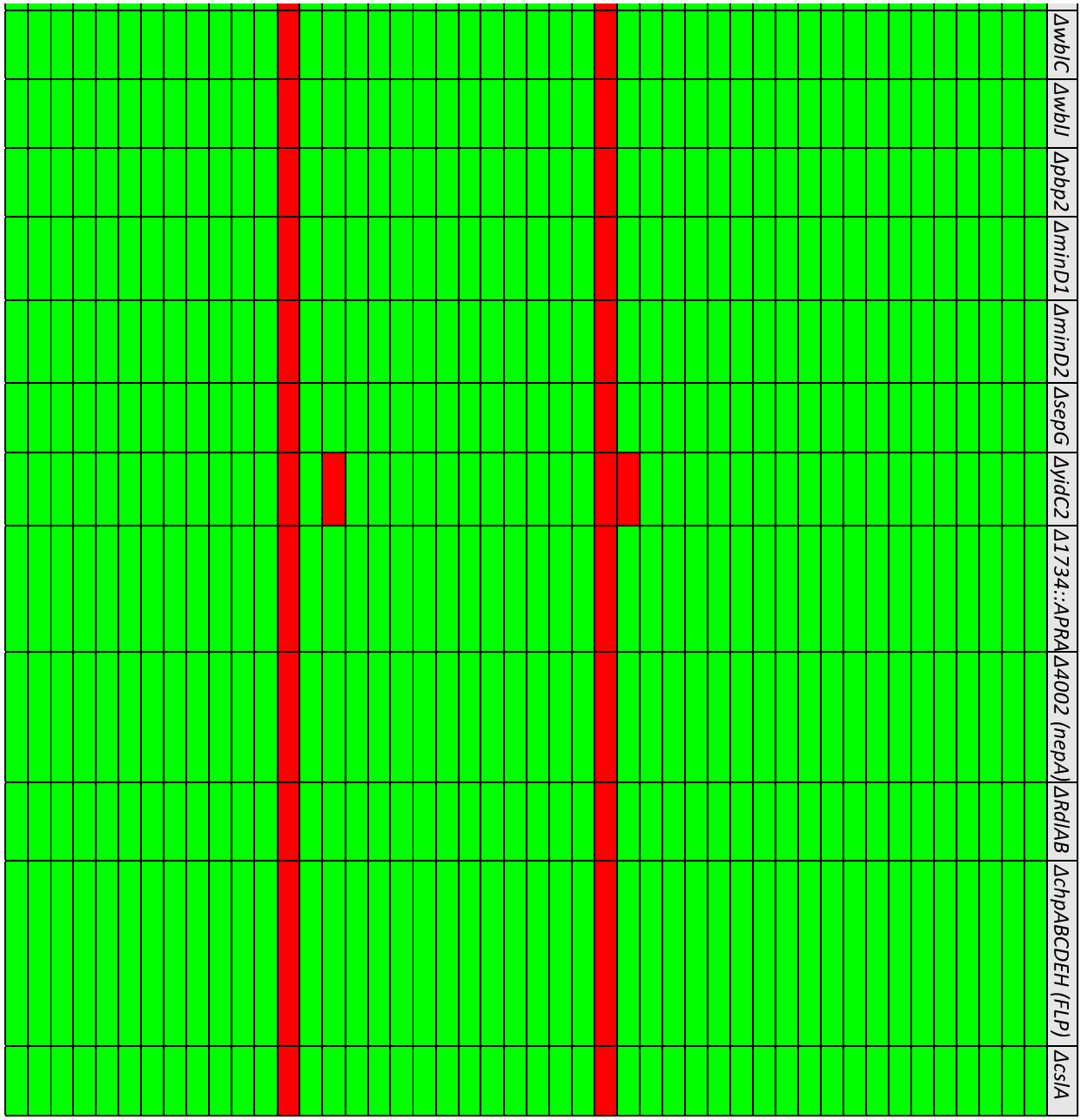

Figure S1. Phage-host interactions of *S. coelicolor* mutants against our phage library. Bacteria-phage interactions are depicted as plaque formation, both turbid and clear (green) or no visible plaque formation (red). Note that not all phages have been sequenced and we therefore suspect that phage CF3, CF2, CD8 and CE10 have a similar lifecycle.

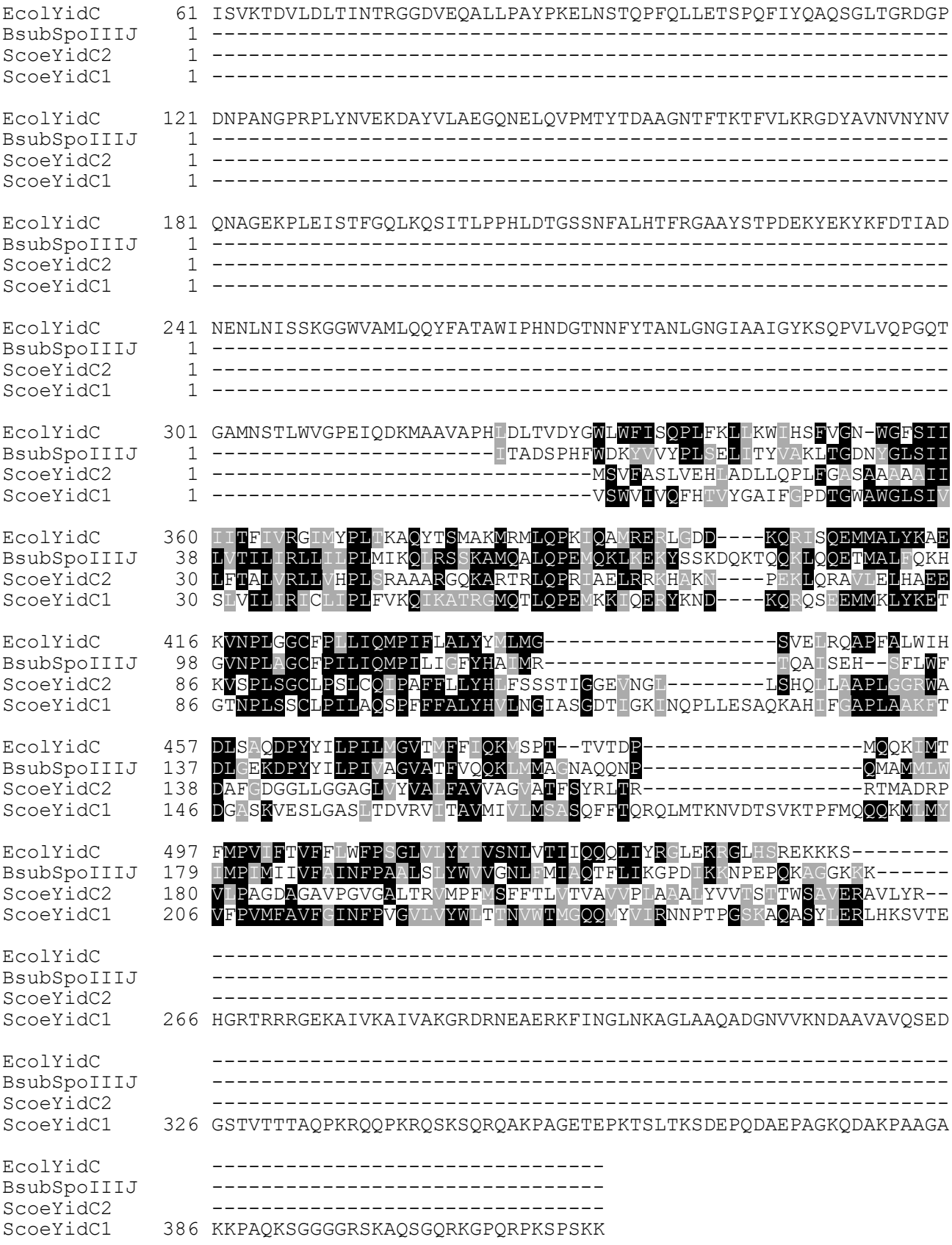
EcolYidC 61 ISVKTDVLDLTINTRGGDVEQALLPAYPKELNSTQPFQLLETSPQFIYQAQSGLTGRDGP
BsubSpoIIIJ 1
ScoeYidC2 1
ScoeYidC1 1
EcolYidC 121 DNPANGPRPLYNVEKDAYVLAEGQNELQVPMTYTDAAGNTFTKTFVLKRGDYAVNVNYNV
BsubSpoIIIJ 1
ScoeYidC2 1
ScoeYidC1 1
EcolYidC 181 QNAGEKPLEISTFGQLKQSITLPPHLDTGSSNFALHTFRGAAYSTPDEKYEKYKFDTIAD
BsubSpoIIIJ 1
ScoeYidC2 1
ScoeYidC1 1
EcolYidC 241 NENLNISSKGGWVAMLQQYFATAWIPHNDGTNNFYTANLGNGIAAIGYKSQPVLVQPGQT
BsubSpoIIIJ 1
ScoeYidC2 1
ScoeYidC1 1
EcolYidC 301 GAMNSTLWVGPEIQDKMAAVAPHLDLTVDYGWLWFISQPLFKLLKWIHSFVGN-WGFSII
BsubSpoIIIJ 1 ITADSPHFWDKYVVYPLSELITYVAKLTGDNYGLSII
ScoeYidC2 1 MSVFASLVEHLADLLQPLFGASAAAAAII
ScoeYidC1 1 VSWVIVQFHTVYGAIFGPDTGWAWGLSIV
EcolYidC 360 IITFIVRGIMYPLIKAQYTSMAKMRMLQPKIQAMRERLGDD----KQRISQEMMALYKAE
BsubSpoIIIJ 38 LVTILIRLLILPLMIKQLRSSKAMQALQPEMQKLKEKYSSKDQKTQQKLQQETMALFQKH
ScoeYidC2 30 LFTALVRLLVHPLSRAAARGQKARTRLQPRIAELRRKHAKN----PEKLQRAVLELHAEE
ScoeYidC1 30 SLVILIRICLIPLFVKQIKATRGMQTLQPEMKKIQERYKND----KQRQSEEMMKLYKET
EcolYidC 416 KVNPLGGCFPLLIQMPIFLALYYMLMG----------SVELRQAPFALWIH
BsubSpoIIIJ 98 GVNPLAGCFPILIQMPILIGFYHAIMR----------TQAISEH--SFLWF
ScoeYidC2 86 KVSPLSGCLPSLCQIPAFFLLYHLFSSSTIGGEVNGL--------LSHQLLAAPLGGRWA
ScoeYidC1 86 GTNPLSSCLPILAQSPFFFALYHVLNGIASGDTIGKINQPLLESAQKAHIFGAPLAAKFT
EcolYidC 457 DLSAQDPYYILPILMGVTMFFIQKMSPT--TVTDP----------MQQKIMT
BsubSpoIIIJ 137 DLGEKDPYYILPIVAGVATFVQQKLMMAGNAQQNP----------QMAMMLW
ScoeYidC2 138 DAFGDGGLLGGAGLVYVALFAVVAGVATFSYRLTR----------RTMADRP
ScoeYidC1 146 DGASKVESLGASLTDVRVITAVMIVLMSASQFFTQRQLMTKNVDTSVKTPFMQQQKMLMY
EcolYidC 497 FMPVIFTVFFLWFPSGLVLYYIVSNLVTIIQQQLIYRGLEKRGLHSREKKKS--------
BsubSpoIIIJ 179 IMPIMIIVFAINFPAALSLYWVVGNLFMIAQTFLIKGPDIKKNPEPQKAGGKKK------
ScoeYidC2 180 VLPAGDAGAVPGVGALTRVMPFMSFFTLVTVAVVPLAAALYVVISITWSAVERAVLYR--
ScoeYidC1 206 VFPVMFAVFGINFPVGVLVYWLTTNVWTMGQQMYVIRNNPTPGSKAQASYLERLHKSVTE
EcolYidC
BsubSpoIIIJ
ScoeYidC2
ScoeYidC1 266 HGRTRRRGEKAIVKAIVAKGRDRNEAERKFINGLNKAGLAAQADGNVVKNDAAVAVQSED
EcolYidC
BsubSpoIIIJ
ScoeYidC2
ScoeYidC1 326 GSTVTTTAQPKRQQPKRQSKSQRQAKPAGETEPKTSLTKSDEPQDAEPAGKQDAKPAAGA
EcolYidC
BsubSpoIIIJ
ScoeYidC2
ScoeYidC1 386 KKPAQKSGGGGRSKAQSGQRKGPQRPKSPSKK

Figure S2. Alignment of *E. coli* YidC (NP_418161), *B. subtilis* SPOIIIJ (Z14225), *S. coelicolor* YidC1 (Y16311; SCO3883) and YidC2 (NP_627080; SCO2851). Black boxes indicate identical aa residues, while grey boxes indicate conserved aa changes. Note that amino acids 1-60 of *E. coli* YidC are not shown.

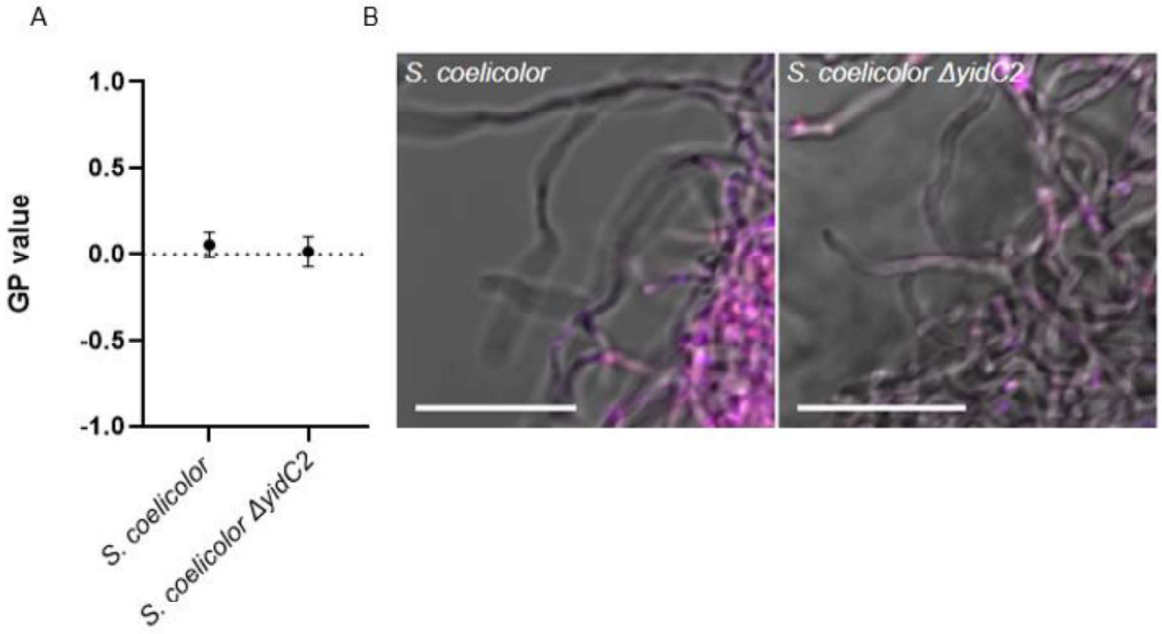

Figure S3. Membrane fluidity of *S. coelicolor* Δ*yidC2*. (A) Analysis to measure membrane fluidity using Laurdan staining. 24-hour old mycelia of both strains were labeled with 1mM 100µM Laurdan. The generalized polarization (GP) values range from +1 (less fluid) to -1 (more fluid). No significance in membrane fluidity of *S. coelicolor* Δ*yidC2* was observed. (B) Representative images of the Laurdan staining. Scalebar represents 10 µm.

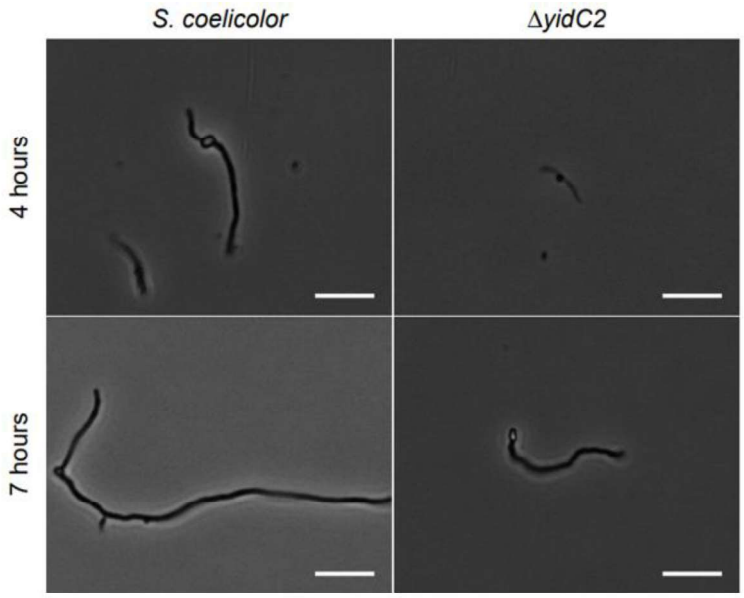

Figure S4. Growth speed. The *yidC2* mutant has a reduced growth speed in DNB medium at 30°C compared to the parental strain. After 7 hours of incubation, the mutant strains has developed germ tubes of approximately the same length as the parental strain at 4 hours.

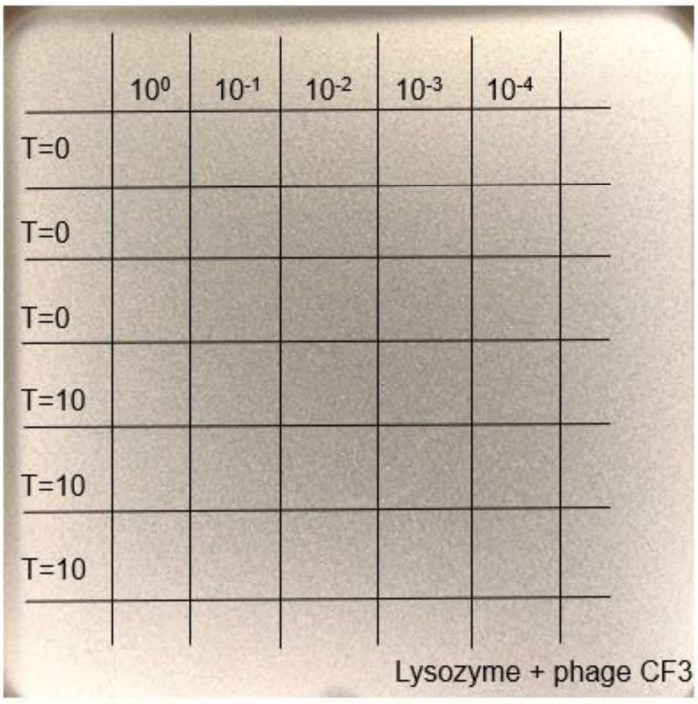

Figure S5. Phage CF3 does not survive an adsorption assay with lysozyme. When an adsorption assay of the *yidC2* mutant was supplemented with 0.2 mg ml^{-1} lysozyme and phage CF3, the phage did not give any plaques on *Streptomyces* strain MBT61, even at timepoint zero.

Table S1. Bacterial strains and phages used in this study.

Strains	Description	Reference
Bacterial strains		
Streptomyces coelicolor M145	Wildtype	Lab collection [94]
Streptomyces coelicolor Δ*yidC2*	Δ*yidC2*::aac(IV)3	This work
Streptomyces sp. MBT61	Wildtype	Lab collection [94]
Escherichia coli BW25113/pIJ790	K12 derivative: Δ*araBAD*, Δ*rhaBAD*	Lab collection [157]
Escherichia coli ET12567/pUZ8002	*dam, dcm, hsdS, cat, tet*	Lab collection [157, 184]
Phages		
Phage CF3	Wildtype, host: *Streptomyces coelicolor*	This work
Phage CD8	Wildtype, host: *Streptomyces coelicolor*	This work

Table S2. Plasmids used in this study.

	Description	Reference
Plasmids		
pIJ790	λ-RED (*gam, bet, exo*), *cat, araC, rep101*^{ts}	[157]
pUZ8002	*tra, neo*, RP4	[185]
S. coelicolor cosmid	Carb^{R}, Kan^{R}	[157]
pCB-1	addgene, #210387	[159]
pGWS758	Used to amplify coding sequence of eGFP	[160]

pIJ82	Streptomyces integrative plasmid	[130]
pIJ82Cu	pIJ82 containing the cumate-inducible promoter	This study
pIJ82Cu-SecGFP	pIJ82 plasmid expressing *signal peptide of SCO5376-eGFP* fragment from cumate inducible promoter	This study
pIJ82Cu-SecEndo	pIJ82 plasmid expressing *signal peptide of SCO5376-endolysin* fragment from cumate inducible promoter	This study
pIJ82Cu-GFP	pIJ82 plasmid expressing eGFP from cumate inducible promoter	This study
pIJ82Cu-Endo	pIJ82 plasmid expressing endolysin from cumate inducible promoter	This study
pKT25	pSU40 derivative expressing the T25 fragment of CyaA (amino acids 1–224)	[186]
pUT18C	pUC19 derivative expressing the T18 fragment of CyaA (amino acids 225–339)	[186]
pKT25-YidC2	pKT25 containing nucleotides 1–714 of YidC2	This study
pKT25-Holin	pKT25 containing nucleotides 1–279 of holin	This study
pKT25-Endolysin	pKT25 containing nucleotides 1–861 of endolysin	This study
pUT18C-YidC2	pUT18C containing nucleotides 1–714 of YidC2	This study
pUT18C-Holin	pUT18C containing nucleotides 1–279 of holin	This study
pUT18C-Endolysin	pUT18C containing nucleotides 1–861 of endolysin	This study

Table S3. Primers used in this study.

	Description
Primers	
E20_KOF	ACGTACTGGACCGTAGGCACGCACCGGACCGGCCCGTGTTCAATTCCGGGGATCCGT
E20_KOR	CTTGCCCGGCACGACGAGACCCTCGGAGGGCTCACCCACCCATGTAGGCTGGAGCTGCTTC

IDProm-F	AATTCGATATCGCGCGCGGCCGCGAACAATAAGGCCTCCCTAACGG
IDProm-R	GGCTGCAGGTCGACTCTAGACATATGGACACTCCTTACTTAGAATAATAC AAACAG
SecGFP-F1	TTATTCTAAGTAAGGAGTGTCCATATGCGCTTCAGACACAAAGCCGCGG CACTCGCAGC
SecGFP-F2	CGAGCCCGGCCCAGGCGGCCACGATGGTGAGCAAGGGCGAG
GFP-F	TTATTCTAAGTAAGGAGTGTCCATATGGTGAGCAAGGGCGAG
TatGFP-R2	GGCTGCAGGTCGACTCTAGAGCATATTACTTGTACAGCTCGTCCATGCCG AG
TatEndo-F2	CACCCGCCGCTCATGCCGCAGACGTGAGTGCAGTGCAGAAGGTCATC
SecEndo-R1	ATGACCTTCTGCACTGCACTCACCGTGGCCGCCTGGGCCGGGCTC
SecEndo-F2	CGAGCCCGGCCCAGGCGGCCACGGTGAGTGCAGTGCAGAAGGTCATC
Endo-F	TTATTCTAAGTAAGGAGTGTCCATGTGAGTGCAGTGCAGAAGGTCATC
ThYidC2-F	gccTCTAGAaATGTCCGTTTTCGCCAGCCTGGTCGAGCAC
ThYidC2-R	cggGAATTCtcaTCAGCGGTACAGCACGGCCCGC
ThHolin-F	gccTCTAGAaATGGGCCGACACACCGCAC
ThHolin-R	cggGAATTCtcaTCAGCCCTCGTAGGCCGACTCG
ThEndo-F	gccTCTAGAaGTGAGTGCAGTGCAGAAGGTCATC
ThEndo-R	cggGAATTCtcaTCAGCGACGACCACACTGCTTC

Chapter 7

Summary and general discussion

Streptomyces are filamentous bacteria that flourish in soil, where they encounter a wide array of environmental fluctuations. Their ability to adapt and withstand many stressors relies on their capacity to switch to different morphological states, including the formation of aerial hyphae, spores and likely cell wall-deficient (CWD) cells that can be extruded under hyperosmotic stress conditions [11, 12, 93]. One of the common stressors bacteria are exposed to are bacteriophages, as they are the most abundant biological entities on this planet [19].

In general, phages recognize their host by binding to receptor proteins attached to, or located on, the bacterial cell wall. Next, phages eject their genome, make progeny phages and eventually lyse the host. However, little is known about the infection cycle of phages in multicellular bacteria. So far, we know that *Streptomyces* phages are unable to attach to spores, and prefer replication in young vegetative mycelium [15, 16]. Interestingly, older mycelium can even protect younger germinating spores by producing molecules, like daunorubicin and actinomycin D, that kill phages [51, 187]. Recent research has shown that the viral impact on a colony can be restricted by increasing the formation of aerial hyphae and spores near the site of an infection [17]. This transient phage resistance by morphological differentiation is not only observed for spores, but also during the production of cell wall-deficient cells.

The work presented in this thesis provides new insights into the biology of phage-*Streptomyces* interactions and analyzes the ecological role of CWD cells in nature.

Cell wall-deficiency as an escape mechanism from phage infection

For phages to complete a successful infection cycle, the first step is to recognize and attach to a suitable bacterial host. The receptor-binding proteins (RBPs) on the phages' tail fibers, tail spike or even head fibers, play a crucial role in viral attachment and subsequent genome delivery in the host bacterium [188]. The RBPs recognize surface associated macromolecules on the cell envelope, like lipopolysaccharides, transporter proteins or substrate receptors for diderm bacteria and peptidoglycan and (lipo)teichoic acids on monoderm bacteria. However, some phages can also recognize receptor proteins on structures like flagella, pili and capsule layers [35]. Many defense

systems have been discovered recently that interfere with this initial step of phage infection [189]. In **Chapter 2**, we hypothesized that shedding of the cell wall might be an efficient strategy for transient resistance against phages. Many bacteria are known to shed their cell wall in response to environmental stressors, and most receptor proteins that phages are able to recognize are usually located, associated with, or attached to the bacterial cell wall [190]. Therefore, we reasoned that CWD bacteria could temporarily render immunity from phage attachment and infection by losing the cell wall, before reverting to the walled mode-of-growth.

To test this hypothesis, we exposed several bacterial strains under hyperosmotic stress to bacteriophages in **Chapter 5**. As we predicted, the mycelium of *Streptomyces* strain MBT86 was entirely converted into cell wall-deficient cells after infection with phage LA7 (which was later named Pablito, in **Chapter 3**) in osmoprotective medium. These CWD cells could revert to the mycelial mode-of-growth and significantly more colony forming units were obtained after phage infection, indicating that a greater fraction of this multicellular population could survive an infection in osmoprotective medium compared to the standard *Streptomyces* growth medium (see Fig. 1). Not only this strain, but all tested *Streptomyces* strains became CWD after infection with a susceptible phage, although some strains seemed to make more CWD cells compared to others. This might be explained by the different phage-host pairs and therefore differences in infection mechanisms, or the timing of phage infection, since there seems to be an ecological trade-off between phage reproduction rate and progeny release [191]. Some phages quickly assemble and release new progeny phages, leading to early lysis of the host and perhaps the bacteria have less time to grow into long hyphae, resulting in less CWD cells.

Not only multicellular bacteria, but also *Escherichia coli* and *Bacillus subtilis* were able to shed their cell wall after phage infection. Therefore, we expected that many other bacteria are capable of shedding the cell wall after phage infection, which was later also shown in detail for *Listeria monocytogenes* and *Enterococcus faecalis* [153]. The interaction between *E. coli*, *B. subtilis* and their respective phages was also imaged using cryo-electron microscopy. This revealed that phage T4 could no longer bind to *E. coli* CWD cells, probably because the receptor proteins that phage T4 recognizes are located on the

outer membrane [31]. Interestingly, phage φ29 could still attach and infect CWD cells of *B. subtilis*. The RBPs of this phage are likely recognizing lipoteichoic acids, which are anchored in the membrane, and remnants could still be present in CWD cells and exposed to the environment [142].

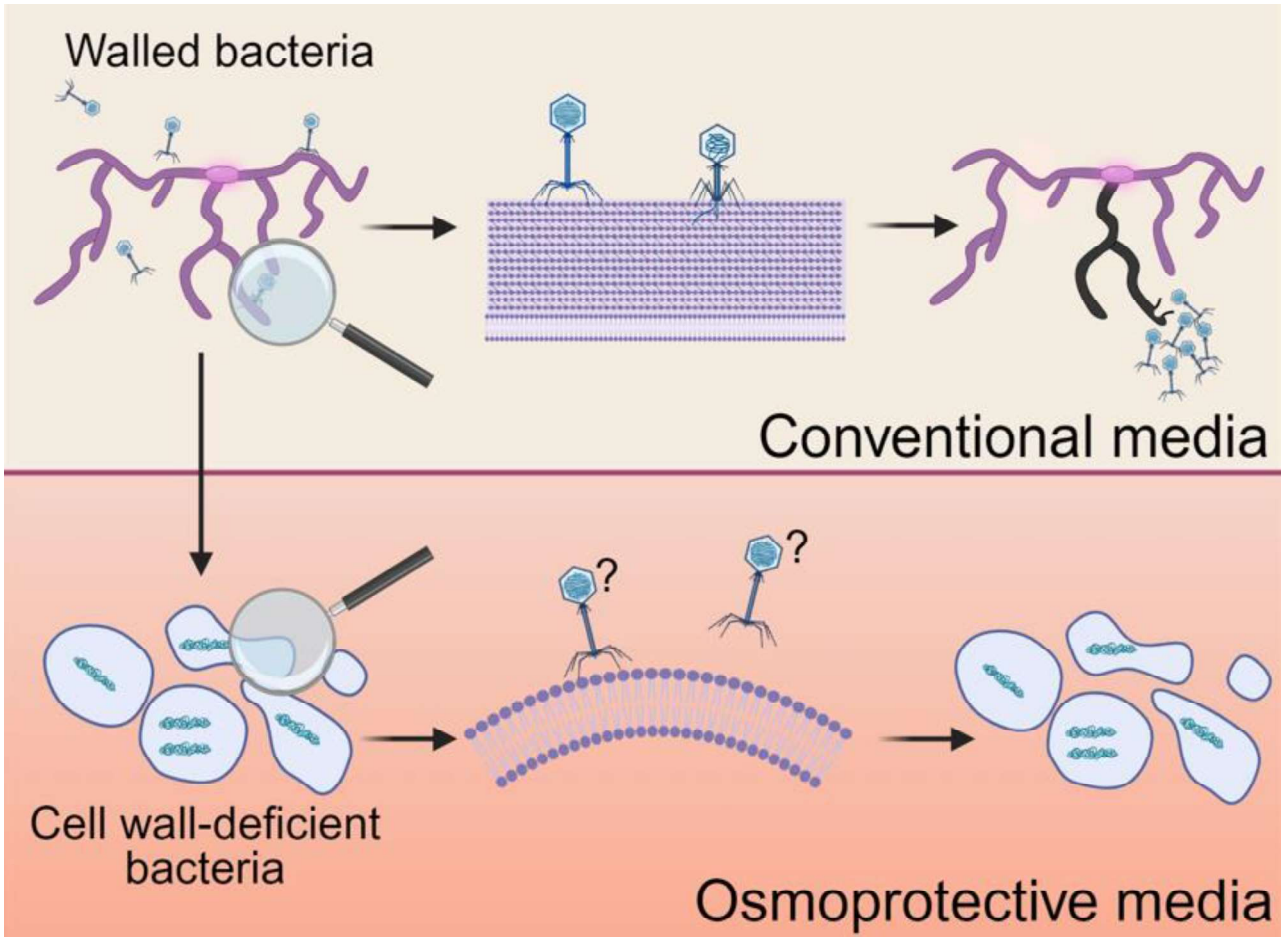

Figure 1. Schematic overview of phage infection in Streptomycetes in conventional and osmoprotective medium. In normal medium, phages recognize the RPBs on the bacterial cell wall and the hyphae lyses. In osmoprotective medium, the mycelium can become cell wall-deficient and phages no longer recognize their usual host, which therefore stays uninfected.

Although the mechanism of shedding the cell wall after phage infection in osmoprotective medium still remains unclear, it was later shown that the endolysins released from lysed *L. monocytogenes* bacteria cause degradation of the cell walls of uninfected cells [153], where this transition to cell wall-deficiency was also observed. However, when we added spent medium of a CWD culture after phage infection to an uninfected culture of *B. subtilis*, we did not observe formation of CWD cells (**Chapter 5**). This suggest that either

the concentration of endolysins was too low, or that *B. subtilis* does not become CWD due to endolysin release of neighboring bacteria. These results emphasize that every phage-host pair might react differently and that not all research on model organisms can be extrapolated to other bacteria.

Identifying new *Streptomyces* phage species

Characterizing and sequencing more phages that infect multicellular bacteria to increase our knowledge on this viral dark matter is of extreme importance. In **Chapter 3** and **4** we have isolated three new phage species. *Streptomyces* phage Pablito could be characterized as a new species in the genus *Janusvirus*, while *Streptomyces* phage Verabelle and Vanseggelen were classified as new species in the genus *Camvirus*. All three phages have a dsDNA genome with a relative high G+C content of over 65% and are predicted to have a temperate lifestyle. Compared to other phages from model organisms like *E. coli*, relatively few *Streptomyces* phages have been accurately sequenced, classified and characterized [173]. Additionally, mostly dsDNA phages have been isolated and ssDNA, ssRNA and dsRNA *Streptomyces* phages are highly underrepresented [76]. This bias could be due to the standardized isolation methods and difficulties sequencing phages with a single-stranded genome [98, 130, 192]. However, new high-throughput isolation methods could really benefit this field, for example by using the Mimetas microfluidics platform [193]. Here, 96 different *Streptomyces* strains can be tested simultaneously for susceptibility to phage infection in environmental samples, speeding-up the usually time-consuming protocol of phage enrichment, isolation and microscopic characterization of the phage-host interaction.

Isolating and characterizing more *Streptomyces* phages could in the long run lead to a BASEL-like collection for these multicellular bacteria. The BASEL collection [194] is a phage library consisting of *E. coli* phages that are all well-sequenced, phenotypically characterized and for which host receptors proteins are known. This collection is broadly used and facilitates the discovery of the molecular mechanisms of phage-host interactions [195-197]. For *Streptomyces* phages, there is the Actinobacteriophage database [76], but this consists solely of phage genomes and is not readily available for experiments. Since we only know the tip of the iceberg of the interaction

between phages and their multicellular bacterial hosts, a library of sequenced and characterized *Streptomyces* phages would greatly benefit the field and hopefully contribute to more open science and collaborations between different research groups worldwide.

Mechanism of phage infection in multicellular bacteria is largely unknown

Since a commonly used *Streptomyces* phage library is not readily available, we have infected 29 different *Streptomyces coelicolor* mutant strains lacking distinct cell wall-associated proteins, with 46 phages of our own collection to begin to understand the molecular mechanism of phage infection in multicellular bacteria. In **Chapter 6**, we identified that phage CF3 could no longer successfully infect *S. coelicolor* lacking YidC2. This protein is predicted to be a membrane protein insertase in *E. coli* and *B. subtilis*, but little is known about its function in *Streptomyces* [155, 156]. Unlike its parent, *S. coelicolor* Δ*yidC2* did not form CWD cells after phage infection. CWD cells of the Δ*yidC2* mutant could only be formed by exposing the strain to lysozyme, indicating that YidC2 plays an important role in shedding of the cell wall after phage infection. Interestingly, phage CF3 could still attach to *S. coelicolor* Δ*yidC2*. However, using biochemistry and cryo-electron microscopy, we found that the progeny phages could no longer be released into the environment due to a block in degradation of the host cell wall.

To enhance our understanding of YidC2's role in the infection process, we hypothesized that the phage might exploit this protein to insert some of its own proteins into the membrane. Since most known phage holins are membrane-associated proteins, we closely examined the holin-endolysin system of phage CF3. Previous studies showed that holin proteins disrupt the membrane by making holes, through which the endolysin protein can exit and subsequently break down the peptidoglycan layer [182]. However, some holins do not form the typical "holes", but can be used for non-lytic protein translocation, by temporarily permeabilizing the membrane, so that endolysins can passage [183]. Using Alphafold3 combined with a bacterial two-hybrid assay and characterization of endolysin secretion mutants, we could show that YidC2 interacts with the holin-endolysin system of phage CF3. We propose that YidC2 facilitates insertion of the holin and endolysin of phage CF3 into the

membrane. Through non-lytic protein translocation, the endolysin is flipped across the membrane, allowing it to enzymatically degrade the peptidoglycan layer. This mechanism allows the cell membrane to remain intact and the bacteria will form CWD cells.

Outlook and future directions

The results of this thesis are a promising starting point to further improve our understanding of the ecological value of cell wall-deficient bacteria in nature and the interaction between phages and their multicellular hosts. The combination of several techniques, like confocal microscopy, electron microscopy, genetics and many more, made this work possible and allowed for the discovery of unprecedented new insights. However, several questions remain to be explored. For example, can phages traverse though mycelial hyphae? This hypothesis could be investigated by live-imaging of a fluorescent *Streptomyces* phage during infection [198]. However, deleting or adding genes in *Streptomyces* phages is relatively complicated, probably due to the high G+C content, low burst sizes and small capsid heads. One way to circumvent these disadvantages is by integrating temperate *Streptomyces* phages into their host, and manipulating the phage genome inside the bacteria with genome editing systems like CRISPR-Cas9 [162, 199], after which the engineered phages can be isolated from their host with mitomycin C, which induced excision of temperate phages from the bacterial genome [200]. Live-imaging of a fluorescent phage during infection in *Streptomyces* could resolve whether phages can actually travel though hyphae and may also shed a light on the mechanism-of-action of cell wall-deficiency after phage infection in a multicellular host.

Since most research on phage-host interactions has been done in unicellular bacteria [19, 48, 54], multicellular bacteria might respond with a completely different mode-of-action. In phage research, the ratio between phages and bacteria during infection, or Multiplicity of Infection (MOI) is an important concept. An MOI of 1, for example, is calculated as one bacterium getting infected by one phage, and an MOI of 0.1 means that for every 10 bacteria, only one is infected by a phage. *Streptomyces* spores can make one or two germ tubes and further in the lifecycle, the mycelial network gets counted as one colony forming unit. So, MOI calculations with multicellular bacteria loses

its significance, once a spore has germinated [98] and when *Streptomyces* are infected with phages at low MOI, only one or two hyphae of a whole mycelium will be infected. Perhaps, the multicellular mycelial colony signals to uninfected hyphae to produce CWD cells in order to save the population, similar to abortive infection in unicellular bacteria [46]. For these reasons, calculating MOI in multicellular bacteria like *Streptomyces*, should be optimized and a new and more accurate formula for MOI in multicellular bacteria would benefit this research field.

However, the most urgent question that remains to be resolved would be to answer the impact of shedding the bacterial cell wall in phage therapy. Phage therapy is a promising strategy for treating antibiotic-resistant bacteria. However, my work has shown that bacteria can readily become CWD upon exposure to phages, which provides a protective mechanism for the population of bacteria. Interestingly, previous research has shown that cell wall-deficient bacteria were found in blood samples and in patients with recurrent urinary tract infections [66, 201, 202]. This indicates that urine and blood can sustain the transient morphological state of CWD cells and that clinical trials testing phage therapy should take this morphological switch into consideration. For example, phage therapy shows promising outcomes when treating mycobacterial infections, but there never is a 100% success rate [203, 204], which might be explained by the ability of many mycobacterial strain to form viable cell wall-deficient cells [205]. Alongside conventional diagnostics tools, a next step would be to also monitor the formation of CWD cells after phage infection during experimental procedures and clinical trials for phage therapy treatments, which have likely been overlooked in the past [206]. This would increase our knowledge on the occurrence and impact of CWD cells after phage therapy and will contribute to our battle against antibiotic-resistant bacteria.

Nederlandse samenvatting

Streptomyces zijn filamenteuze bacteriën die goed gedijen in de bodem, waar ze te maken krijgen met een breed scala aan milieufluctuaties. Hun vermogen om zich aan te passen en vele stressfactoren te weerstaan, berust op hun capaciteit om zich te veranderen in verschillende morfologische gedaantes, waaronder luchthyfen, sporen en celwandloze cellen, die kunnen worden gevormd onder hyperosmotische stressomstandigheden [11,12,93]. Eén van de meest voorkomende stressfactoren waaraan bacteriën worden blootgesteld, zijn bacteriofagen, aangezien dit de meest aanwezige biologische entiteiten op deze planeet zijn [19].

In het algemeen herkennen fagen hun gastheer door zich te binden aan receptoreiwitten die aan, of op de bacteriële celwand zijn bevestigd. Vervolgens injecteren fagen hun genoom, maken ze nieuwe fagen, en lyseren uiteindelijk de bacteriële cel. Desalniettemin, is er weinig bekend over de infectiecyclus van fagen in multicellulaire bacteriën. Tot nu toe weten we dat *Streptomyces* fagen niet kunnen binden aan sporen en de voorkeur geven aan replicatie in jong vegetatief mycelium [15,16]. Interessant genoeg kan ouder mycelium, jongere kiemende sporen zelfs beschermen door moleculen te produceren, zoals daunorubicine en actinomycine D, die fagen kunnen doden [51,186]. Recent onderzoek heeft aangetoond dat de virale impact op een kolonie kan worden beperkt door de vorming van luchthyfen en sporen nabij de plaats van een infectie te vergroten [17]. Deze tijdelijke faagresistentie door morfologische differentiatie wordt niet alleen waargenomen bij sporen, maar ook tijdens de aanmaak van celwandloze cellen.

Het werk dat is gepresenteerd in dit proefschrift biedt nieuwe inzichten in de biologie van faag-*Streptomyces* interacties en analyseert de ecologische rol van celwandloze cellen in de natuur.

Celwandloze cellen als ontsnappingsmechanisme voor faaginfectie

Om een succesvolle faag infectiecyclus te voltooien, is de eerste stap het herkennen en binden aan een geschikte bacteriële gastheer. De receptorbindende eiwitten op de staartvezels, staartspike of zelfs kopvezels van de fagen, spelen een cruciale rol in virale hechting en de daaropvolgende

genoominjectie in de bacterie [187]. De receptorbindende eiwitten herkennen oppervlaktegeassocieerde macromoleculen op de celwand, zoals lipopolysacchariden, transportereiwitten of substraatreceptoren voor Gram-negatieve bacteriën en peptidoglycaan en (lipo)teichoïnezuren voor Gram-positieve bacteriën. Sommige fagen kunnen echter ook receptoreiwitten op structuren zoals flagellen, pili en capsule lagen herkennen [35]. Veel afweersystemen die recent zijn ontdekt, interfereren met deze eerste stap van de faaginfectie [188]. In **Hoofdstuk 2** heb ik de hypothese opgesteld dat het afwerpen van de celwand een efficiënte strategie zou kunnen zijn voor tijdelijke resistentie tegen fagen. Van veel bacteriën weten we dat ze hun celwand af kunnen werpen als reactie op omgevingsstressfactoren, en de meeste receptoreiwitten die fagen kunnen herkennen zijn meestal gelokaliseerd, geassocieerd met of bevestigd aan de bacteriële celwand [189]. Daarom redeneerden we dat celwandloze bacteriën tijdelijk immuniteit tegen faaghechting en -infectie zouden kunnen verkrijgen door het verliezen van de celwand, voordat ze terugkeren naar de groei met celwand.

Om deze hypothese te testen, hebben we verschillende bacteriestammen blootgesteld aan hyperosmotische stress en bacteriofagen in **Hoofdstuk 5**. Zoals we voorspelden, werd het mycelium van de *Streptomyces* bacterie MBT86 volledig omgezet in celwandloze cellen na infectie met faag LA7 (die we later Pablito hebben genoemd in **Hoofdstuk 3**). Deze celwandloze cellen konden terugkeren naar de filamenteuze groeiwijze en er werden significant meer kolonievormende eenheden geobserveerd na faaginfectie, wat aangeeft dat een groter deel van deze multicellulaire populatie een infectie in hyperosmotisch medium kon overleven in vergelijking met het standaard *Streptomyces* groei medium (zie Figuur 1). Niet alleen deze stam, maar alle geteste *Streptomyces* stammen werden celwandloos na infectie met een faag, hoewel sommige stammen meer celwandloze cellen leken te maken in vergelijking met andere. Dit zou kunnen worden verklaard door de verschillende faag-bacterie combinaties en daarom dus verschillen in infectiemechanismen, of door het tijdstip van faaginfectie, aangezien er een ecologische afweging lijkt te zijn tussen de faagreproductiesnelheid en de afgifte van nakomelingen [190]. Sommige fagen produceren snel nieuwe fagen, wat leidt tot vroege lysis van de gastheer en misschien minder tijd voor de bacteriën om lange hyfen te vormen, resulterend in minder celwandloze cellen.

Niet alleen multicellulaire bacteriën, maar ook de eencellige bacteriën *Escherichia coli* en *Bacillus subtilis* waren in staat hun celwand af te werpen na faaginfectie. Daarom verwachtten we dat veel andere bacteriën ook in staat zijn hun celwand af te werpen na faaginfectie, wat later ook gedetailleerd werd aangetoond voor *Listeria monocytogenes* en *Enterococcus faecalis* [153]. De interactie tussen *E. coli*, *B. subtilis* en hun respectieve fagen werd in beeld gebracht met behulp van cryo-elektronenmicroscopie. Dit toonde aan dat faag T4 niet langer kon binden aan celwandloze cellen van *E. coli*, waarschijnlijk omdat de receptoreiwitten die T4 herkent, zich op het buitenmembraan bevinden [31]. Interessant genoeg kon faag φ29 nog steeds hechten en infecteren aan celwandloze cellen van *B. subtilis*. De receptorbindende eiwitten van deze faag herkennen waarschijnlijk lipoteichoïnezuren, die verankerd zijn in het membraan, en restanten daarvan kunnen nog steeds aanwezig zijn in celwandloze cellen en daarom blootgesteld zijn aan de omgeving [142].

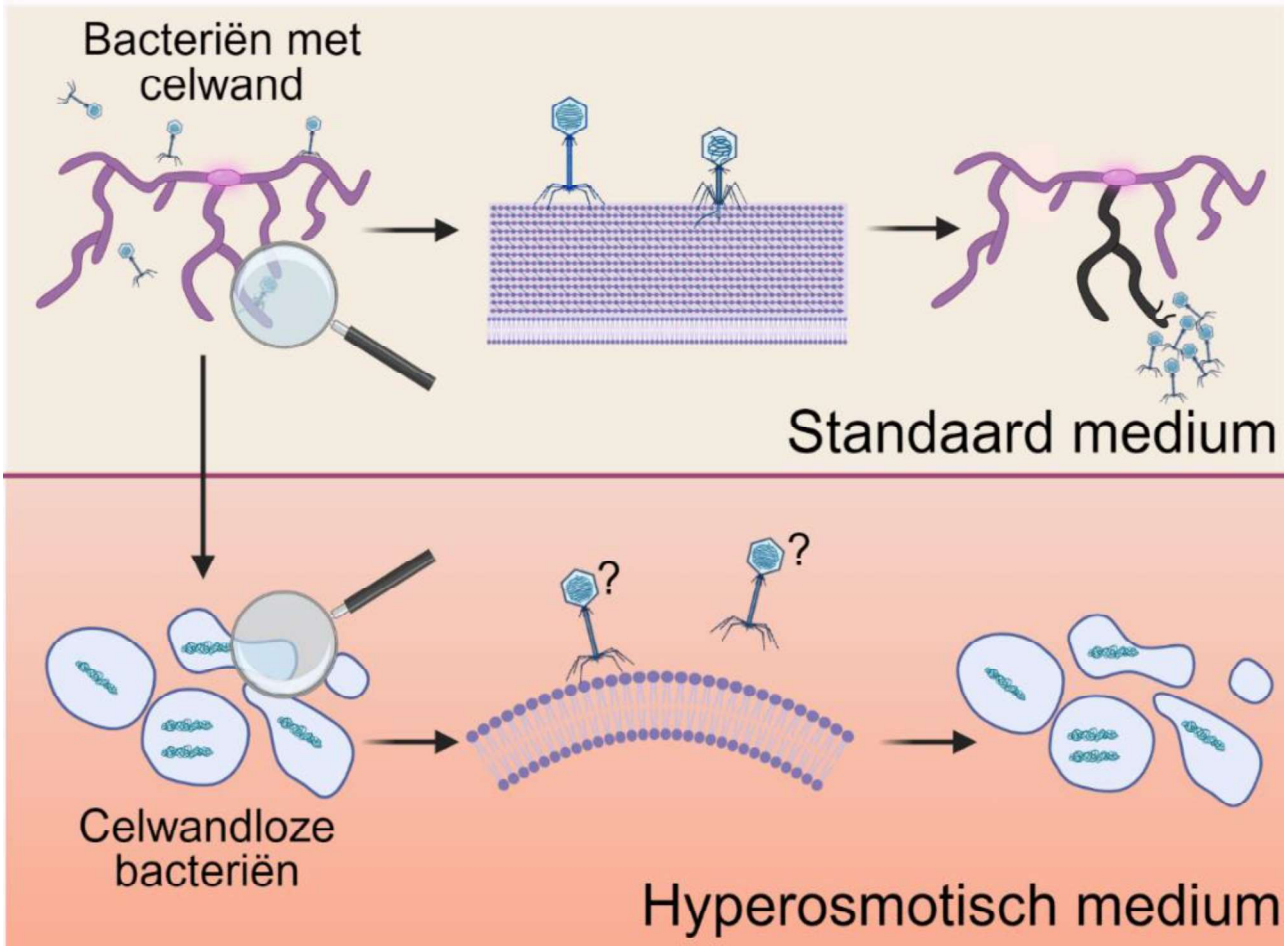

Figuur 1. Schematisch overzicht van faaginfectie in Streptomyceten in standaard en hyperosmotisch medium. In normaal medium herkennen fagen de receptorbindende eiwitten op de bacteriële celwand en de hyfe van het mycelium lyseert. In hyperosmotisch medium kan het mycelium veranderen in celwandloze cellen en herkennen fagen hun gebruikelijke gastheer niet meer, waardoor deze ongeïnfecteerd blijft.

Hoewel het mechanisme van het afwerpen van de celwand na faaginfectie in hyperosmotisch medium nog steeds onduidelijk blijft, werd later aangetoond dat de "endolysin" eiwitten die vrijkomen uit gelyseerde *L. monocytogenes* bacteriën, de celwanden van ongeïnfecteerde cellen afbreken [153], waarbij de overgang naar celwand-deficiënte cellen ook werd waargenomen. Echter, toen wij medium van een celwandloze cultuur gecreëerd na faaginfectie, toevoegden aan een ongeïnfecteerde cultuur van *B. subtilis*, observeerden we geen vorming van celwandloze cellen (**Hoofdstuk 5**). Dit suggereert dat ofwel de concentratie van endolysin eiwitten te laag was, of dat *B. subtilis* niet celwandloos wordt door de endolysin afgifte van naburige bacteriën. Deze resultaten benadrukken dat elk faag-bacterie paar anders kan reageren en dat niet al het onderzoek op modelorganismen kan worden geëxtrapoleerd naar andere bacteriën.

Het identificeren van nieuwe *Streptomyces* fagensoorten

Het karakteriseren en sequencen van meer fagen die multicellulaire bacteriën infecteren om onze kennis over deze virale "dark matter" te vergroten, is van groot belang. In **Hoofdstukken 3** en **4** hebben we drie nieuwe fagensoorten geïsoleerd. *Streptomyces* faag Pablito kon worden gekarakteriseerd als een nieuwe soort in het geslacht *Janusvirus*, terwijl *Streptomyces* fagen Verabelle en Vanseggelen werden geclassificeerd als nieuwe soorten in het geslacht *Camvirus*. Alle drie de fagen hebben een dsDNA-genoom met een relatief hoog G+C-gehalte van meer dan 65% en hebben waarschijnlijk een lysogene levensstijl. In vergelijking met andere fagen van modelorganismen, zoals *E. coli*, zijn relatief weinig *Streptomyces* fagen accuraat gesequenced, geclassificeerd en gekarakteriseerd [172]. Bovendien zijn meestal dsDNA-fagen geïsoleerd en zijn ssDNA-, ssRNA- en dsRNA *Streptomyces* fagen sterk ondervertegenwoordigd [76]. Deze bias zou te wijten kunnen zijn aan de gestandaardiseerde isolatiemethoden en moeilijkheden bij het sequencen van fagen met een enkelstrengs genoom [98,130,191]. Nieuwe "high-throughput" isolatiemethoden zouden dit veld daarentegen aanzienlijk kunnen bevorderen, bijvoorbeeld door gebruik te maken van het "Mimetas

microfluïdics platform" [192]. Hier kunnen 96 verschillende *Streptomyces* stammen gelijktijdig worden getest op vatbaarheid voor faaginfectie uit verschillende milieumonsters, wat het gebruikelijk tijdrovende protocol van faagverrijking, isolatie en microscopische karakterisering van de faag-bacterie interactie versnelt.

Het isoleren en karakteriseren van meer *Streptomyces* fagen zou op de lange termijn kunnen leiden tot een BASEL-achtige collectie voor deze multicellulaire bacteriën. De BASEL-collectie [193] is een faagbibliotheek bestaande uit *E. coli* fagen die allemaal goed gesequenced, fenotypisch gekarakteriseerd zijn, en waarvan de bacteriële receptoreiwitten bekend zijn [194-196]. Deze collectie wordt breed gebruikt en faciliteert de ontdekking van de moleculaire mechanismen van faag-bacterie interacties. Voor *Streptomyces* fagen is er de Actinobacteriofaag-database [76], maar deze bestaat uitsluitend uit faaggenomen en is niet direct beschikbaar voor experimenten. Aangezien we slechts het topje van de ijsberg kennen van de interactie tussen fagen en hun multicellulaire bacteriële gastheren, zou een bibliotheek van gesequenced en gekarakteriseerde *Streptomyces* fagen het veld enorm ten goede komen en hopelijk bijdragen aan meer open wetenschap en samenwerkingen tussen verschillende onderzoeksgroepen wereldwijd.

Het mechanisme van faaginfectie in multicellulaire bacteriën is grotendeels onbekend

Aangezien een veelgebruikte *Streptomyces* fagenbibliotheek niet direct beschikbaar is, hebben we 29 verschillende *Streptomyces coelicolor* mutantstammen, die specifieke celwand-geassocieerde eiwitten missen, geïnfecteerd met 46 fagen uit onze eigen collectie om het moleculaire mechanisme van faaginfectie in multicellulaire bacteriën te begrijpen. In **Hoofdstuk 6** observeerden we dat faag CF3 niet langer succesvol *S. coelicolor* kon infecteren die YidC2 miste. Dit eiwit is waarschijnlijk een membraaneiwit insertase in *E. coli* en *B. subtilis*, maar er is weinig bekend over zijn functie in *Streptomyces* [155,156]. In tegenstelling tot de wildtype, vormde *S. coelicolor* Δ*yidC2* geen celwandloze cellen na faaginfectie. Celwandloze cellen van de Δ*yidC2* mutant konden alleen worden gevormd door de stam bloot te stellen aan lysozym, wat aangeeft dat YidC2 een belangrijke rol speelt bij het afwerpen van de celwand na faaginfectie.

Interessant genoeg kon faag CF3 nog steeds hechten aan de Δ*yidC2* mutant. Met behulp van biochemie en cryo-elektronenmicroscopie, ontdekten we dat de nieuwe fagen die werden geproduceerd in de Δ*yidC2* mutant, niet langer werden vrijgegeven in de omgeving vanwege een blokkade in de afbraak van de bacteriële celwand.

Om ons begrip van YidC2's rol in het infectieproces te verbeteren, stelden we de hypothese dat de faag dit eiwit zou kunnen gebruiken om enkele van zijn eigen eiwitten in het membraan te zetten. Aangezien “holins” de meest bekende membraan-geassocieerde eiwitten van de faag zijn, hebben we het holin-endolysin systeem van faag CF3 nauwkeurig onderzocht. Eerdere studies toonden aan dat holin eiwitten het membraan verstoren door gaten te maken, waardoor endolysin eiwitten naar buiten kunnen om vervolgens de peptidoglycaanlaag af te breken [181]. Sommige holins vormen echter niet de typische "gaten", maar kunnen ook worden gebruikt voor niet-lytische eiwittranslocatie, door tijdelijk het membraan permeabel te maken, zodat endolysinen kunnen passeren [182]. Met behulp van Alphafold3, in combinatie met een bacteriële two-hybrid assay en karakterisering van endolysin-secretie mutanten, konden we aantonen dat YidC2 een interactie aangaat met het holin-endolysin systeem van faag CF3. Daarom denken we dat YidC2 de insertie van de holin en het endolysin eiwit van faag CF3 in het membraan vergemakkelijkt. Door middel van niet-lytische proteïnetranslocatie wordt dan het endolysin eiwit door de holin door het membraan geflipt, waardoor het de peptidoglycaanlaag enzymatisch kan afbreken. Dit mechanisme zorgt ervoor dat het celmembraan intact blijft en de bacteriën celwandloze cellen vormen.

Conclusie en toekomstige visie

De resultaten van dit proefschrift vormen een veelbelovend startpunt om ons begrip van de ecologische waarde van celwandloze bacteriën in de natuur en de interactie tussen fagen en hun multicellulaire gastheren verder te verbeteren. De combinatie van verschillende technieken, zoals licht en fluorescentie microscopie, elektronenmicroscopie, genetica en nog veel meer, maakte dit werk mogelijk en stelde ons in staat ongekende nieuwe inzichten te ontdekken. Echter, er blijven nog verschillende vragen over die onderzocht moeten worden. Bijvoorbeeld, kunnen fagen door hyfen van een mycelium reizen? Deze hypothese zou kunnen worden onderzocht door live-imaging van een fluorescerende *Streptomyces* faag tijdens infectie [197]. Het

verwijderen of toevoegen van genen in *Streptomyces* fagen is relatief ingewikkeld, waarschijnlijk vanwege het hoge G+C-gehalte, lage opbrengst van nieuwe fagen na infectie, en kleine fagenhoofdjes. Eén manier om deze nadelen te omzeilen is door lysogene *Streptomyces* fagen te integreren in hun gastheer en het faaggenoom binnenin de bacterie te manipuleren met genoom bewerkingssystemen zoals CRISPR-Cas9 [162,198], waarna de gemanipuleerde fagen kunnen worden geïsoleerd uit hun gastheer met mitomycine C, wat excisie van lysogene fagen uit het bacteriële genoom induceert [199]. Live-imaging van een fluorescerende faag tijdens infectie in *Streptomyces* zou kunnen onthullen of fagen daadwerkelijk door hyfen kunnen reizen en kan ook licht werpen op het mechanisme van celwandloosheid na faaginfectie in een multicellulaire bacterie.

Aangezien het meeste onderzoek naar faag-bacterie interacties is uitgevoerd in eencellige bacteriën [19,48,54], zouden multicellulaire bacteriën op een geheel andere manier kunnen reageren. In faagonderzoek is de verhouding tussen fagen en bacteriën tijdens infectie, of “Multiplicity of Infection” (MOI) een belangrijk concept. Een MOI van 1, bijvoorbeeld, betekent dat één bacterie wordt geïnfecteerd door één faag, en een MOI van 0,1 betekent dat er voor elke 10 bacteriën slechts één wordt geïnfecteerd door een faag. *Streptomyces* sporen kunnen één of twee kiembuizen maken en verder in de levenscyclus wordt het mycelium geteld als één kolonievormende eenheid. Dus, MOI-berekeningen met multicellulaire bacteriën verliezen hun betekenis zodra een spoor gekiemd is [98]. Wanneer *Streptomyces* geïnfecteerd wordt met fagen bij lage MOI, zullen slechts één of twee hyfen van een heel mycelium worden geïnfecteerd. Misschien signaleert de multicellulaire kolonie naar ongeïnfecteerde hyfen om celwandloze cellen te produceren om de populatie te redden, vergelijkbaar met abortieve infectie in eencellige bacteriën [46]. Om deze redenen zouden MOI-berekeningen in multicellulaire bacteriën, zoals *Streptomyces,* geoptimaliseerd moeten worden en zou een nieuwe en meer accurate formule voor MOI in multicellulaire bacteriën dit onderzoeksveld ten goede komen.

Echter, de meest urgente vraag die beantwoord moet worden, is de impact van het afwerpen van de bacteriële celwand tijdens faagtherapie. Faagtherapie is een veelbelovende strategie voor de behandeling van antibioticaresistente bacteriën. Mijn werk daarentegen, heeft aangetoond dat bacteriën gemakkelijk celwandloze cellen kunnen vormen na blootstelling aan fagen, wat een beschermend mechanisme biedt voor de bacteriepopulatie.

Interessant genoeg heeft eerder onderzoek aangetoond dat celwandloze bacteriën werden gevonden in bloedmonsters en ook bij patiënten met terugkerende urineweginfecties [66,200,201]. Dit geeft aan dat urine en bloed de tijdelijke morfologische staat van celwandloze cellen kunnen ondersteunen en dat klinische proeven die faagtherapie testen, deze morfologische verandering in overweging zouden moeten nemen. Bijvoorbeeld, faagtherapie toont veelbelovende resultaten bij de behandeling van mycobacteriële infecties, maar er is nooit een 100% succespercentage [202,203], wat mogelijk kan worden verklaard door het vermogen van veel mycobacteriële stammen om levensvatbare celwandloze cellen te vormen [204]. Naast conventionele diagnostische hulpmiddelen zou een volgende stap zijn om ook de vorming van celwandloze cellen na faaginfectie te monitoren tijdens experimentele procedures en klinische proeven voor faagtherapie behandelingen, die waarschijnlijk in het verleden over het hoofd zijn gezien [205]. Dit zou onze kennis over het voorkomen en de impact van celwandloze cellen na faagtherapie vergroten en bijdragen aan onze strijd tegen antibioticaresistente bacteriën.

References

[1] N. Arefa, A. K. Sarker, and M. A. Rahman, "Resistance-guided isolation and characterization of antibiotic-producing bacteria from river sediments," *BMC microbiology,* vol. 21, pp. 1-12, 2021.

[2] E. A. Barka *et al.*, "Taxonomy, physiology, and natural products of Actinobacteria," *Microbiology and molecular biology reviews,* vol. 80, no. 1, pp. 1-43, 2016.

[3] A. Van der Meij, S. F. Worsley, M. I. Hutchings, and G. P. van Wezel, "Chemical ecology of antibiotic production by actinomycetes," *FEMS microbiology reviews,* vol. 41, no. 3, pp. 392-416, 2017.

[4] K. Flärdh and M. J. Buttner, "Streptomyces morphogenetics: dissecting differentiation in a filamentous bacterium," *Nature Reviews Microbiology,* vol. 7, no. 1, pp. 36-49, 2009.

[5] P. Yagüe *et al.*, "Subcompartmentalization by cross-membranes during early growth of Streptomyces hyphae," *Nature Communications,* vol. 7, no. 1, p. 12467, 2016.

[6] M. Kontro, U. Lignell, M. R. Hirvonen, and A. Nevalainen, "pH effects on 10 Streptomyces spp. growth and sporulation depend on nutrients," *Letters in Applied Microbiology,* vol. 41, no. 1, pp. 32-38, 2005.

[7] D. Lapwood, "The Relative Importance of Weather, Soil-and Seed-borne Inoculum in determining the Incidence of Common Scab (Streptomyces scabies) in Potato Crops," *Plant Pathology,* vol. 21, no. 3, pp. 105-108, 1972.

[8] E. M. Shepherdson, C. R. Baglio, and M. A. Elliot, "Streptomyces behavior and competition in the natural environment," *Current Opinion in Microbiology,* vol. 71, p. 102257, 2023.

[9] P. Marsh and E. Wellington, "Interactions between actinophage and their streptomycete hosts in soil and the fate of phage borne genes," in *Gene Transfers and Environment: Proceedings of the Third European Meeting on Bacterial Genetics and Ecology (BAGECO-3),*

20–22 November 1991, Villefranche-sur-Mer, France, 1992: Springer, pp. 135-142.

[10] D. Claessen and J. Errington, "Cell wall-deficiency as a coping strategy for stress," in *Trends in Microbiology* vol. 27, ed: Elsevier Ltd, 2019, pp. 1025-1033.

[11] K. Ramijan *et al.*, "Stress-induced formation of cell wall-deficient cells in filamentous actinomycetes," *Nature Communications,* vol. 9, 2018, doi: 10.1038/s41467-018-07560-9.

[12] E. Ultee, K. Ramijan, R. T. Dame, A. Briegel, and D. Claessen, "Stress-induced adaptive morphogenesis in bacteria," *Advances in Microbial Physiology,* vol. 74, pp. 97-141, 2019, doi: 10.1016/bs.ampbs.2019.02.001.

[13] K. Kohm and R. Hertel, "The lifecycle of SPβ and related phages," *Archives of Virology,* vol. 166, no. 8, pp. 2119-2130, 2021.

[14] A. Washizaki, T. Yonesaki, and Y. Otsuka, "Characterization of the interactions between Escherichia coli receptors, LPS and OmpC, and bacteriophage T4 long tail fibers," *Microbiologyopen,* vol. 5, no. 6, pp. 1003-1015, 2016.

[15] M. H. V. Alstyne, R. H. Otto, and E. McCoy, "Characteristics of *Streptomyces griseus* strains resistant to phage," *Journal of bacteriology,* vol. 70, no. 1, pp. 113-119, 1955.

[16] L. A. Jones and S. Bradley, "The life-cycle of an actinophage for *Streptomyces venezuelae*," *Microbiology,* vol. 40, no. 2, pp. 191-198, 1965.

[17] T. Luthe *et al.*, "Streptomyces development is involved in the efficient containment of viral infections," *Microlife,* vol. 4, p. uqad002, 2023.

[18] L.-C. Fortier and O. Sekulovic, "Importance of prophages to evolution and virulence of bacterial pathogens," vol. 5, pp. 354-365, 2013, doi: 10.4161/viru.24498.

[19] G. P. C. Salmond and P. C. Fineran, "A century of the phage: past, present and future," in *Nature Reviews Microbiology* vol. 13, ed: Nature Publishing Group, 2015, pp. 777-786.

[20] M. Simmons, K. Drescher, C. D. Nadell, and V. Bucci, "Phage mobility is a core determinant of phage-bacteria coexistence in biofilms," *ISME Journal,* vol. 12, pp. 532-543, 2018, doi: 10.1038/ismej.2017.190.

[21] B. L. Beaman, "Induction of L-phase variants of *Nocardia caviae* within intact murine lungs," *Infection and Immunity,* vol. 29, pp. 244-251, 1980, doi: 10.1128/iai.29.1.244-251.1980.

[22] F. Germano, D. Testi, L. Campagnolo, M. Scimeca, and C. Arcuri, "Cell-wall-deficient bacteria in oral biofilm: association with periodontitis," in *medRxiv*, ed: medRxiv, 2020, p. 2020.07.13.20120428.

[23] H. W. Ackermann, "Phage classification and characterization.," *Methods in molecular biology (Clifton, N.J.),* vol. 501, pp. 127-140, 2009, doi: 10.1007/978-1-60327-164-6_13.

[24] E. J. Lefkowitz, D. M. Dempsey, R. C. Hendrickson, R. J. Orton, S. G. Siddell, and D. B. Smith, "Virus taxonomy: the database of the International Committee on Taxonomy of Viruses (ICTV)," *Nucleic Acids Research,* vol. 46, pp. D708-D717, 2018, doi: 10.1093/NAR/GKX932.

[25] M. Seoane-Blanco, M. J. van Raaij, and M. Granell, "Bacteriophage tail fibres, tailspikes, and bacterial receptor interaction," *Encyclopedia of Virology,* pp. 194-205, 2021, doi: 10.1016/B978-0-12-814515-9.00152-1.

[26] Y. Sun *et al.*, "Structural changes of tailless bacteriophage Φx174 during penetration of bacterial cell walls," *Proceedings of the National Academy of Sciences of the United States of America,* vol. 114, pp. 13708-13713, 2017, doi: 10.1073/pnas.1716614114.

[27] Q. Zhong *et al.*, "Transcriptomic analysis reveals the dependency of *Pseudomonas aeruginosa* genes for double-stranded RNA bacteriophage phiYY infection cycle," *iScience,* vol. 23, p. 101437, 2020, doi: 10.1016/j.isci.2020.101437.

[28] E. Stone, K. Campbell, I. Grant, and O. McAuliffe, "Understanding and exploiting phage–host interactions," in *Viruses* vol. 11, ed: MDPI AG, 2019, p. 567.

[29] Z. Chen *et al.*, "Cryo-EM structure of the bacteriophage T4 isometric head at 3.3-Å resolution and its relevance to the assembly of icosahedral viruses," *Proceedings of the National Academy of Sciences of the United States of America,* vol. 114, pp. E8184-E8193, 2017, doi: 10.1073/pnas.1708483114.

[30] A. Washizaki, T. Yonesaki, and Y. Otsuka, "Characterization of the interactions between *Escherichia coli* receptors, LPS and OmpC, and bacteriophage T4 long tail fibers," *MicrobiologyOpen,* vol. 5, pp. 1003-1015, 2016, doi: 10.1002/mbo3.384.

[31] M. L. Yap and M. G. Rossmann, "Structure and function of bacteriophage T4," in *Future Microbiology* vol. 9, ed: Future Medicine Ltd., 2014, pp. 1319-1337.

[32] A. A. Lindberg, "Bacteriophage receptors," in *Annual review of microbiology* vol. 27, ed, 1973, pp. 205-241.

[33] J.-V. Höltje, "Growth of the stress-bearing and shape-maintaining murein sacculus of *Escherichia coli*," *Microbiology and Molecular Biology Reviews,* vol. 62, pp. 181-203, 1998, doi: 10.1128/mmbr.62.1.181-203.1998.

[34] F. C. Neuhaus and J. Baddiley, "A continuum of anionic charge: structures and functions of d-alanyl-teichoic acids in gram-positive bacteria," *Microbiology and Molecular Biology Reviews,* vol. 67, pp. 686-723, 2003, doi: 10.1128/mmbr.67.4.686-723.2003.

[35] J. Bertozzi Silva, Z. Storms, and D. Sauvageau, "Host receptors for bacteriophage adsorption," *FEMS Microbiology Letters,* vol. 363, p. fnw002, 2016, doi: 10.1093/femsle/fnw002.

[36] D. V. Rakhuba, E. I. Kolomiets, E. Szwajcer Dey, and G. I. Novik, "Bacteriophage receptors, mechanisms of phage adsorption and penetration into host cell," in *Polish Journal of Microbiology* vol. 59, ed: Polish Society of Microbiologists, 2010, pp. 145-155.

[37] D. B. Datta, B. Arden, and U. Henning, "Major proteins of the *Escherichia coli* outer cell envelope membrane as bacteriophage receptors," *Journal of Bacteriology,* vol. 131, pp. 821-829, 1977, doi: 10.1128/jb.131.3.821-829.1977.

[38] K. Hantke, "Major outer membrane proteins of *E. coli* K12 serve as receptors for the phages T2 (protein Ia) and 434 (protein Ib)," *MGG Molecular & General Genetics,* vol. 164, pp. 131-135, 1978, doi: 10.1007/BF00267377.

[39] R. Marti, K. Zurfluh, S. Hagens, J. Pianezzi, J. Klumpp, and M. J. Loessner, "Long tail fibres of the novel broad-host-range T-even bacteriophage S16 specifically recognize *Salmonella* OmpC," *Molecular Microbiology,* vol. 87, pp. 818-834, 2013, doi: 10.1111/mmi.12134.

[40] M. Roa, "Interaction of bacteriophage K10 with its receptor, the lamB protein of *Escherichia coli*," *Journal of Bacteriology,* vol. 140, pp. 680-686, 1979, doi: 10.1128/jb.140.2.680-686.1979.

[41] H. Shin, J. H. Lee, H. Kim, Y. Choi, S. Heu, and S. Ryu, "Receptor diversity and host interaction of bacteriophages infecting *Salmonella enterica* Serovar Typhimurium," *PLoS ONE,* vol. 7, p. e43392, 2012, doi: 10.1371/journal.pone.0043392.

[42] R. C. Guerrero-Ferreira *et al.*, "Alternative mechanism for bacteriophage adsorption to the motile bacterium *Caulobacter crescentus*," *Proceedings of the National Academy of Sciences of the United States of America,* vol. 108, pp. 9963-9968, 2011, doi: 10.1073/pnas.1012388108.

[43] Z. Yu, C. Schwarz, L. Zhu, L. Chen, Y. Shen, and P. Yu, "Hitchhiking behavior in bacteriophages facilitates phage infection and enhances carrier bacteria colonization," *Environmental Science & Technology,* 2020, doi: 10.1021/acs.est.0c06969.

[44] A. K. Nichith Ratheesh, C. A. Calderon, A. M. Zdimal, and A. Shrivastava, "Swarm-mediated phage transport disrupts a biofilm inherently protected from phage penetration," doi: 10.1101/2021.06.25.449910.

[45] M. R. Tock and D. T. F. Dryden, "The biology of restriction and anti-restriction," in *Current Opinion in Microbiology* vol. 8, ed: Elsevier Current Trends, 2005, pp. 466-472.

[46] A. Lopatina, N. Tal, and R. Sorek, "Abortive infection: bacterial suicide as an antiviral immune strategy," in *Annual Review of Virology* vol. 7, ed: Annual Reviews Inc., 2020, pp. 371-384.

[47] A. Harms, D. E. Brodersen, N. Mitarai, and K. Gerdes, "Toxins, targets, and triggers: an overview of toxin-antitoxin biology," in *Molecular Cell* vol. 70, ed: Cell Press, 2018, pp. 768-784.

[48] H. G. Hampton, B. N. J. Watson, and P. C. Fineran, "The arms race between bacteria and their phage foes," in *Nature* vol. 577, ed: Nature Research, 2020, pp. 327-336.

[49] A. B. Isaev, O. S. Musharova, and K. V. Severinov, "Microbial arsenal of antiviral defenses – part I," in *Biochemistry (Moscow)* vol. 86, ed: Pleiades journals, 2021, pp. 319-337.

[50] K. Bhushan, "BacteRiophage EXclusion (BREX): a novel anti-phage mechanism in the arsenal of bacterial defense system," *Journal of Cellular Physiology,* vol. 233, pp. 771-773, 2018, doi: 10.1002/JCP.25973.

[51] S. Kronheim *et al.*, "A chemical defence against phage infection," *Nature,* vol. 564, pp. 283-286, 2018, doi: 10.1038/s41586-018-0767-x.

[52] A. H. Azam and Y. Tanji, "Bacteriophage-host arm race: an update on the mechanism of phage resistance in bacteria and revenge of the phage with the perspective for phage therapy," in *Applied Microbiology and Biotechnology* vol. 103, ed: Springer Verlag, 2019, pp. 2121-2131.

[53] X. Wu, J. Zhu, P. Tao, and V. B. Rao, "Bacteriophage T4 escapes CRISPR attack by minihomology recombination and repair," *mBio,* 2021, doi: 10.1128/mbio.01361-21.

[54] A. Bernheim and R. Sorek, "The pan-immune system of bacteria: antiviral defence as a community resource," in *Nature Reviews Microbiology* vol. 18, ed: Nature Research, 2020, pp. 113-119.

[55] H. G. Hampton, L. M. Smith, S. Ferguson, S. Meaden, S. A. Jackson, and P. C. Fineran, "Functional genomics reveals the toxin–antitoxin

repertoire and AbiE activity in serratia," *Microbial Genomics,* vol. 6, pp. 1-15, 2020, doi: 10.1099/mgen.0.000458.

[56] S. van Houte, A. Buckling, and E. R. Westra, "Evolutionary ecology of prokaryotic immune mechanisms," *Microbiology and Molecular Biology Reviews,* vol. 80, pp. 745-763, 2016, doi: 10.1128/mmbr.00011-16.

[57] L. Vidakovic, P. K. Singh, R. Hartmann, C. D. Nadell, and K. Drescher, "Dynamic biofilm architecture confers individual and collective mechanisms of viral protection," *Nature Microbiology,* vol. 3, pp. 26-31, 2017, doi: 10.1038/s41564-017-0050-1.

[58] T. Reyes-Robles *et al.*, "*Vibrio cholerae* outer membrane vesicles inhibit bacteriophage infection," *Journal of Bacteriology,* vol. 200, 2018, doi: 10.1128/JB.00792-17.

[59] H. Harvey, J. Bondy-Denomy, H. Marquis, K. M. Sztanko, A. R. Davidson, and L. L. Burrows, "*Pseudomonas aeruginosa* defends against phages through type IV pilus glycosylation," *Nature Microbiology,* vol. 3, pp. 47-52, 2018, doi: 10.1038/s41564-017-0061-y.

[60] J. T. Rostøl and L. Marraffini, "(Ph)ighting phages: how bacteria resist their parasites," in *Cell Host and Microbe* vol. 25, ed: Cell Press, 2019, pp. 184-194.

[61] D. Scholl, S. Adhya, and C. Merril, "*Escherichia coli* K1's capsule is a barrier to bacteriophage T7," *Applied and Environmental Microbiology,* vol. 71, pp. 4872-4874, 2005, doi: 10.1128/AEM.71.8.4872-4874.2005.

[62] S. Lemire, K. M. Yehl, and T. K. Lu, "Phage-based applications in synthetic biology," *Annual Review of Virology,* vol. 5, pp. 453-476, 2018, doi: 10.1146/annurev-virology-092917-043544.

[63] E. Ultee, A. Briegel, and D. Claessen, "Formation of wall-less cells in *Kitasatospora viridifaciens* requires cytoskeletal protein FilP in oxygen-limiting conditions," pp. 1-10, 2020, doi: 10.1101/2020.05.26.116947.

[64] R. Mercier, Y. Kawai, and J. Errington, "General principles for the formation and proliferation of a wall-free (L-form) state in bacteria," *eLife,* vol. 3, 2014, doi: 10.7554/eLife.04629.

[65] R. Mercier, Y. Kawai, and J. Errington, "Excess membrane synthesis drives a primitive mode of cell proliferation," *Cell,* vol. 152, pp. 997-1007, 2013, doi: 10.1016/j.cell.2013.01.043.

[66] K. M. Mickiewicz *et al.*, "Possible role of L-form switching in recurrent urinary tract infection," *Nature Communications,* vol. 10, 2019, doi: 10.1038/s41467-019-12359-3.

[67] J. T. Park and J. L. Strominger, "Mode of action of penicillin. Biochemical basis for the mechanism of action of penicillin and for Its selective toxicity," in *New Series*, 1957, vol. 125, pp. 99-101.

[68] G. Slavchev, L. Michailova, and N. Markova, "Stress-induced L-forms of *Mycobacterium bovis*: a challenge to survivability," in *NEW MICROBIOLOGICA*, 2013, vol. 36, pp. 157-166.

[69] N. Markova, G. Slavchev, L. Michailova, and M. Jourdanova, "Survival of *Escherichia coli* under lethal heat stress by L-form conversion," *International Journal of Biological Sciences,* vol. 6, pp. 303-315, 2010, doi: 10.7150/ijbs.6.303.

[70] T. Onoda, A. Oshima, S. Nakano, and A. Matsuno, "Morphology, growth and reversion in a stable L-form of *Escherichia coli* K12," *Journal of General Microbiology,* vol. 133, pp. 527-534, 1987, doi: 10.1099/00221287-133-3-527.

[71] M. Osawa and H. P. Erickson, "L form bacteria growth in low-osmolality medium," *Microbiology (United Kingdom),* vol. 165, pp. 842-851, 2019, doi: 10.1099/mic.0.000799.

[72] T. Chikada, T. Kanai, M. Hayashi, T. Kasai, T. Oshima, and D. Shiomi, "Direct observation of conversion from walled cells to wall-deficient L-form and vice versa in *Escherichia coli* indicates the essentiality of the outer membrane for proliferation of L-form cells," *Frontiers in Microbiology,* vol. 12, p. 537, 2021, doi: 10.3389/fmicb.2021.645965.

[73] E. R. Rojas *et al.*, "The outer membrane is an essential load-bearing element in Gram-negative bacteria," *Nature,* vol. 559, pp. 617-621, 2018, doi: 10.1038/s41586-018-0344-3.

[74] A. Du Toit, "Living without the cell wall," *Nature Reviews Microbiology,* vol. 17, p. 65, 2019, doi: 10.1038/s41579-018-0142-9.

[75] F. A. Hussain *et al.*, "Rapid evolutionary turnover of mobile genetic elements drives microbial resistance to viruses," doi: 10.1101/2021.03.26.437281.

[76] D. A. Russell and G. F. Hatfull, "PhagesDB: the actinobacteriophage database," *Bioinformatics,* vol. 33, pp. 784-786, 2017, doi: 10.1093/bioinformatics/btw711.

[77] I. Groth, C. Rodríguez, B. Schütze, P. Schmitz, E. Leistner, and M. Goodfellow, "Five novel *Kitasatospora* species from soil: *Kitasatospora arboriphila* sp. nov., *K. gansuensis* sp. nov., *K. nipponensis* sp. nov., *K. paranensis* sp., nov. and *K. terrestris* sp. nov," *International Journal of Systematic and Evolutionary Microbiology,* vol. 54, pp. 2121-2129, 2004, doi: 10.1099/ijs.0.63070-0.

[78] E. M. H. Wellington, E. Stackebrandt, D. Sanders, J. Wolstrup, and N. O. G. Jorgensen, "Taxonomic status of *Kitasatosporia*, and proposed unification with *Streptomyces* on the basis of phenotypic and 16S rRNA analysis and emendation of *Streptomyces Waksman* and *Henrici* 1943, 339(AL)," *International Journal of Systematic Bacteriology,* vol. 42, pp. 156-160, 1992, doi: 10.1099/00207713-42-1-156.

[79] A. Petrovic Fabijan *et al.*, "L-form switching confers antibiotic, phage and stress tolerance in pathogenic *Escherichia coli*," *bioRxiv,* p. 2021.06.21.449206, 2021, doi: 10.1101/2021.06.21.449206.

[80] J. Gumpert, I. Zimmermann, and U. Taubeneck, "Phage adsorption and productive lysis in stable protoplast type L-forms of *Bacillus subtilis* and *Streptomyces hygroscopicus*," *Journal of Basic Microbiology,* vol. 26, pp. 15-25, 1986, doi: 10.1002/jobm.3620260106.

[81] E. D. Jacobson1, O. E. Landman2, and H. Rogers, "Interaction of protoplasts, L forms, and bacilli of *Bacillus subtilis* with 12 strains of

bacteriophage," *JOURNAL OF BACTERIOLOGY,* vol. 124, pp. 445-458, 1975.

[82] J. Maniloff and K. Dybvig, "Mycoplasma viruses," *CRC Critical Reviews in Microbiology,* vol. 15, pp. 339-389, 1988, doi: 10.3109/10408418809104462.

[83] T. Azimi, M. Mosadegh, M. J. Nasiri, S. Sabour, S. Karimaei, and A. Nasser, "Phage therapy as a renewed therapeutic approach to mycobacterial infections: a comprehensive review," in *Infection and Drug Resistance* vol. 12, ed: Dove Medical Press Ltd., 2019, pp. 2943-2959.

[84] S. Kilcher, P. Studer, C. Muessner, J. Klumpp, M. J. Loessner, and S. Adhya, "Cross-genus rebooting of custom-made, synthetic bacteriophage genomes in L-form bacteria," *Proceedings of the National Academy of Sciences of the United States of America,* vol. 115, pp. 567-572, 2018, doi: 10.1073/pnas.1714658115.

[85] R. Monteiro, D. P. Pires, A. R. Costa, and J. Azeredo, "Phage therapy: going temperate?," in *Trends in Microbiology* vol. 27, ed: Elsevier Ltd, 2019, pp. 368-378.

[86] L. T. Fernández-Martínez *et al.*, "New insights into chloramphenicol biosynthesis in *Streptomyces venezuelae* ATCC 10712," *Antimicrobial Agents and Chemotherapy,* vol. 58, no. 12, pp. 7441-7450, 2014.

[87] R. E. d. L. Procópio, I. R. d. Silva, M. K. Martins, J. L. d. Azevedo, and J. M. d. Araújo, "Antibiotics produced by *Streptomyces*," *Brazilian Journal of Infectious Diseases,* vol. 16, no. 5, pp. 466-471, 2012.

[88] J. Zheng, Y. Li, H. Guan, J. Zhang, and H. Tan, "Enhancement of neomycin production by engineering the entire biosynthetic gene cluster and feeding key precursors in *Streptomyces fradiae* CGMCC 4.576," *Applied microbiology and biotechnology,* vol. 103, no. 5, pp. 2263-2275, 2019.

[89] K.-S. Hwang, H. U. Kim, P. Charusanti, B. Ø. Palsson, and S. Y. Lee, "Systems biology and biotechnology of *Streptomyces* species for the production of secondary metabolites," *Biotechnology advances,* vol. 32, no. 2, pp. 255-268, 2014.

[90] G. P. van Wezel and K. J. McDowall, "The regulation of the secondary metabolism of *Streptomyces*: new links and experimental advances," *Natural product reports,* vol. 28, no. 7, pp. 1311-1333, 2011.

[91] P. A. Hoskisson, P. Sumby, and M. C. Smith, "The phage growth limitation system in *Streptomyces coelicolor* A (3) 2 is a toxin/antitoxin system, comprising enzymes with DNA methyltransferase, protein kinase and ATPase activity," *Virology,* vol. 477, pp. 100-109, 2015.

[92] P. Sumby and M. C. Smith, "Genetics of the phage growth limitation (Pgl) system of *Streptomyces coelicolor* A3 (2)," *Molecular microbiology,* vol. 44, no. 2, pp. 489-500, 2002.

[93] V. Ongenae, A. S. Mabrouk, M. Crooijmans, D. Rozen, A. Briegel, and D. Claessen, "Reversible bacteriophage resistance by shedding the bacterial cell wall," *Open Biology,* vol. 12, no. 6, 2022, doi: 10.1098/rsob.210379.

[94] H. Zhu *et al.*, "Eliciting antibiotics active against the ESKAPE pathogens in a collection of actinomycetes isolated from mountain soils," *Microbiology (United Kingdom),* vol. 160, pp. 1714-1726, 2014, doi: 10.1099/mic.0.078295-0.

[95] J. Dowding, "Characterization of a bacteriophage virulent for Streptomyces coelicolor A3 (2)," *Microbiology,* vol. 76, no. 1, pp. 163-176, 1973.

[96] J. R. Garneau, F. Depardieu, L.-C. Fortier, D. Bikard, and M. Monot, "PhageTerm: a tool for fast and accurate determination of phage termini and packaging mechanism using next-generation sequencing data," *Scientific reports,* vol. 7, no. 1, pp. 1-10, 2017.

[97] R. C. Edgar, "MUSCLE: multiple sequence alignment with high accuracy and high throughput," *Nucleic acids research,* vol. 32, no. 5, pp. 1792-1797, 2004.

[98] A. Hardy, V. Sharma, L. Kever, and J. Frunzke, "Genome sequence and characterization of five bacteriophages infecting Streptomyces coelicolor and Streptomyces venezuelae: Alderaan, Coruscant, Dagobah, Endor1 and Endor2," *Viruses,* vol. 12, no. 10, p. 1065, 2020.

[99] D. Turner, E. M. Adriaenssens, I. Tolstoy, and A. M. Kropinski, "Phage annotation guide: guidelines for assembly and high-quality annotation," *PHAGE,* vol. 2, no. 4, pp. 170-182, 2021.
[100] C. Moraru, A. Varsani, and A. M. Kropinski, "VIRIDIC—A novel tool to calculate the intergenomic similarities of prokaryote-infecting viruses," *Viruses,* vol. 12, no. 11, p. 1268, 2020.
[101] A. C. Groth and M. P. Calos, "Phage integrases: biology and applications," *Journal of molecular biology,* vol. 335, no. 3, pp. 667-678, 2004.
[102] J. J. Dennehy and S. T. Abedon, "Phage Infection and Lysis," *Bacteriophages: Biology, Technology, Therapy,* pp. 341-383, 2021.
[103] R. Seshadri *et al.*, "Expanding the genomic encyclopedia of Actinobacteria with 824 isolate reference genomes," *Cell genomics,* vol. 2, no. 12, 2022.
[104] M. J. Bibb, "Understanding and manipulating antibiotic production in actinomycetes," *Biochemical Society Transactions,* vol. 41, no. 6, pp. 1355-1364, 2013.
[105] N. Lu *et al.*, "Characterization and genome analysis of the temperate bacteriophage ϕSAJS1 from Streptomyces avermitilis," *Virus research,* vol. 265, pp. 34-42, 2019.
[106] D. Turner *et al.*, "Abolishment of morphology-based taxa and change to binomial species names: 2022 taxonomy update of the ICTV bacterial viruses subcommittee," *Archives of Virology,* vol. 168, no. 2, p. 74, 2023.
[107] H.-W. Ackermann, "Frequency of morphological phage descriptions," *Archives of virology,* vol. 124, pp. 201-209, 1992.
[108] D. A. Russell and G. F. Hatfull, "PhagesDB: the actinobacteriophage database," *Bioinformatics,* vol. 33, no. 5, pp. 784-786, 2017.
[109] D. A. Benson *et al.*, "GenBank," *Nucleic Acids Research,* vol. 41, no. D1, pp. D36-D42, 2012, doi: 10.1093/nar/gks1195.
[110] N. S. Olsen, W. Kot, L. M. Junco, and L. H. Hansen, "Exploring the remarkable diversity of Escherichia coli phages in the Danish

Wastewater Environment, including 91 Novel Phage Species," *bioRxiv,* p. 2020.01. 19.911818, 2020.

[111] V. Ongenae, J. Azeredo, A. M. Kropinski, D. Rozen, A. Briegel, and D. Claessen, "Genome sequence and characterization of Streptomyces phage Pablito, representing a new species within the genus Janusvirus," *Scientific Reports,* vol. 12, no. 1, p. 17785, 2022.

[112] A. Rosner and R. Gutstein, "Adsorption of actinophage Pal 6 to developing mycelium of Streptomyces albus," *Canadian Journal of Microbiology,* vol. 27, no. 2, pp. 254-257, 1981.

[113] A. Prjibelski, D. Antipov, D. Meleshko, A. Lapidus, and A. Korobeynikov, "Using SPAdes de novo assembler," *Current protocols in bioinformatics,* vol. 70, no. 1, p. e102, 2020.

[114] Y. Nishimura, T. Yoshida, M. Kuronishi, H. Uehara, H. Ogata, and S. Goto, "ViPTree: the viral proteomic tree server," *Bioinformatics,* vol. 33, no. 15, pp. 2379-2380, 2017.

[115] M. van den Belt, C. Gilchrist, T. J. Booth, Y.-H. Chooi, M. H. Medema, and M. Alanjary, "CAGECAT: The CompArative GEne Cluster Analysis Toolbox for rapid search and visualisation of homologous gene clusters," *BMC Bioinformatics,* vol. 24, no. 1, p. 181, 2023/05/03 2023, doi: 10.1186/s12859-023-05311-2.

[116] Y. Takahashi, "Genus *Kitasatospora,* taxonomic features and diversity of secondary metabolites," in *Journal of Antibiotics* vol. 70, ed: Nature Publishing Group, 2017, pp. 506-513.

[117] C. Gilmour, E. Noller, and B. Watkins, "Studies on Streptomyces Phage: I. Growth Characteristics of the Streptomyces griseus Host-Phage System," *Journal of Bacteriology,* vol. 78, no. 2, pp. 186-192, 1959.

[118] E. Jończyk, M. Kłak, R. Międzybrodzki, and A. Górski, "The influence of external factors on bacteriophages," *Folia microbiologica,* vol. 56, pp. 191-200, 2011.

[119] V. Zsuzsanna, C. Gabriella, H. Levente, and K. Miklós, "Temperature-dependent nanomechanics and topography of bacteriophage T7," 2018.

[120] M. R. Olson, R. P. Axler, and R. E. Hicks, "Effects of freezing and storage temperature on MS2 viability," *Journal of virological methods,* vol. 122, no. 2, pp. 147-152, 2004.
[121] M. Sharma, D. Kumar, and K. M. Poluri, "Elucidating the pH-dependent structural transition of T7 bacteriophage endolysin," *Biochemistry,* vol. 55, no. 33, pp. 4614-4625, 2016.
[122] A. Das, S. Mandal, V. Hemmadi, V. Ratre, and M. Biswas, "Studies on the gene regulation involved in the lytic–lysogenic switch in *Staphylococcus aureus* temperate bacteriophage Phi11," *The Journal of Biochemistry,* vol. 168, pp. 659-668, 2020, doi: 10.1093/jb/mvaa080.
[123] R. Edgar *et al.*, "Bacteriophage infection is targeted to cellular poles," *Molecular Microbiology,* vol. 68, pp. 1107-1116, 2008, doi: 10.1111/j.1365-2958.2008.06205.x.
[124] R. L. Dy, R. Przybilski, K. Semeijn, G. P. C. Salmond, and P. C. Fineran, "A widespread bacteriophage abortive infection system functions through a type IV toxin-antitoxin mechanism," *Nucleic Acids Research,* vol. 42, pp. 4590-4605, 2014, doi: 10.1093/nar/gkt1419.
[125] F. Hille, H. Richter, S. P. Wong, M. Bratovič, S. Ressel, and E. Charpentier, "The biology of CRISPR-Cas: backward and forward," in *Cell* vol. 172, ed: Cell Press, 2018, pp. 1239-1259.
[126] C. M. Johnson, M. M. Harden, and A. D. Grossman, "An integrative and conjugative element encodes an abortive infection system to protect host cells from predation by a bacteriophage," in *bioRxiv*, ed: bioRxiv, 2020, p. 2020.12.13.422588.
[127] K. S. Makarova *et al.*, "Evolutionary classification of CRISPR–Cas systems: a burst of class 2 and derived variants," in *Nature Reviews Microbiology* vol. 18, ed: Nature Research, 2020, pp. 67-83.
[128] L. M. Malone, N. Birkholz, and P. C. Fineran, "Conquering CRISPR: how phages overcome bacterial adaptive immunity," in *Current Opinion in Biotechnology* vol. 68, ed: Elsevier Ltd, 2021, pp. 30-36.

[129] Y. Qiu, S. Wang, Z. Chen, Y. Guo, and Y. Song, "An active type I-E CRISPR-cas system identified in *Streptomyces avermitilis*," *PLoS ONE,* vol. 11, 2016, doi: 10.1371/journal.pone.0149533.

[130] T. Kieser, M. J. Bibb, M. J. Buttner, K. F. Chater, and D. A. Hopwood, "Practical streptomyces genetics," vol. 291, 2000.

[131] C. Stuttard, "Temperate phages of *Streptomyces venezuelae*: lysogeny and host specificity shown by phages SV1 and SV2," *Journal of General Microbiology,* vol. 128, pp. 115-121, 1982, doi: 10.1099/00221287-128-1-115.

[132] C. Allan *et al.*, "OMERO: flexible, model-driven data management for experimental biology," *Nat Methods,* vol. 9, no. 3, pp. 245-53, Feb 28 2012, doi: 10.1038/nmeth.1896.

[133] J. R. Kremer, D. N. Mastronarde, and J. R. McIntosh, "Computer visualization of three-dimensional image data using IMOD," *Journal of Structural Biology,* vol. 116, pp. 71-76, 1996, doi: 10.1006/jsbi.1996.0013.

[134] F. U. Battistuzzi, A. Feijao, and S. B. Hedges, "A genomic timescale of prokaryote evolution: insights into the origin of methanogenesis, phototrophy, and the colonization of land," *BMC evolutionary biology,* vol. 4, no. 1, pp. 1-14, 2004.

[135] A. Bravo and M. Salas, "Polymerization of bacteriophage ø29 replication protein p1 into protofilament sheets," *The EMBO journal,* vol. 17, no. 20, pp. 6096-6105, 1998.

[136] A. B. Isaev, O. S. Musharova, and K. V. Severinov, "Microbial arsenal of antiviral defenses. part II," *Biochemistry (Moscow) 2021 86:4,* vol. 86, pp. 449-470, 2021, doi: 10.1134/S0006297921040064.

[137] E. J, "L-form bacteria, cell walls and the origins of life," *Open biology,* vol. 3, 2013, doi: 10.1098/RSOB.120143.

[138] M. Toyofuku *et al.*, "Prophage-triggered membrane vesicle formation through peptidoglycan damage in *Bacillus subtilis*," *Nature Communications,* vol. 8, pp. 1-10, 2017, doi: 10.1038/s41467-017-00492-w.

[139] V. Grosboillot, "Revertant *Listeria monocytogenes* and conditions for their persistence as intracellular L-forms," 2021, doi: 10.3929/ETHZ-B-000490596.
[140] A. M. Paton and C. M. J. Innes, "Methods for the establishment of intracellular associations of L-forms with higher plants," *Journal of Applied Bacteriology,* vol. 71, pp. 59-64, 1991, doi: 10.1111/J.1365-2672.1991.TB04663.X.
[141] J. M. Wood, "Bacterial responses to osmotic challenges," *The Journal of General Physiology,* vol. 145, p. 381, 2015, doi: 10.1085/JGP.201411296.
[142] F. E. Youngt, "Requirement of glucosylated teichoic acid for adsorption of phage in *Bacillus subtilis*."
[143] M. M. Farley, J. Tu, D. B. Kearns, I. J. Molineux, and J. Liu, "Ultrastructural analysis of bacteriophage Φ29 during infection of *Bacillus subtilis*," *Journal of structural biology,* vol. 197, p. 163, 2017, doi: 10.1016/J.JSB.2016.07.019.
[144] E. D. Jacobson and O. E. Landman, "Adsorption of bacteriophages phi 29 and 22a to protoplasts of *Bacillus subtilis* 168," *Journal of Virology,* vol. 21, pp. 1223-1227, 1977, doi: 10.1128/JVI.21.3.1223-1227.1977.
[145] N. Pett *et al.*, "T4 Bacteriophage and E. coli Interaction in the Murine Intestine: A Prototypical Model for Studying Host-Bacteriophage Dynamics In Vivo," *Journal of Visualized Experiments: Jove,* no. 203, 2024.
[146] N. Li *et al.*, "Characterization of phage resistance and their impacts on bacterial fitness in Pseudomonas aeruginosa," *Microbiology Spectrum,* vol. 10, no. 5, pp. e02072-22, 2022.
[147] A. R. Costa *et al.*, "Accumulation of defense systems in phage-resistant strains of Pseudomonas aeruginosa," *Science Advances,* vol. 10, no. 8, p. eadj0341, 2024.
[148] R. E. d. L. Procópio, I. R. d. Silva, M. K. Martins, J. L. d. Azevedo, and J. M. d. Araújo, "Antibiotics produced by Streptomyces," *Brazilian Journal of Infectious Diseases,* vol. 16, pp. 466-471, 2012.

[149] M. G. Watve, R. Tickoo, M. M. Jog, and B. D. Bhole, "How many antibiotics are produced by the genus Streptomyces?," *Archives of microbiology,* vol. 176, pp. 386-390, 2001.

[150] J. Hamedi, N. Poorinmohammad, and R. Papiran, "Growth and lifecycle of Actinobacteria," *Biology and Biotechnology of Actinobacteria,* pp. 29-50, 2017.

[151] L. Kever, Q. Zhang, A. Hardy, P. Westhoff, Y. Yu, and J. Frunzke, "Decoupling the molecular versatility of aminoglycosides via drug or target modification enables community-wide antiphage defense," *bioRxiv,* p. 2024.02.27.582341, 2024, doi: 10.1101/2024.02.27.582341.

[152] H. Georjon, F. Tesson, H. Shomar, and A. Bernheim, "Genomic characterization of the antiviral arsenal of Actinobacteria," *Microbiology,* vol. 169, no. 8, p. 001374, 2023.

[153] J. C. Wohlfarth *et al.*, "L-form conversion in Gram-positive bacteria enables escape from phage infection," *Nature Microbiology,* vol. 8, no. 3, pp. 387-399, 2023.

[154] B. Roucourt and R. Lavigne, "The role of interactions between phage and bacterial proteins within the infected cell: a diverse and puzzling interactome," *Environmental microbiology,* vol. 11, no. 11, pp. 2789-2805, 2009.

[155] J. C. Samuelson *et al.*, "YidC mediates membrane protein insertion in bacteria," *Nature,* vol. 406, no. 6796, pp. 637-641, 2000.

[156] H. Tjalsma, S. Bron, and J. M. van Dijl, "Complementary impact of paralogous Oxa1-like proteins of Bacillus subtilis on post-translocational stages in protein secretion," *Journal of Biological Chemistry,* vol. 278, no. 18, pp. 15622-15632, 2003.

[157] B. Gust, G. L. Challis, K. Fowler, T. Kieser, and K. F. Chater, "PCR-targeted Streptomyces gene replacement identifies a protein domain needed for biosynthesis of the sesquiterpene soil odor geosmin," *Proceedings of the National Academy of Sciences,* vol. 100, no. 4, pp. 1541-1546, 2003.

[158] D. Russel and J. Sambrook, "Molecular cloning: a laboratory manual," *New,* 2001.
[159] Y. Lee, S. Hwang, W. Kim, J. H. Kim, B. O. Palsson, and B.-K. Cho, "CRISPR-aided genome engineering for secondary metabolite biosynthesis in Streptomyces," *Journal of Industrial Microbiology and Biotechnology,* p. kuae009, 2024.
[160] L. Zhang, J. Willemse, P. A. Hoskisson, and G. P. van Wezel, "Sporulation-specific cell division defects in ylmE mutants of Streptomyces coelicolor are rescued by additional deletion of ylmD," *Scientific Reports,* vol. 8, no. 1, p. 7328, 2018.
[161] M. B. Hamed, J. Anné, S. Karamanou, and A. Economou, "Streptomyces protein secretion and its application in biotechnology," *FEMS microbiology letters,* vol. 365, no. 22, p. fny250, 2018.
[162] C. Bai and G. P. van Wezel, "CUBIC: A Versatile Cumate-Based Inducible CRISPRi System in Streptomyces," *ACS Synthetic Biology,* vol. 12, no. 10, pp. 3143-3147, 2023.
[163] A. Froger and J. E. Hall, "Transformation of plasmid DNA into E. coli using the heat shock method," *JoVE (Journal of visualized experiments),* no. 6, p. e253, 2007.
[164] X. Zhong, L. Zhang, G. P. van Wezel, E. Vijgenboom, and D. Claessen, "Role for a lytic polysaccharide monooxygenase in cell wall remodeling in Streptomyces coelicolor," *Mbio,* vol. 13, no. 2, pp. e00456-22, 2022.
[165] J. N. Bach and M. Bramkamp, "Flotillins functionally organize the bacterial membrane," (in eng), *Mol Microbiol,* vol. 88, no. 6, pp. 1205-17, Jun 2013, doi: 10.1111/mmi.12252.
[166] R. Kapteijn *et al.*, "Endocytosis-like DNA uptake by cell wall-deficient bacteria," *Nature Communications,* vol. 13, no. 1, p. 5524, 2022/09/22 2022, doi: 10.1038/s41467-022-33054-w.
[167] C. Allan *et al.*, "OMERO: flexible, model-driven data management for experimental biology," *Nature methods,* vol. 9, no. 3, pp. 245-253, 2012.

[168] J. Abramson *et al.*, "Accurate structure prediction of biomolecular interactions with AlphaFold 3," *Nature,* pp. 1-3, 2024.
[169] J. Hallgren *et al.*, "DeepTMHMM predicts alpha and beta transmembrane proteins using deep neural networks," *bioRxiv,* p. 2022.04.08.487609, 2022, doi: 10.1101/2022.04.08.487609.
[170] S. H. Rangwala *et al.*, "Accessing NCBI data using the NCBI sequence viewer and genome data viewer (GDV)," *Genome research,* vol. 31, no. 1, pp. 159-169, 2021.
[171] P. Wang, A. Kuhn, and R. E. Dalbey, "Global change of gene expression and cell physiology in YidC-depleted Escherichia coli," *Journal of bacteriology,* vol. 192, no. 8, pp. 2193-2209, 2010.
[172] D. Claessen *et al.*, "The stomatin-like protein StlP organizes membrane microdomains to govern polar growth in filamentous actinobacteria under hyperosmotic stress," 2024.
[173] V. Ongenae *et al.*, "Genome sequence and characterization of Streptomyces phages Vanseggelen and Verabelle, representing two new species within the genus Camvirus," *Scientific Reports,* vol. 13, no. 1, p. 20153, 2023.
[174] R. R. Yocum, J. R. Rasmussen, and J. L. Strominger, "The mechanism of action of penicillin. Penicillin acylates the active site of Bacillus stearothermophilus D-alanine carboxypeptidase," *Journal of Biological Chemistry,* vol. 255, no. 9, pp. 3977-3986, 1980.
[175] H. G. Floss and T.-W. Yu, "Rifamycin mode of action, resistance, and biosynthesis," *Chemical reviews,* vol. 105, no. 2, pp. 621-632, 2005.
[176] Z. Wu *et al.*, "The holin-endolysin lysis system of the OP2-Like phage X2 infecting Xanthomonas oryzae pv. oryzae," *Viruses,* vol. 13, no. 10, p. 1949, 2021.
[177] M. Youle, *Thinking like a phage*. Wholon, 2017.
[178] V. A. Fischetti, "Bacteriophage endolysins: a novel anti-infective to control Gram-positive pathogens," *International Journal of Medical Microbiology,* vol. 300, no. 6, pp. 357-362, 2010.

[179] M. Schneider, J. R. Johnson, N. J. Krogan, and S. K. Chanda, "The virus–host interactome: Knowing the players to understand the game," in *Viral Pathogenesis*: Elsevier, 2016, pp. 157-167.
[180] A. A. Pohane and V. Jain, "Insights into the regulation of bacteriophage endolysin: Multiple means to the same end," *Microbiology,* vol. 161, no. Pt_12, pp. 2269-2276, 2015.
[181] R. Young, "Bacteriophage holins: deadly diversity," *Journal of molecular microbiology and biotechnology,* vol. 4, no. 1, pp. 21-36, 2002.
[182] I.-N. Wang, D. L. Smith, and R. Young, "Holins: the protein clocks of bacteriophage infections," *Annual Reviews in Microbiology,* vol. 54, no. 1, pp. 799-825, 2000.
[183] T. Brüser and D. Mehner-Breitfeld, "Occurrence and potential mechanism of holin-mediated non-lytic protein translocation in bacteria," *microbial Cell,* vol. 9, no. 10, p. 159, 2022.
[184] D. J. MacNeil, K. M. Gewain, C. L. Ruby, G. Dezeny, P. H. Gibbons, and T. MacNeil, "Analysis of Streptomyces avermitilis genes required for avermectin biosynthesis utilizing a novel integration vector," *Gene,* vol. 111, no. 1, pp. 61-68, 1992.
[185] M. S. Paget, L. Chamberlin, A. Atrih, S. J. Foster, and M. J. Buttner, "Evidence that the extracytoplasmic function sigma factor ςE is required for normal cell wall structure in Streptomyces coelicolor A3 (2)," *Journal of bacteriology,* vol. 181, no. 1, pp. 204-211, 1999.
[186] G. Karimova, J. Pidoux, A. Ullmann, and D. Ladant, "A bacterial two-hybrid system based on a reconstituted signal transduction pathway," *Proceedings of the National Academy of Sciences,* vol. 95, no. 10, pp. 5752-5756, 1998.
[187] L. Kever *et al.*, "Aminoglycoside antibiotics inhibit phage infection by blocking an early step of the infection cycle," *MBio,* vol. 13, no. 3, pp. e00783-22, 2022.
[188] R. Ouyang, V. Ongenae, A. Muok, D. Claessen, and A. Briegel, "Phage fibers and spikes: a nanoscale Swiss army knife for host infection," *Current Opinion in Microbiology,* vol. 77, p. 102429, 2024.

[189] H. Georjon and A. Bernheim, "The highly diverse antiphage defence systems of bacteria," *Nature Reviews Microbiology,* vol. 21, no. 10, pp. 686-700, 2023.
[190] V. Ongenae, A. Briegel, and D. Claessen, "Cell wall-deficiency as an escape mechanism from phage infection," *Open Biology,* vol. 11, p. 210199, 2021, doi: 10.1098/RSOB.210199.
[191] M. Blazanin and P. E. Turner, "Community context matters for bacteria-phage ecology and evolution," *The ISME Journal,* pp. 1-10, 2021, doi: 10.1038/s41396-021-01012-x.
[192] B. Rackow, C. Rolland, I. Mohnen, J. Wittmann, J. Overmann, and J. Frunzke, "Isolation and characterization of the new Streptomyces phages Kamino, Geonosis, Abafar and Scarif infecting a broad range of host species," *bioRxiv,* p. 2024.02. 26.582091, 2024.
[193] A. Sidi Mabrouk, V. Ongenae, D. Claessen, S. Brenzinger, and A. Briegel, "A flexible and efficient microfluidics platform for the characterization and isolation of novel bacteriophages," *Applied and Environmental Microbiology,* vol. 89, no. 1, pp. e01596-22, 2023.
[194] E. Maffei *et al.*, "Systematic exploration of Escherichia coli phage–host interactions with the BASEL phage collection," *PLoS Biology,* vol. 19, no. 11, p. e3001424, 2021.
[195] T. Mets *et al.*, "Mechanism of phage sensing and restriction by toxin-antitoxin-chaperone systems," *Cell Host & Microbe,* 2024.
[196] A. A. Hossain *et al.*, "DNA glycosylases provide antiviral defence in prokaryotes," *Nature,* pp. 1-7, 2024.
[197] S. Erdrich, U. Schurr, J. Frunzke, and B. Arsova, "Seed coating with phages for sustainable plant biocontrol of plant pathogens and influence of the seed coat mucilage," *bioRxiv,* p. 2024.01. 12.575253, 2024.
[198] H. Shomar *et al.*, "A family of lanthipeptides with anti-phage function," *bioRxiv,* p. 2024.06.26.600839, 2024, doi: 10.1101/2024.06.26.600839.

[199] R. E. Cobb, Y. Wang, and H. Zhao, "High-efficiency multiplex genome editing of Streptomyces species using an engineered CRISPR/Cas system," *ACS synthetic biology,* vol. 4, no. 6, pp. 723-728, 2015.
[200] L. Pan *et al.*, "Induction and genomic analysis of a lysogenic phage of Hafnia paralvei," *Current Microbiology,* vol. 79, no. 2, p. 50, 2022.
[201] N. Markova, "Blood Microbiota and Cancer: Cell Wall-Deficient L-Forms of Bacteria and Fungi as Cancer-Promoting Environment," *Journal of Biosciences and Medicines,* vol. 10, no. 9, pp. 148-159, 2022.
[202] F. Davison, J. Chapman, and K. Mickiewicz, "Isolation of L-form bacteria from urine using filtration method," *JoVE (Journal of Visualized Experiments),* no. 160, p. e61380, 2020.
[203] R. M. Dedrick *et al.*, "Phage therapy of Mycobacterium infections: compassionate use of phages in 20 patients with drug-resistant mycobacterial disease," *Clinical infectious diseases,* vol. 76, no. 1, pp. 103-112, 2023.
[204] F. Yang *et al.*, "Bacteriophage therapy for the treatment of Mycobacterium tuberculosis infections in humanized mice," *Communications Biology,* vol. 7, no. 1, p. 294, 2024.
[205] N. Dannenberg *et al.*, "Mycobacteria form viable cell wall-deficient cells that are undetectable by conventional diagnostics," *bioRxiv,* p. 2022.11.16.516772, 2022, doi: 10.1101/2022.11.16.516772.
[206] J.-P. Pirnay *et al.*, "Personalized bacteriophage therapy outcomes for 100 consecutive cases: a multicentre, multinational, retrospective observational study," *Nature Microbiology,* pp. 1-20, 2024.

Curriculum vitae

Véronique Margiet Antoinette Ongenae was born in Enschede, The Netherlands on the 26th of June, 1996. She attended secondary school at the Bonhoeffer College Van der Waalslaan, following the 'Science and Health' profile, from which she graduated in 2014.

After graduation, she moved from Enschede to Leiden to follow the Bachelor Biology at Leiden University. During this time, she discovered her passion for microbes and ecology and therefore continued her studies by following the Master "From Cells to Organisms" again at Leiden University. During her first Master internship, supervised by dr. Sjoerd Seekles in the fungal biotechnology group of prof. dr. Arthur Ram, she studied the impact of environmental conditions on the stress-resistance of *Aspergillus niger* conidia. This internship really sparked her interest for doing research. She then did her second Master internship at the Westerdijk fungal biodiversity institute in the group of dr. Jos Houbraken under the supervision of dr. Jan Dijksterhuis and dr. Tom Van den Brule, where she identified and annotated genes involved in the heat-resistance of *Paecilomyces variotii* conidia. After graduating her Masters during the pandemic in 2020, she continued to work at the Westerdijk institute as a technician in the Fungal physiology department.

Véronique started her PhD programme at the Institute of Biology at Leiden University in 2021. Under the joint supervision of prof. dr. Dennis Claessen and prof. dr. Ariane Briegel. The work done as a PhD student is described in this thesis.

Publications

Ongenae, V., Briegel, A., & Claessen, D. (2021). Cell wall-deficiency as an escape mechanism from phage infection. *Open biology*, *11*(9), 210199.

Ongenae, V., Mabrouk, A. S., Crooijmans, M., Rozen, D., Briegel, A., & Claessen, D. (2022). Reversible bacteriophage resistance by shedding the bacterial cell wall. *Open Biology*, *12*(6), 210379.

Ongenae, V., Azeredo, J., Kropinski, A. M., Rozen, D., Briegel, A., & Claessen, D. (2022). Genome sequence and characterization of *Streptomyces* phage Pablito, representing a new species within the genus *Janusvirus*. *Scientific Reports*, *12*(1), 17785.

Ongenae, V.[*], Kempff, A.[*], van Neer, V.[*] *et al.* (2023) Genome sequence and characterization of *Streptomyces* phages Vanseggelen and Verabelle, representing two new species within the genus *Camvirus*. *Scientific Reports* 13, 20153.

Sidi Mabrouk, A., **Ongenae, V.**, Claessen, D., Brenzinger, S., & Briegel, A. (2023). A flexible and efficient microfluidics platform for the characterization and isolation of novel bacteriophages. *Applied and Environmental Microbiology*, *89*(1), e01596-22.

Britton A.P., Visser K.A., **Ongenae V.M.A.,** Zhang P., Wassink H., Doerksen T.A., Welke C.A., Lynch K.H., Belkum M.J. van, Dennis J.J., Yang X., Claessen D., Briegel A. & Martin-Visscher L.A. (2023), Characterization of bacteriophage cd2, a siphophage infecting *Carnobacterium divergens* and a representative species of a new genus of phage, *Microbiology Spectrum*.

Ongenae, V.[*], Ouyang, R.[*], Muok, A., Claessen, D., Briegel, A. (2024) Phage fibers and spikes: a nanoscale Swiss army knife for host infection. Curr Opin Microbiol. 2024 Feb;77:102429. doi: 10.1016/j.mib.2024.102429. Epub 2024 Jan 26. PMID: 38277900.

Zhong, X., Baur, S., **Ongenae, V.** *et al.* (2024) The stomatin-like protein StlP organizes membrane microdomains to govern polar growth in filamentous actinobacteria under hyperosmotic stress. *Research square* https://doi.org/10.21203/rs.3.rs-3811693/v1

Shomar, H., Tesson, F., Guillaume, M., **Ongenae, V.**, *et al.* (2024) A family of lanthipeptides with anti-phage function. Biorxiv. DOI: 10.1101/2024.06.26.600839.